Benedikt Kien, BSc

# Investigation of Omega-O-Acylceramide Biosynthesis in Mammalian Cells using a Bicistronic Expression System

**MASTER'S THESIS**

to achieve the university degree of

Master of Science

Master's degree programme: Biochemistry and Molecular Biomedical Sciences

submitted to

**Graz University of Technology**

Supervisor

Mag. Dr.rer.nat. Franz Radner

Institute of Molecular Biosciences, University of Graz

Assoz. Prof. Mag. Dr.rer.nat. Achim Lass
Institute of Molecular Biosciences, University of Graz

Graz, March 2017

## AFFIDAVIT

I declare that I have authored this thesis independently, that I have not used other than the declared sources/resources, and that I have explicitly indicated all material which has been quoted either literally or by content from the sources used. The text document uploaded to TUGRAZonline is identical to the present master‘s thesis.

Date

Signature

# Danksagung

*"Always remember people who have helped you along the way,*
*and don't forget to lift someone up."* – Roy T. Bennett

*"We often take for granted the very things that most deserve our gratitude."*
- Cynthia Ozick

An dieser Stelle möchte ich mich herzlich bei all jenen Menschen bedanken, ohne die ich es nicht geschafft hätte so weit zu kommen und mein Studium zu beenden.

Ich bedanke mich bei Mag. Dr.rer.nat. Franz Radner für die geduldige, freundliche und fachlich exzellente Betreuung meiner Masterarbeit. Das Fachwissen, die präzise Arbeitsweise und die vielen methodischen Tricks die ich mir dank ihm aneignen konnte sind von sehr hohem Wert für mich und werden mir auf meinem weiteren Weg von großem Nutzen sein.

Weiters bedanke ich mich bei Assoz. Prof. Mag. Dr.rer.nat. Achim Lass für die freundliche Betreuung und die Korrektur meiner Masterarbeit.

Ich danke meinem Vater und meiner Mutter, Peter und Ursula, für das Ermöglichen meines Studiums, ihr Vertrauen, ihren Rat und ihre bedingungslose Unterstützung in jeder Situation. Mir ist bewusst, dass diese Dinge nicht selbstverständlich sind und auch wenn ich es zu selten ausspreche schätze ich mich sehr glücklich euch als Eltern zu haben.

Meinen Kolleginnen und Kollegen vom Institut für molekulare Biowissenschaften, von denen ich viele als Freunde betrachte, danke ich für die schöne Zeit, die angenehme Arbeitsatmosphäre, die fachliche und persönliche Unterstützung und die enorme Hilfsbereitschaft.

Zuletzt möchte ich mich bei Michael, Isabel und Lisa für ihre Freundschaft bedanken, die mir mehr bedeutet als ihnen vielleicht bewusst ist.

# Abstract

Members of the patatin-like phospholipase domain containing (PNPLA) protein family are key enzymes in lipid metabolism and exhibit diverse lipolytic and acyltransferase activities. Until lately, the physiological role and enzymatic activity of PNPLA1 remained unclear. However, in recent publications it was demonstrated that *PNPLA1* mutations are associated with autosomal recessive congenital ichthyosis (ARCI) in humans and Golden Retriever dogs. Moreover, the generation of *Pnpla1* knockout mice revealed that such animals display an ichthyosiform skin phenotype and die shortly after birth due to skin barrier dysfunction. It was demonstrated that the permeability barrier defect in *Pnpla1* -/- mice was most probably caused by impaired corneocyte-bound lipid envelope (CLE) formation due to epidermal ω-O-acylceramide (ω-O-AcylCer) deficiency, which indicated defective ω-O-AcylCer synthesis. On the other hand, free extractable ω-hydroxyceramides (ω-OH-Cers), which are the supposed precursor lipids of ω-O-AcylCers, strongly accumulated in the epidermises of PNPLA1 deficient mice.

Based on these results it has been hypothesized that PNPLA1 is the yet unknown acyltransferase/transacylase, which catalyzes the final step of ω-O-AcylCer synthesis, the esterification of ω-OH-Cers with linoleic acid. To investigate this hypothesis *in vivo*, I generated a 2A peptide-based lentiviral co-expression system, which I then used to co-express the three identified crucial enzymes of ω-OH-Cer synthesis, ELOVL4, CYP4F22 and CERS3, together with PNPLA1 in HEK-293T, HaCaT or COS-7 cells. As a negative control, I expressed a putative enzymatically inactive PNPLA1 p.S53A mutant variant or an enzymatically inert yellow fluorescent protein (YFP) instead of wild-type PNPLA1.

To investigate ω-O-AcylCer synthesis *in vivo*, resulting cell lines overproducing the target enzymes were radiolabeled using [$^{14}$C]linoleic acid, [$^{14}$C]palmitic acid or [3-$^{3}$H]D-erythro-sphingosine, respectively, and the lipid profiles were examined by TLC analysis. The expected formation of ω-O-AcylCers in HEK-293T, HaCaT or COS-7 cells expressing ELOVL4, CYP4F22 and CERS3 together with PNPLA1 was not observed, which argued against the proposed hypothesis and indicated the need for further research.

# Zusammenfassung

Enzyme der „patatin-like phospholipase domain containing" (PNPLA) Proteinfamilie besitzen diverse Acyltransferase- und Hydrolaseaktivitäten und spielen eine Schlüsselrolle im Lipidmetabolismus und der Signalübertragung. Die physiologische Funktion und enzymatische Aktivität von PNPLA1 waren bis vor kurzem unklar. Jedoch wurde in aktuellen Publikationen eine Korrelation von *PNPLA1* Mutationen und autosomal rezessiver kongenitaler Ichthyose (ARCI) in Menschen und Golden Retriever Hunden nachgewiesen. In der Folge generierte *Pnpla1* Knockout-Mäuse wiesen ebenfalls einen ichthyotischen Phänotyp auf und starben aufgrund eines Hautbarriere-Defekts kurz nach der Geburt. Es wurde gezeigt, dass dieser Permeabilitätsbarriere-Defekt mit hoher Wahrscheinlichkeit auf einer gestörten Bildung des „corneocyte-bound lipid envelope" (CLE) beruhte, welchem eine beinahe vollständige ω-O-Acylceramid (ω-O-AcylCer) Defizienz der Epidermis zugrunde lag. Weiterhin wurde eine starke Akkumulation von ω-Hydroxyceramiden (ω-OH-Cers), den vermuteten Vorläuferlipiden von ω-O-AcylCers, in den Epidermen von PNPLA1-defizienten Mäusen beobachtet.

Diese Resultate führten zu der Hypothese, dass es sich bei PNPLA1 um eine bisher unbekannte Acyltransferase oder Transacylase handelt, welche den letzten Schritt der ω-O-AcylCer Synthese, die Veresterung von ω-OH-Cers mit Linolsäure, katalyisiert. Um diese Theorie *in vivo* zu untersuchen etablierte ich ein 2A-Peptid basierendes lentivirales Co-Expressionssystem, welches ich anschließend für die transiente oder stabile Co-Expression von drei bekannten essentiellen Enzymen der ω-OH-Cer Synthese (ELOVL4, CYP4F22 und CERS3) gemeinsam mit PNPLA1 in HEK-293T, HaCaT oder COS-7 Zellen verwendete. Als Negativkontrolle exprimierte ich eine vermutete inaktive PNPLA1 Mutante (p.S53A) oder ein enzymatisch inertes gelb fluoreszierendes Protein (YFP) anstelle von Wildtyp-PNPLA1.

In weiterer Folge markierte ich Lipide in den hergestellten überexprimierenden Zelllinien mit [$^{14}$C]Linolsäure, [$^{14}$C]Palmitinsäure oder [3-$^{3}$H]D-Erythro-Sphingosin und untersuchte die Lipidprofile mittels Dünnschichtchromatographie Analyse. Die erwartete ω-O-AcylCer Synthese in ELOVL4, CYP4F22, CERS3 und PNPLA1 co-exprimierenden Zellen konnte nicht beobachtet und damit die aufgestellte Hypothese nicht bestätigt werden. Zur Aufklärung der tatsächlichen enzymatischen Aktivität von PNPLA1 ist somit weitere Forschung unerlässlich.

# Table of Contents

# 1 Introduction

## 1.1 Anatomy and functions of the mammalian skin

The mammalian skin is a large, complex and dynamic organ, which is essential for survival in a terrestrial environment. It consists of three major layers - epidermis, dermis and hypodermis (also called subcutis). Depending on the body region, full thickness of the skin varies from 1.5 to 4.0 mm, whereas thickness of the epidermis ranges from 0.4 to 1.5 mm [1]. A schematic of human skin and its different layers is depicted in Figure 1.1.

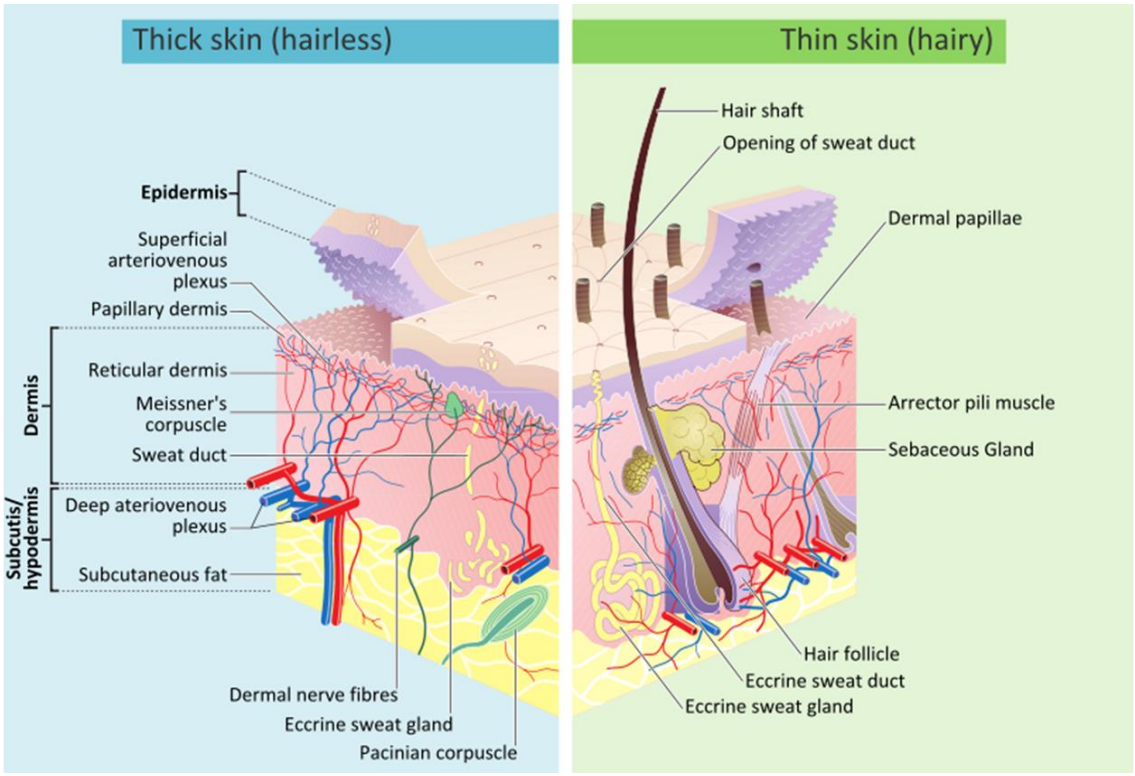


**Figure 1.1: Schematic cross section of the different layers and features of human skin.**[1] The image illustrates the complex anatomy of the skin, which consists of multiple layers of tissue and encloses a variety of components like blood- and lymphatic vessels, sensory nerve endings, muscles, hair follicles and eccrine glands.

Besides determining physical appearance, the skin provides a variety of different functions, including sensation of heat and cold, touch, pressure, vibration and tissue injury. An essential function of the skin is thermoregulation. Cooling is mainly achieved by evaporation of sweat, secreted by eccrine glands. Furthermore, dilation of cutaneous blood vessels results in increased perfusion and a better heat loss rate, thereby lowering body temperature. On the other hand, the insulation provided by subcutaneous fat and constriction of dermal blood vessels aid in the conservation of heat [1].

[1] Image source: https://en.wikipedia.org/wiki/File:Skin_layers.svg, August 2016.

Another major function of the skin is to protect its host from harmful influences, by providing an efficient, physical barrier between the hostile environment and the internal milieu. The skin barrier prevents intrusion of pathogenic microorganisms and protects the body from allergens, chemicals, toxins, mechanical insults and ultraviolet light. However, skin lesions or wounds may allow pathogens to penetrate the skin barrier. In such an event, the skin provides the organism's first line of defense as it contains components of the innate immune system, as well as patrolling immune cells of the adaptive immune system [1,2].

In the epidermis four distinct cellular layers, the stratum basale (SB), stratum spinosum (SS), stratum granulosum (SG) and stratum corneum (SC) can be distinguished (Figure 1.2). The latter, outermost layer (SC) is the location of the highly hydrophobic and water sealing epidermal permeability barrier, which provides the possibly most important function of the skin - the prevention of excessive transcutaneous loss of water and electrolytes to the environment [2–5].

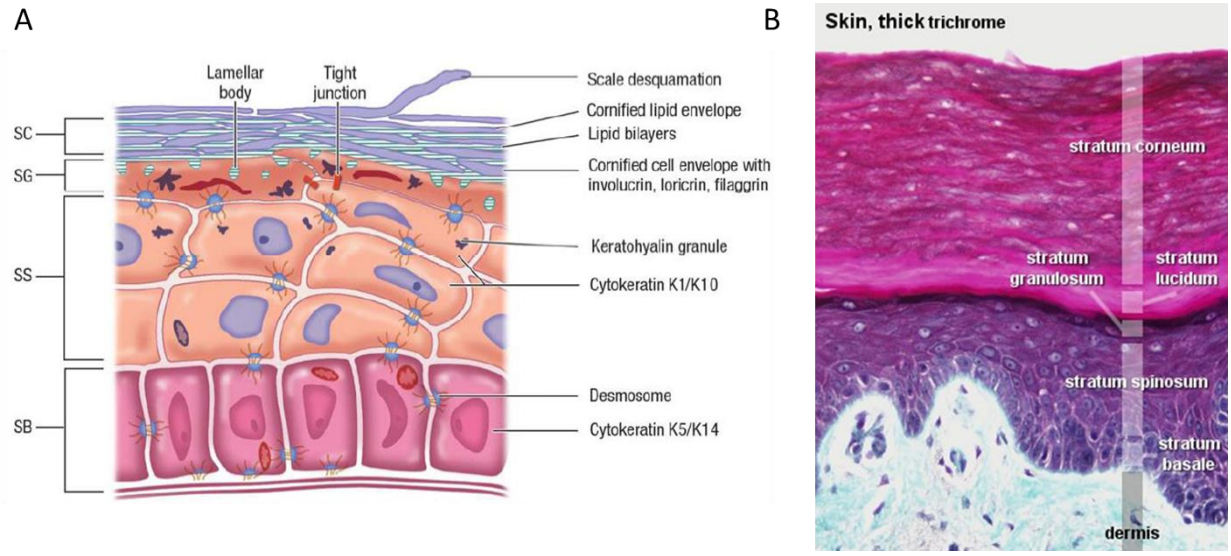


**Figure 1.2: Anatomy of the human epidermis. A)** Schematic drawing of the epidermis and its four distinct cellular layers[2]: Stratum basale, SB; stratum spinosum, SS; stratum granulosum, SG; stratum corneum, SC. **B)** Histological cross section of human skin[3]. The different cellular layers were stained by trichrome staining.

[2] Image source: Fitzpatrick's Dermatology in General Medicine [1].
[3] Image source: http://www.nku.edu/~dempseyd/skin%20layers.jpg, October 2016.

## 1.2 The role of ceramides in skin barrier formation

The lowest layer of the epidermis (SB) consists of proliferating keratinocytes, which subsequently migrate towards the SC. In the next layer (SS) migrating keratinocytes begin to differentiate due to an increasing $Ca^{2+}$ gradient and initiate synthesis of precursor lipids like glucosylceramides, phospholipids, cholesterolsulfate and cholesterol [3–6]. These lipids are essential for the subsequent formation of the permeability barrier.

The major lipid constituents of the skin barrier are ceramides (Cer). To date there are twelve different free extractable Cer species known in human SC, which differ in the hydroxylation pattern of their sphingoid base and in their amide-linked fatty acid moiety [4]. Four of those ceramide species, Cer 1 (EOS), Cer 4 (EOH), Cer 9 (EOP) and Cer 12 (EODS) are exclusively found in mammalian epidermis and are critical for barrier formation. These so-called ω-O-acylceramides (ω-O-AcylCers) are characterized by a unique structure, consisting of a sphingosine backbone that is amide-linked to an ω-hydroxylated ultra-long chain fatty acid (ULFA, ≥C26-36), which itself is further esterified with linoleic acid (Figure 1.3) [4,5].

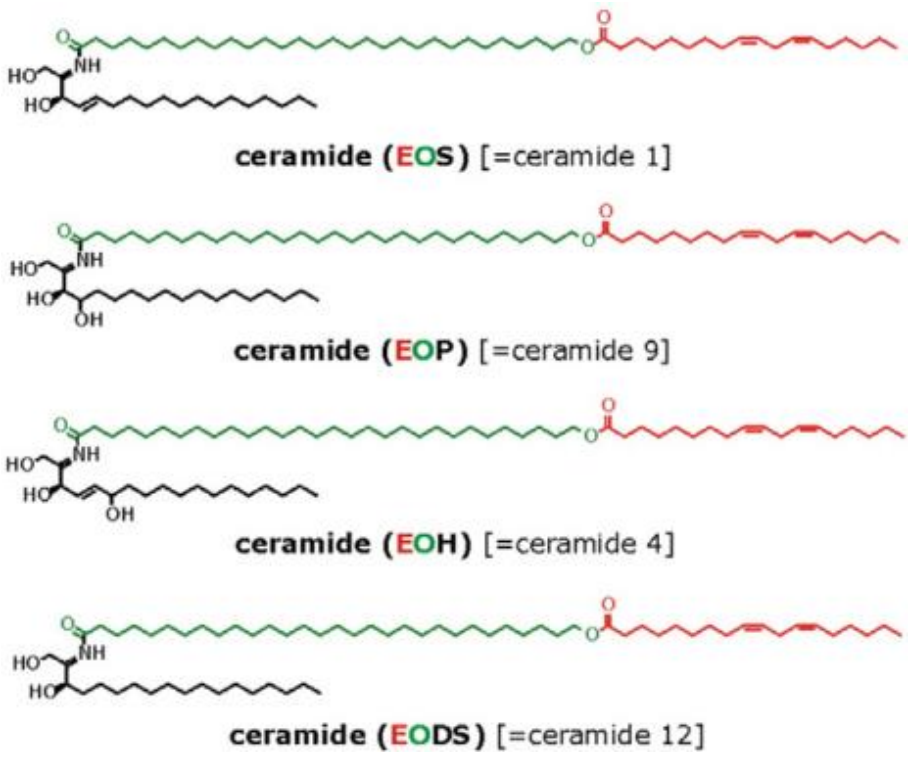


**Figure 1.3: Molecular structures of the four known ω-O-acylceramides, found in mammalian stratum corneum.[4]**

[4] Image source: Breiden & Sandhoff, 2013 [4].

### 1.2.1 The ω-O-AcylCer pathway and associated pathologies

The pathway leading to the formation of ω-O-AcylCer is not fully understood yet. It is known that the synthesis occurs in a multi-step process, involving several key-enzymes. In differentiating keratinocytes, ω-O-AcylCer formation starts with *de novo* sphinganine synthesis from L-serine and palmitoyl-CoA (catalyzed by serine palmitoyltransferase and 3-keto-sphinganine reductase) at the endoplasmic reticulum (ER) membrane [5].

#### *1.2.1.1* Generation of ULFAs (≥C26) by fatty acid elongase 4 (ELOVL4)

The required fatty acids (FAs, ≥C16) for subsequent elongation are either taken up by the diet or are *de novo* synthesized from acetyl-CoA and malonyl-CoA by the cytosolic fatty acid synthase complex I (FAS-I) and the mitochondrial FAS-II complex [4,7]. The stepwise elongation of FAs (≥C16) is catalyzed by multiple homologous ER-bound fatty acid elongases (ELOVL1-7), which vary in their substrate specificity for saturated or (poly)unsaturated FAs with different chain lengths [4,5,8]. The elongation of ULFAs (≥C26) up to a chain length of 36 carbon atoms is catalyzed by ELOVL4 (UniProtKB Q9GZR5, OMIM #614457), thereby making the enzyme indispensable for ω-O-AcylCer formation [4,9–11]. Heterozygous mutations of *ELOVL4* have been identified as causative for autosomal dominant Stargardt-like macular dystrophy (STGD3), whereas recessive *ELOVL4* mutations are associated with intellectual disability, spastic quadriplegia and ichthyosis (a severe skin barrier defect) in humans [11,12]. Furthermore the skins of *Elovl4* knockout mice (*Elovl4* -/-) and mice with a homozygous 5 bp-deletion in the *Elovl4* gene (*Elovl4*$^{del/del}$) are depleted of ULFAs and ULFA-Cers (including ω-O-AcylCers), resulting in ichthyosis and neonatal death [13,14].

#### 1.2.1.2 ω-hydroxylation of ULFAs by cytochrome P450 4F22 (CYP4F22)

Performing co-expression experiments and subsequent radiolabeling of lipids in HEK-293T cells (as well as LC-MS analysis), Ohno *et. al.* demonstrated that the next step of the pathway, the ω-hydroxylation of ULFAs (≥C28), is catalyzed by CYP4F22 (UniProtKB Q6NT55, OMIM #611495). The authors further suggested that this reaction likely occurs at the cytoplasmic side of the ER [10]. The identification of CYP4F22 as an ULFA-specific ω-hydroxylase explains the previously observed association of *CYP4F22* mutations with congenital ichthyosis in humans [15–17].

#### 1.2.1.3 Amide bond formation by ceramide synthase 3 (CERS3)

After activation by esterification with Coenzyme A (CoA; possibly catalyzed by FATP4 [10]), ω-hydroxylated ULFAs are subsequently amide-linked to a sphingoid base by the integral ER-membrane protein ceramide synthase 3 (CERS3, formerly known as LASS3, UniProtKB Q8IU89, OMIM #615276), forming ω-hydroxyceramides (ω-OH-Cers) [18–23]. In

accordance with this enzymatic function, the skins of humans and mice with CERS3-deficiency are depleted of ω-OH-Cer (and consequently ω-O-AcylCer), resulting in autosomal recessive congenital ichthyosis (ARCI) [20,21,23]. Similar to *Elovl4* -/- mice, CERS3-deficient mice ($Cers3^{d/d}$) die shortly after birth, due to a defective skin barrier [23].

#### 1.2.1.4 Esterification of ω-OH-Cers with linoleic acid by an unknown enzyme

Finally, a yet unknown putative acyltransferase or transacylase catalyzes the last step of the pathway by esterifying ω-OH-Cer with linoleic acid, yielding ω-O-AcylCer [4,5,10,24].

### 1.2.2 ω-O-AcylCer processing and permeability barrier formation

In the Golgi apparatus, ceramides are further processed to glucosylceramides (GlcCers) and sphingomyelin (SM). Glucosylation of ω-O-AcylCers (and other Cers) is catalyzed by ceramide-glucosyltransferase, yielding ω-O-acylglucosylceramides (ω-O-acylGlcCers, Figure 1.4) [5].

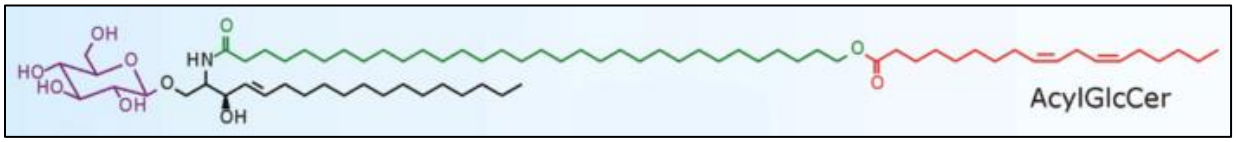


**Figure 1.4: Molecular structure of a ω-O-acylglucosylceramide (GlcEOS), found in mammalian SC.[5]**

Together with certain hydrolytic enzymes and probarrier lipids (such as GlcCers, SM and phospholipids) ω-O-acylGlcCers are packed into specialized secretory organelles, which are known as lamellar bodies (LBs) [4]. In the SG, high numbers of such granular LBs are associated with the plasma membranes of keratinocytes. Subsequently, the contents of LBs are secreted into the intercellular space at the SG-SC interface by exocytosis [3–5].

The SC consists of 10-25 layers of flattened and enucleated, terminally differentiated keratinocytes (hence called corneocytes), which are constantly removed from the skin (desquamation) and replaced by new cells from lower layers [3]. During cornification, the plasma membranes of corneocytes are replaced by a cross-linked, cornified protein envelope (CE), which mainly consists of filaggrin, involucrin and loricrin [4,5,25]. In the SG-SC interstitium, the linoleic acid moiety of ω-O-acylGlcCer is removed by successive oxygenation and hydrolysis catalyzed by lipoxygenases 12R-LOX and eLOX3 [25]. The resulting ω-OH-GlcCer are then covalently linked to glutamine residues of CE-proteins by transesterification via transglutaminase 1 (TGase 1) and glucose residues are removed by β-glucocerebrosidase (β-GlcCerase) and SAP-C. Furthermore, some of the esterified ω-O-Cer

[5] Image source: Breiden & Sandhoff, 2013 [4].

are depleted of their sphingosine moiety by hydrolysis via acid ceramidase, Sap-D and Sap-C [4,5,25,26].

The described process (summarized in Figure 1.5) leads to the formation of a highly hydrophobic monolayer of ω-O-Cer and ω-O-ULFAs that are covalently linked to amino acid residues of CE-proteins. This monolayer is known as the corneocyte-bound lipid envelope (CLE) and essential for the development of a functional permeability barrier [5,27].

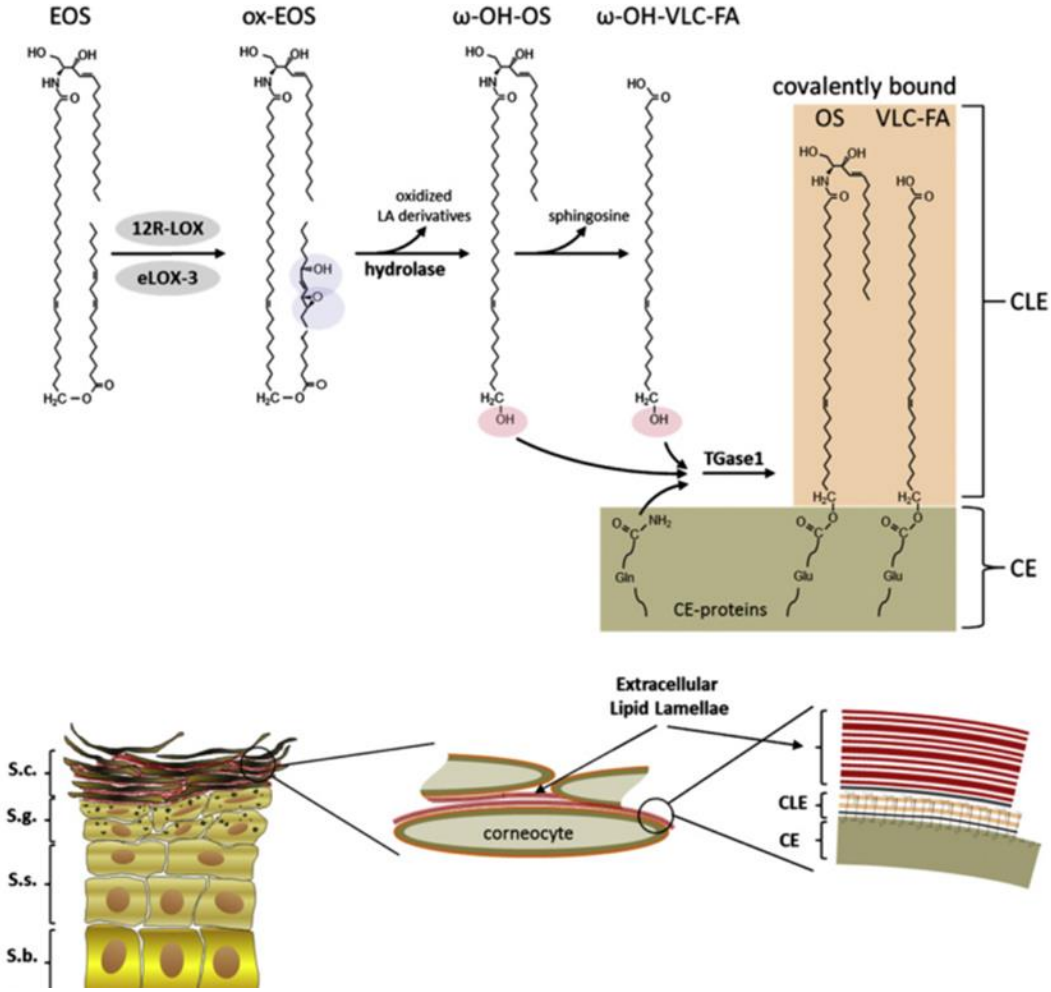


**Figure 1.5: Overview of corneocyte-bound lipid envelope (CLE) formation in human stratum corneum.**[6] In the SG-SC interstitium, ω-O-acylGlcCer (EOS) are extracellularly processed and covalently linked to glutamine residues of cornified envelope (CE) proteins. The resulting lipid monolayer (CLE) serves as a template for the formation of highly hydrophobic extracellular lipid lamellae, which (in combination with the cornified corneoecytes) provide the permeability barrier function of the skin.

The CLE serves as an essential scaffold for the formation of highly hydrophobic, extracellular lipid lamellae, which are located between the corneocytes (Figure 1.5). These bilayered lamellae account for approximately 10% of the SC tissue mass and consist of ceramides (50%), cholesterol (25%) and very long chain FAs (15%). In combination with the cornified

[6] Image source: Krieg & Fürstenberger, 2013 [25].

corneocytes, the lipid lamellae provide the vital permeability barrier function of the skin [3–5,25].

A lack of ω-O-AcylCers prevents the formation of a functional CLE and thereby obstructs the subsequent development of the hydrophobic lipid lamellae. This may explain the above mentioned skin barrier defects that affect ichthyosis patients lacking crucial enzymes for ω-O-AcylCer synthesis (such as ELOVL4, CYP4F22 and CERS3) [11,12,15,16,20,21].

## 1.3 Patatin-like phospholipase domain-containing protein 1 (PNPLA1) and its role in ichthyosis

**Figure 1.6: Typical phenotype of a newborn baby suffering from harlequin ichthyosis.**

Human ichthyoses are a very heterogeneous group of hereditary skin disorders. They usually affect the entire integument and are characterized by a reddish, dry and thick phenotype of the skin, as well as abnormal scaling and impaired terminal keratinocyte differentiation. The genetic causes and severity of symptoms vary significantly. Currently, about forty genes have been identified to be involved in various types of ichthyoses [28]. Mild forms, like the relatively common autosomal ichthyosis vulgaris, are well treatable by application of moisturizing lotions. On the other hand, very rare and severe forms, like congenital harlequin ichthyosis (Figure 1.6[7]), are potentially lethal. Yet, patients can survive, if given adequate intensive care [24,28–30].

Ichthyoses typically involve a defective skin permeability barrier. Therefore, common symptoms include increased dehydration, high susceptibility to infections and overheating, due to impaired thermoregulation. Because of the abnormal appearance of their skin, patients also often suffer from isolation, low self-esteem and depression [31].

Autosomal recessive congenital ichthyosis (ARCI), as indicated by its name, is an autosomal recessive transmitted, nonsyndromic form of ichthyosis. It is commonly diagnosed right after birth. Examples for diseases classified as ARCI are harlequin ichthyosis, lamellar ichthyosis or congenital ichthyosiform erythroderma [29].

[7] Image source: Akiyama, 2013 [30].

In 2012, Grall *et. al.* investigated a spontaneous mutant Golden Retriever dog model, displaying lamellar ichthyosis with similar symptoms as present in patients affected by ARCI [28]. Using a genomewide association study, the authors have identified a causative, homozygous insertion-deletion (indel) mutation in *PNPLA1,* resulting in C-terminal truncation of the protein. Furthermore, Grall and colleagues have also found a homozygous nonsense and a homozygous missense mutation in human *PNPLA1* in six individuals from two consanguineous families affected by ARCI. Based on these findings, several novel *PNPLA1* mutations in patients suffering from ARCI have been identified so far [32–36]. To date, the enzymatic function of PNPLA1 still remains unclear [24,37]. However, it obviously appears to play a major role in skin lipid metabolism and permeability barrier formation.

### 1.3.1 PNPLA1 is essential for ω-O-AcylCer formation

PNPLA1 (UniProtKB Q8N8W4, OMIM #612121) is a member of the patatin domain containing proteins (Pfam01734). In humans, this protein family consists of nine members (PNPLA1-9) that are characterized by a patatin-like phospholipase domain, containing the evolutionary conserved Gly-X-Ser-X-Gly consensus serine hydrolase motif with a nucleophilic serine [37]. In contrast to “classic” hydrolytic enzymes (e.g. hormone-sensitive lipase, HSL) that exhibit an α/β-hydrolase fold with a Ser-Asp/Glu-His catalytic triad, PNPLAs display a distinct Pat17 fold topology, which shares similarities with the cytosolic phospholipase $A_2$ ($cPLA_2$, a lipid acyl hydrolase) fold and contains a Ser-Asp catalytic diad [37,38]. Human PNPLAs exhibit diverse lipolytic and acyltransferase activities and play crucial roles in lipid metabolism, as well as signaling [37]. For instance, PNPLA2, also known as ATGL (adipose triglyceride lipase), is the rate limiting enzyme of triacylglycerol (TG) catabolism (lipolysis) [37,39,40].

The human *PNPLA1* gene is encoded by eight exons at chromosomal region 6p21 [28]. By alternative splicing, three different isoforms of PNPLA1 exist[8]. However, there are no data available, regarding which of the isoforms are expressed in humans. The longest version (isoform 1) has a length of 532 amino acids. As the other two isoforms (isoform 2 and 3) lack a large part of the N-terminal patatin domain, including the catalytic Ser-Asp dyad, isoform 1 is presumably the only active variant[9]. Strong *PNPLA1* mRNA expression was observed in the digestive system and in keratinocytes of the granular layer [41][10]. Interestingly, PNPLA1 protein expression appears to be more pronounced in upper epidermal and lower cornified layers, suggesting a possible function in cornification and/or skin barrier formation [28]. To date, no experimental 3D structures of PNPLA1 are available.

[8] https://www.ncbi.nlm.nih.gov/gene/285848; 2017.
[9] http://www.uniprot.org/uniprot/Q8N8W4 ; 2017
[10] https://www.ncbi.nlm.nih.gov/gene/285848/?report=expression ; 2017

Very recently, Grond *et. al.* generated and characterized PNPLA1-deficient (*Pnpla1 -/-*) mice [24]. Newborn *Pnpla1 -/-* pups were significantly smaller and lighter than their wild-type and heterozygous littermates. Furthermore, they displayed a dry, wrinkled and reddish skin phenotype (similar to those present in ARCI), which resembled the appearance of newborn *Elovl4* and *Cers3* knockout mice (Figure 1.7). Due to severe skin barrier dysfunction, trans-epidermal water loss of *Pnpla1 -/-* mice was approximately four-fold increased and (just like *Elovl4* and *Cers3* knockout mice) the pups died shortly after birth.

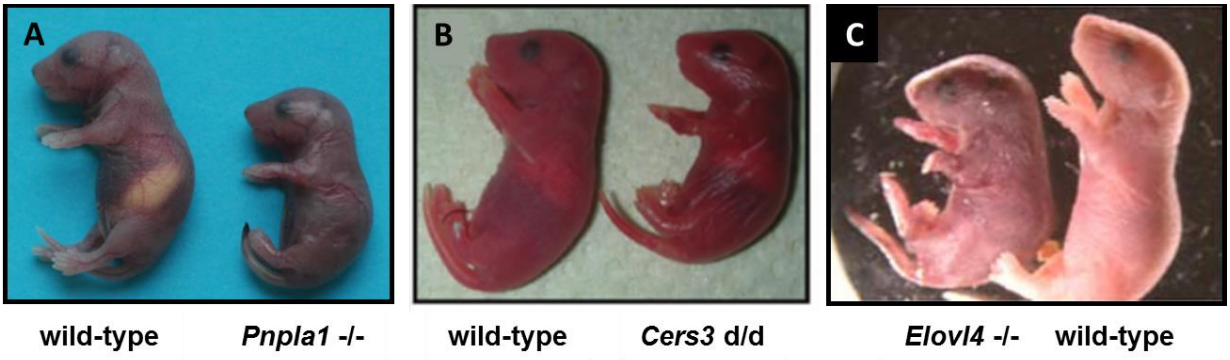


**Figure 1.7: Comparison of the phenotypes of newborn *Pnpla1* (A[11]), *Cers3* (B[12]) and *Elovl4* (C[13]) knockout mice.** The different knockout animals are significantly smaller than their corresponding wild-type littermates and they display an ichthyotic, wrinkled skin phenotype. The mutant animals die shortly after birth due to a severe permeability barrier defect.

Grond and colleagues further investigated the epidermal neutral and polar lipids of newborn wild-type and *Pnpla1 -/-* mice by UPLC-qTOF. The analysis revealed that *Pnpla1* knockout mice suffered from an impaired epidermal ceramide homeostasis, as their epidermis were completely depleted of free extractable ω-O-(18:2)AcylCers and their glucosylated derivates. On the other hand, the PNPLA1-deficient animals exhibited a distinct accumulation of free extractable ω-OH-Cers (the supposed precursor lipids of ω-O-AcylCers) and their glucosylated derivatives [24]. In accordance with the absence of ω-O-AcylCers, covalently bound ω-OH-Cers were almost undetectable in the epidermises of *Pnpla1 -/-* mice [24]. This finding strongly indicated a defective CLE, which most probably accounted for the impaired permeability barrier formation in *Pnpla1* knockout mice. Labelling epidermal lipids using [$^{14}$C]linoleic acid, Grond and colleagues have demonstrated an identical ω-O-AcylCer synthesis defect in primary keratinocytes that were obtained from a patient affected by a homozygous nonsense mutation in *PNPLA1*. Based on these results the authors concluded that PNPLA1 function is conserved among mammals and indispensable for adequate ω-O-AcylCer synthesis to provide normal skin function [24].

[11] Image source: Modified from Grond *et. al.* (2016) [24].
[12] Image source: Modified from Jennemann *et.al.* (2012) [23].
[13] Image source: Modified from Li *et. al.* (2007) [14].

## 1.4 Internal ribosomal entry sites (IRES) and 2A peptides allow co-expression of multiple genes from a single multicistronic vector construct

For many applications and experimental settings, it is necessary to reliably co-express two or more genes of interest in a cell culture model. However, co-transfection of multiple single-gene constructs does not guarantee that every cell actually carries all desired plasmids and, in turn, expresses all desired gene products. This may result in biased or irreproducible data. To overcome this problem, the use of multicistronic constructs is of high value. Such constructs often contain certain elements, like an internal ribosomal entry site (IRES) or a 2A peptide sequence [42–48] to allow expression of multiple genes driven by a single promoter. The use of viral multicistronic expression vectors for gene therapeutic approaches also offers highly promising results [49,50]. Therefore, they have the potential to become important tools for future treatments of genetic diseases.

### 1.4.1 IRES

IRES elements were first discovered in the poliovirus genome in 1988 [42,43]. Subsequently, various IRES sequences were found in other viruses, but also in cellular mRNAs from humans, mice, dogs, yeast, and fruit flies [44]. IRES elements themselves are non-coding. However, they allow a non-standard, 5' cap-independent initiation of translation by a mechanism that is not fully understood so far [44,45]. This enables independent co-expression of one or more genes, encoded on a single, long mRNA transcript (Figure 1.8).

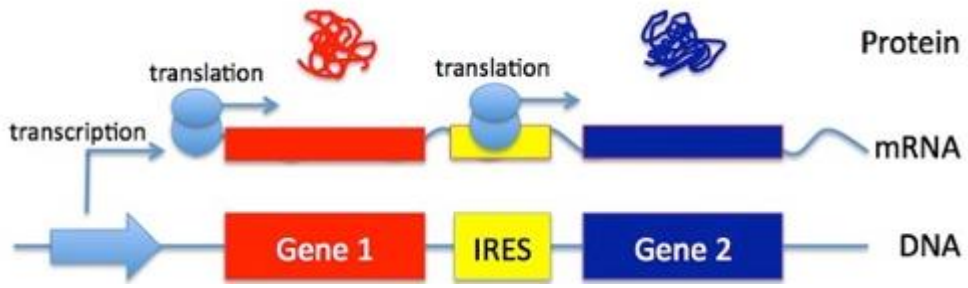


**Figure 1.8: IRES elements allow un-coupled co-expression of multiple ORFs by 5' cap-independent translation initiation.[14]**

IRES elements are usually relatively large in size (~600 bp). This can be of disadvantage, when they are used in viral expression systems, as packaging capacity of viral particles is limited [51]. Another frequently observed problem of IRES-constructs is the low expression of the 3' gene, which depends on the gene per se and the used cell types for expression [48,50,51].

[14] Image source: http://blog.addgene.org/plasmids-101-multicistronic-vectors ; November 2016

### 1.4.2 2A peptides

2A peptides are small “self-cleaving” peptides, consisting of about 18-22 amino acids [52]. They were first discovered in picornaviruses in the 1980’s [46]. To exploit the co-translational self-cleaving mechanism, two genes must be linked in frame by a 2A peptide sequence. The upstream gene must not contain a stop codon. Transcription results in a long mRNA, encoding a Protein1-2A-Protein2 fusion protein. Translation is initiated in a standard 5’ cap-dependent fashion.

During translation of the 2A peptide sequence, a peptide bond between the conserved C-terminal glycine and proline is not formed. This “translational skipping” is assumed to occur due to interaction of the nascent 2A peptide with the exit tunnel of the ribosome [46]. Despite the “skip”, the ribosome is able to continue translating the downstream gene until it reaches the stop codon to dissociate. The resulting upstream protein is C-terminally fused to the complete 2A peptide (17-21 amino acids), except its last proline. This, in turn, is fused to the N-terminus of the downstream protein [46,51–53]. The cleavage process is illustrated in Figure 1.9[15].

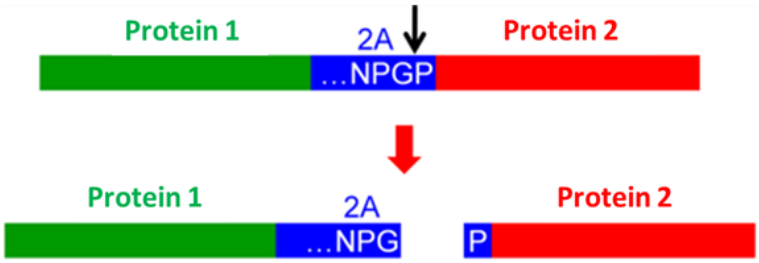


**Figure 1.9: Schema of co-translational, 2A peptide-mediated self-cleavage.** The position of the non-formed peptide bond due to translational skipping is indicated by a black arrow

2A peptides are superior to IRES, in terms of their small size and the ability to produce equimolar levels of target proteins. However, observed expression levels of co-expressed proteins may vary due to their specific stability.

A disadvantage of 2A systems is the C-terminal “2A tag” of the upstream protein. Although it has been reported that this extra sequence has minimal effect on the activity of most proteins and none on their stability [46], negative effects cannot be excluded. For instance, impaired recognition of a C-terminal localization signal or altered interactions with other proteins is discussed[16]. At last, 100% cleavage efficiency is theoretically possible, but cannot be guaranteed [50,52]. Resulting uncleaved fusion proteins might be a problem, depending on the respective application.

[15] Image source: Modified from Kim *et. al.* (2011) [52].
[16] https://www.researchgate.net/post/Does_viral_2A_peptide_really_outperform_IRES_sequence_in_protein_co-expression_in_transgenic_mice ; 2017

# 2 Hypothesis and aim of the study

To investigate the hypothesis that PNPLA1 plays a direct role in the formation of ω-O-AcylCers, I established and tested a 2A peptide-based lentiviral co-expression system. In the following, this system was used for transient or stable co-expression of the three identified crucial enzymes of ω-O-OH-Cer synthesis (ELOVL4, CYP4F22 and CERS3) together with PNPLA1 in HEK-293T, HaCaT or COS-7 cells. As a negative control, a putative enzymatically inactive mutant variant of PNPLA1 (p.S53A) or an enzymatically inert yellow fluorescent protein (YFP) was expressed instead of wild-type PNPLA1.

Similar to the experiments of Ohno *et. al.* [10] identifying the enzymatic function of CYP4F22, I then radiolabeled lipids in the co-expressing cell lines with [$^{14}$C]linoleic acid, [$^{14}$C]palmitic acid or [3-$^{3}$H]D-erythro-sphingosine, extracted the lipids and analyzed the lipid profiles by thin layer chromatography and autoradiography detection. Due to the putative PNPLA1 acyltransferase activity, ω-O-AcylCer biosynthesis was expected in cells expressing ELOVL4, CYP4F22 and CERS3 together with wild-type PNPLA1, but not in cells expressing PNPLA1 p.S53A or YFP instead.

# 3 Materials

## 3.1 Common used buffers and solutions

All used chemicals were purchased from Merck (Darmstadt, Germany), Roth (Karlsruhe, Germany) or Sigma-Aldrich (St. Louis, MO, USA). For preparation of buffers, chemicals were solved in double-distilled, deionized water (dd$H_2O$) and stored as indicated in the list below.

| Buffer / Solution | Composition | Storage temperature |
|---|---|---|
| 10% APS | 10% (w/v) ammonium persulfate | -20°C |
| 30% acrylamide mix | 30% acrylamide<br>0.8% bisacrylamide | 4°C |
| 4x lower Tris buffer | 0.5 M Tris-HCL pH 6.8 | 4°C |
| 4x upper Tris buffer | 0.5 M Tris-HCL pH 8.8<br>0.4% SDS | 4°C |
| 10x SDS-PAGE buffer | 200 mM Tris<br>1.6 M glycine<br>0.83% SDS | RT |
| 4x SDS loading buffer | 0.2 M Tris pH 6.8<br>10% β-mercaptoethanol<br>8% SDS<br>40% glycerine<br>bromophenol blue (tip of a spatula) | -20°C |
| 10x TST pH 7.4 | 1.5 M NaCl<br>500 mM Tris-HCL<br>1% Tween 20 | 4°C |
| 1x CAPS transfer buffer | 10 mM CAPS pH 11<br>10% methanol | RT |

| | | |
|---|---|---|
| Coomassie staining solution | 0.25% coomassie blue<br>6% glacial acetic acid<br>50% ethanol | RT |
| Coomassie destaining solution | 30% methanol<br>8% glacial acetic acid | RT |
| 1x PBS, pH 7.3 | 140 mM NaCl<br>2.7 mM KCl<br>10 mM $Na_2HPO_4$<br>1.8 mM $KH_2PO_4$ | 4°C |
| 1000x protease inhibitor (Pi) | 1 mg/ml pepstatin<br>2 mg/ml antipain<br>20 mg/ml leupeptin | -20°C |
| 1x HSL buffer | 0.25 M sucrose pH 7<br>1 mM EDTA<br>1 mM DTT | -20°C |
| 1x TAE buffer | 40 mM Tris-HCL pH 7.2<br>50 mM EDTA<br>7% glacial acetic acid | RT |
| 5x loading dye | 9% glycerin<br>2.5 mg/ml bromophenol blue<br>2.5 mg/ml xylen-cyanol | -20°C |

| | | |
|---|---|---|
| 1x RIPA buffer | 150 mM NaCl | |
| | 10 mM Tris-HCLpH 7.4 | |
| | 0.1 % SDS | |
| | 1% Triton X-100 | |
| | 1% sodium deoxycholate | |
| | 5 mM EDTA | -20°C |
| 1 M sodium phosphate buffer pH 7.0 | 390 mM $NaH_2PO_4$ | |
| | 610 mM $Na_2HPO_4$ | 4°C |
| β-gal staining solution A | 10 mM sodium phosphate buffer pH 7.0 | |
| | 150 mM NaCl | |
| | 1 mM $MgCl_2$ | |
| | 3.3 mM $K_4Fe(CN)_6$ x $3H_2O$ | |
| | 3.3 mM $K_3Fe(CN)_6$ | 4°C |
| | sterile filtered (0.2 µm pore size) | |
| β-gal staining solution B | 0.02 g X-Gal | |
| | 1 ml DMF | |
| | 9 ml β-gal staining solution A | not storable |
| LB medium/agar pH 7.0 | 10 g/l NaCl | |
| | 5 g/l yeast extract | |
| | 10 g/l tryptone | |
| | (15 g/l agar) autoclaved. | 4°C |
| 1x SOC Outgrowth Medium | 2% Vegetable peptone | |
| | 0.5% Yeast extract | |
| | 10 mM NaCl | |
| | 2.5 mM KCl | |
| | 10 mM MgCl2 | |
| | 10 mM MgSO4 | |
| | 20 mM Glucose | -20°C |

## 3.2 Enzymes and corresponding buffers

| | | |
|---|---|---|
| Phusion High-Fidelity DNA Polymerase<br>5x Phusion GC Buffer | | Thermo Fisher Scientific |
| Q5 Hot Start High-Fidelity DNA Polymerase<br>5x Q5 Reaction Buffer<br>5x Q5 High GC Enhancer | | New England Biolabs |
| DNA Polymerase I, Large (Klenow) Fragment | | New England Biolabs |
| FIREPol DNA Polymerase<br>Optimized 10x DyNAzyme Buffer (F-511) | | Solis Biodyne<br>Thermo Fisher Scientific |
| Calf Intestinal Alkaline Phosphatase (CIP) | | New England Biolabs |
| T4 DNA Ligase<br>10x T4 DNA Ligase Reaction Buffer | | New England Biolabs |
| Acc65I | 5′...G▼GTACC...3′<br>3′...CCATG▲G...5′ | All restriction enzymes:<br>New England Biolabs |
| BamHI<br>BamHI-HF | 5′...G▼GATCC...3′<br>3′...CCTAG▲G...5′ | |
| ClaI | 5′...AT▼CGAT...3′<br>3′...TAGC▲TA...5′ | |
| EcoRI-HF | 5′...G▼AATTC...3′<br>3′...CTTAA▲G...5′ | |
| HindIII-HF | 5′...A▼AGCTT...3′<br>3′...TTCGA▲A...5′ | |
| KpnI-HF | 5′...GGTAC▼C...3′<br>3′...C▲CATGG...5′ | |
| MluI | 5′...A▼CGCGT...3′<br>3′...TGCGC▲A...5′ | |
| NcoI-HF | 5′...C▼CATGG...3′<br>3′...GGTAC▲C...5′ | |
| NotI<br>NotI-HF | 5′...GC▼GGCCGC...3′<br>3′...CGCCGG▲CG...5′ | |
| SalI-HF | 5′...G▼TCGAC...3′<br>3′...CAGCT▲G...5′ | |
| SexAI | 5′...A▼CCWGGT...3′<br>3′...TGGWCC▲A...5′ | |

| | |
|---|---|
| XbaI |  |
| XhoI |  |
| XmaI | 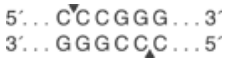 |
| 10x CutSmart Buffer | |
| 10x NEBuffer 3.1 | |
| 10x NEBuffer 2.1 | New England Biolabs |

## 3.3 Plasmid preparation

| | |
|---|---|
| Monarch Plasmid Miniprep Kit | New England Biolabs |
| QIAprep Spin Miniprep Kit | Qiagen |
| NucleoBond Xtra Midi Kit | Macherey-Nagel |

## 3.4 Agarose gel extraction and purification of DNA

| | |
|---|---|
| E.Z.N.A. MicroElute Gel Extraction Kit | Omega Biotek |

## 3.5 Polymerase chain reaction (PCR)

| | |
|---|---|
| C1000 Thermal Cycler with Dual 48/48 Fast Reaction Module | BioRad |

## 3.6 Site-directed mutagenesis

| | |
|---|---|
| Q5 Site-Directed Mutagenesis Kit | New England Biolabs |

## 3.7 *Escherichia coli* strains and eukaryotic cell lines

| | |
|---|---|
| **NEB 5-alpha Competent *E. coli* (High Efficiency)** | **New England Biolabs** |
| ***dam-/dcm-* Competent *E. coli*** | **New England Biolabs** |
| **COS-7**<br>The COS-7 fibroblast-like cell line is derived from African green monkey (*Cercopithecus aethiops*) kidney. It is suitable for transfection by vectors requiring expression of SV40 T antigen. | **ATCC (CRL-1651)** |
| **HaCaT**<br>HaCaT cells are in vitro spontaneously transformed keratinocytes from histologically normal human skin. As they exhibit normal differentiation, they are a suitable model for studying the cellular metabolism of keratinocytes [54]. | **CLS GmbH (Eppelheim, Germany). Article number: 300493** |
| **HEK-293**<br>HEK293 is a hypotriploid cell line derived from human embryonic kidney. It is widely used as a transfection host, for protein expression and enzymatic activity studies. | **ATCC (CRL-1573)** |
| **HEK-293T**<br>The 293T cell line is a highly transfectable derivative of human embryonic kidney 293 cells, and contains the SV40 T-antigen. The cell line is competent to replicate vectors carrying the SV40 region of replication. It gives high titers when used to produce retroviruses. It has been widely used for retroviral production, gene expression and protein production. | **ATCC (CRL-3216)** |

## 3.8 Standards

| | |
|---|---|
| Bovine Serum Albumin Standard [2mg/ml] | Pierce |
| Precision Plus Protein All Blue Standard (Figure 3.1) | BioRad |
| GeneRuler 1 kb DNA Ladder (Figure 3.2) | Thermo Fisher Scientific |
| 100 bp DNA Ladder (Figure 3.3) | Invitrogen |
| Quick-Load Purple 1 kb DNA Ladder (Figure 3.4) | New England Biolabs |
| Quick-Load Purple 100 bp DNA Ladder (Figure 3.5) | New England Biolabs |
| Color Prestained Protein Standard, Broad Range (Figure 3.6) | New England Biolabs |

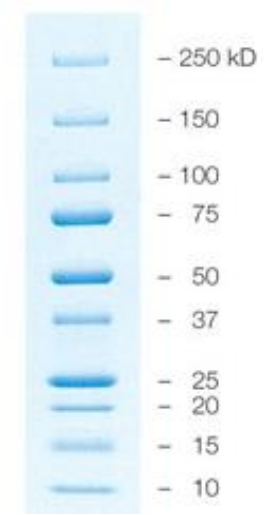


**Figure 3.1:** [17] Precision Plus Protein All Blue Standard (BioRad) for SDS-PAGE.

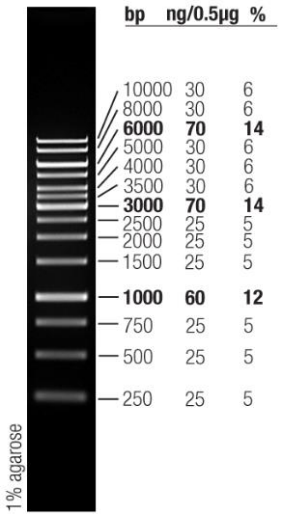


**Figure 3.2:**[18] GeneRuler 1 kb DNA Ladder (Thermo Fisher Scientific) for agarose gel electrophoresis. 0.5 µg/lane, 8 cm length gel, 1x TAE, 7V/cm, 45 min.

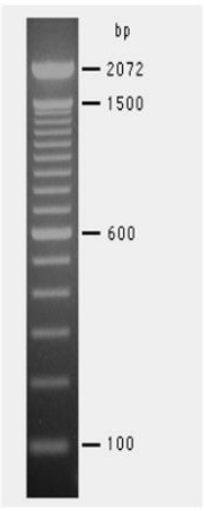


**Figure 3.3:**[19] 100 bp DNA Ladder (Invitrogen) for agarose gel electrophoresis. 0.5 µg/lane, 2% agarose gel stained with ethidium bromide.

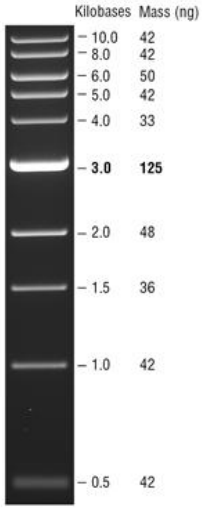


**Figure 3.4:**[20] Quick-Load Purple 1 kb DNA Ladder (New England Biolabs) for agarose gel electrophoresis. Ladder visualized by ethidium bromide staining on a 0.8% TAE agarose gel. Mass values are for 0.5 µg/lane.

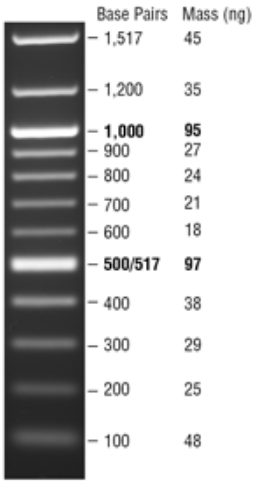


**Figure 3.5:** [21] Quick-Load Purple 100 bp DNA Ladder (New England Biolabs) for agarose gel electrophoresis. Ladder visualized by ethidium bromide staining on a 1.3% TAE agarose gel. Mass values are for 0.5 µg/lane.

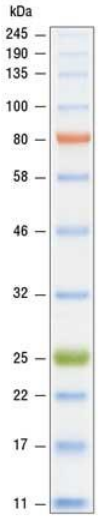


**Figure 3.6:** [22] Color Prestained Protein Standard, Broad Range (New England Biolabs) for SDS-PAGE.

[17] http://www.bio-rad.com/de-at/sku/1610373-precision-plus-protein-all-blue-prestained-protein-standards, 2016.
[18] http://tools.thermofisher.com/content/sfs/manuals/MAN0013006_GeneRuler_1kb_DNALadder_RTU_250ug_UG.pdf
[19] http://www.thermofisher.com/order/catalog/product/15628019, 2016
[20] https://www.neb.com/products/n0552-quick-load-purple-1-kb-dna-ladder,2016
[21] https://www.neb.com/products/n0551-quick-load-purple-100-bp-dna-ladder, 2016
[22] https://www.neb.com/products/p7712-color-prestained-protein-standard-broad-range-11-245-kda, 2016

## 3.9 Lentiviral transduction

| | |
|---|---|
| Lenti-X Tet-Off Advanced Inducible Expression System | Clontech |

## 3.10 Quantification of DNA concentration

| | |
|---|---|
| NanoDrop ND-1000 spectrophotometer | Peqlab |

## 3.11 Quantification of protein concentration

| | |
|---|---|
| Bradford Protein Assay | BioRad |
| BCA Protein Assay | Thermo Fisher Scientific |

## 3.12 Western blot analysis

| | |
|---|---|
| Pierce ECL Plus Western blotting Substrate | Thermo Fisher Scientific |
| Clarity Western ECL Blotting Substrate | BioRad |
| Roti-PVDF Membrane | Carl Roth GmbH |
| Amersham Hyperfilm ECL (8 x 10") | GE Healthcare |
| CL-XPosure Film | Thermo Fisher Scientific |
| ChemiDoc Touch Imaging System | BioRad |

## 3.13 Primers, oligonucleotides and synthetic DNA-constructs

Synthetic DNA-constructs, oligonucleotides (>80 bp) as well as primers for molecular cloning and site-directed mutagenesis were purchased from Eurofins Genomics (Table 3.1 and Table 3.2). Primers for DNA sequencing were purchased from Invitrogen (Table 3.3).

**Table 3.1: Primers for molecular cloning and mutagenesis**. Recognition sites for restriction enzymes are underlined. Bases in primers that introduce point mutations are shaded in grey.

| Primer name | Sequence |
|---|---|
| hCERS3_BamHI_fw | 5′ AGC GGATCC CTT CAC ACC ACT GCC AGA AGA G 3′ |
| hCERS3_EcoRI_rv | 5′ AGC GAATTC CTA ATG GCC ATG CTG GCC 3′ |
| hCERS3_XbaI_fw | 5′ AGC TCTAGA ATG CTT CAC ACC ACT GCC AGA AGA G 3′ |
| hCERS3_FLAG_MluI_rev | 5′ AGC ACGCGT CTA CTT GTC ATC GTC GTC CTT GTA ATC ATG GCC ATG CTG GCC 3′ |
| hCERS3_3F2A_MluI_rev | 5′ AGC ACGCGT CTA ATG GCC ATG CTG GCC 3′ |
| hELOVL4_BamHI_fw | 5′ AGC GGATCC GGG CTC CTG GAC TCG GAG 3′ |
| hELOVL4_XhoI_rv | 5′ AGC CTCGAG TTA ATC TCC TTT TGC TTT TCC ATT TTT C 3′ |
| hELOVL4_BamHI_2_fw | 5′ AGC GGATCC GGG CTC CTG GAC TCG 3′ |
| hELOVL4_XhoI_2_rv | 5′ AGC CTCGAG TTA ATC TCC TTT TGC TTT TCC 3′ |
| hELOVL4_EcoRI_rv | 5′ AGC GAATTC AAC TGG GCT CCA AAA AAT GCT TGT CCT CCT GCA ACC C 3′ |
| hELOVL4_EcoRI_fw | 5′ GC CCA GTT GAATTC CTT TAT C 3′ |
| hELOVL4_XmaI_fw | 5′ AGC CCCGGG ATG GGG CTC CTG GAC TCG 3′ |
| PCMV_SalI_fw | 5′ A CGC GTCGAC AAG CTT GGG AGT TCC GC 3′ |
| PCMV_BamHI_rv | 5′ GC GGATCC TCT AGT AGA GTC GGT GTC TTC TAT G 3′ |
| IRES2_fw | 5′ AGT GGCGGCCGCTCGAGTATCGAT GCC CCT CTC CCT CCC 3′ |
| IRES2_rv | 5′ GCGA ACGCGTCTAGACCCGGG CCA TAT TAT CAT CGT GTT TTT CAA AGG 3′ |
| pBK_4278CG_fw | 5′ ACT TTC CAC AGC TGG TTG CTG ACT AAT TG 3′ |
| pBK_4278CG_rv | 5′ CCC CAG GCT CCC CAG CAG 3′ |
| Neo_EcoRI_rv | 5′ GC GAATTC TGA GGC GGA AAG AAC CAG C 3′ |
| Neo_SexAI_fw | 5′ ATC ACCAGGT CAG AAG AAC TCG TCA AGA AGG C 3′ |
| mPnpla1_5‘_NotI_fw | 5′ ACG GCGGCCGC CCACC ATG GAC GAA CAG GTG TTC AAA G 3′ |
| mPnpla1_5‘_ClaI_rv | 5′ TGC ATCGAT TTA ATG ATG ATG ATG ATG ATG GGA GTT CTG GCC ACT CAC TC 3′ |
| 5’hP1_NotI_fw | 5′ AAC GCGGCCGC CCACC ATG GAA GAA CAG GTG TTC AAG GGG 3′ |
| 5’hP1_P2A_XhoI_rv | 5′ ACG CTCGAG ATC TTG TCA TCG TCG TCC TTG TAA TCC TGC ACT TTG CTG CTT GG 3′ |
| 5’ hP1_3F2A_XhoI_rv | 5′ ACG CTCGAG ATC TGC ACT TTG CTG CTT GG 3′ |

| | |
|---|---|
| CYP_XmaI_fw | 5′ ATA CCCGGG CAA TGC TGC CCA TCA CAG ACC 3′ |
| CYP_XbaI_rv | 5′ ATA TCTAGA ATC AAT GAT GAT GAT GAT GAT GGG CCC GCG GAG G 3′ |
| CYP_XbaI_fw | 5′ AGC TCTAGA ATG CTG CCC ATC ACA GAC CG 3′ |
| CYP_FLAG_MluI_rv | 5′ AGC ACGCGT TCA CTT GTC ATC GTC GTC CTT GTA ATC GGC CCG CGG AGG 3′ |
| hCYP_NotI_fw | 5′ AAC GCGGCCGC CCA CCA TGC TGC CCA TCA CAG ACC G 3′ |
| 5' hCYP_ 3F2A_XhoI_rv | 5′ ACG CTCGAG ATG GCC CGC GGA GG 3′ |
| YFP_NotI_fw | 5′ AAC GCGGCCGC CAC CAT GGT GAG C 3′ |
| YFP_ClaI_rv | 5′ AGC ATCGAT GGT ACC GTC GAC TGC AGA ATT C 3′ |
| LacZ_XmaI_fw | 5′ AGC CCCGGG ATG GAT CCC GTC GTT TTA CAA CG 3′ |
| BGH_MluI_rv | 5′ AGC ACGCGT AGA AGG CAC AGT CGA GGC 3′ |

**Table 3.2: Oligonucleotides (>80 bp) and synthetic DNA-constructs for molecular cloning.** Recognition sites for restriction enzymes are underlined.

| Oligo name | Sequence |
|---|---|
| P2A_ClaI_fw | 5′ TGC ATCGAT GGA AGC GGA GCT ACT AAC TTC AGC CTG CTG AAG CAG GCT GGA GAC GTG GAG GAG AAC CCT GGA CCT AGA CCCGGG TAT 3′ |
| P2A_XmaI_rv | 5′ ATA CCCGGG TCT AGG TCC AGG GTT CTC CTC CAC GTC TCC AGC CTG CTT CAG CAG GCT GAA GTT AGT AGC TCC GCT TCC ATCGAT GCA 3′ |
| 3FP2A3F-insert (synthesized oligo in a pEX-A2 vector, Eurofins Genomics) | 5′ T ATCGAT GAC TAC AAA GAC CAT GAC GGT GAT TAT AAA GAT CAT GAC ATC GAC TAC AAG GAT GAC GAT GAC AAG GGA AGC GGA GCT ACT AAC TTC AGC CTG CTG AAG CAG GCT GGA GAC GTG GAG GAG AAC CCT GGA CCT GAC TAC AAA GAC CAT GAC GGT GAT TAT AAA GAT CAT GAC ATC GAC TAC AAG GAT GAC GAT GAC AAG CCCGGG 3′ |

**Table 3.3: Primers for DNA-sequencing.**

| Primer name | Sequence |
|---|---|
| T7_fw | 5′ TAA TAC GAC TCA CTA TAG G 3′ |
| BGH_rv | 5′ TAG AAG GCA CAG TCG AGG 3′ |
| qRT_ELOVL4_fw | 5′ GAG CCG GGT AGT GTC CTA AAC 3′ |
| pLVX_Tight_Puro_rv | 5′ TCA CGT CCT GCA CGA CG 3′ |
| Seq_PCMV_fw | 5′ GAG CTC GTT TAG TGA ACC GTC 3′ |
| Neo1493_fw | 5′ GCA GCG CAT CGC CTT CTA TC 3′ |
| Seq_IRES_rv | 5′ CTT ATT CCA AGC GGC TTC G 3′ |
| Seq_IRES_fw | 5′ CCT CGG TGC ACA TGC TTT AC 3′ |
| qRT_CERS3_rv | 5′ GAC TCC TAA ACC ATC TTT CCA CC 3′ |
| qRT_CYP4F22_rv | 5′ TAG TGG TGC AAG CGA TAC TGG 3′ |
| qRT_P1_fw | 5′ CGA CTT CCG CAT GTT CAA CTG 3′ |

## 3.14 Antibodies

Antibodies that were used in this study and their specific reaction conditions are listed in Table 3.4.

**Table 3.4: Used antibodies for Western blot analysis.** Dilutions, buffers, incubation times, temperatures and secondary antibodies for detection of the respective primary antibodies are listed. Shown percentages of skimmed dry milk in 1x TST are given in (w/v). Secondary antibodies: horseradish peroxidase (HRP)-conjugated sheep anti-mouse IgG (GE Healthcare), HRP-conjugated goat anti-rabbit IgG (Cell Signaling).

| Primary antibody | Blocking | Primary antibody | Secondary antibody |
|---|---|---|---|
| Anti-His (N-term) (Amersham) | 10% skimmed dry milk<br>1x TST<br>1 hour, RT | 1:5000<br>2% skimmed dry milk<br>1x TST<br>1 hour, RT | 1:10,000 α-mouse HRP<br>3% skimmed dry milk<br>1x TST<br>1 hour, RT |
| Anti-His (C-term) (Reliatech) | 10% skimmed dry milk<br>1x TST<br>1 hour, RT | 1:1000<br>3% skimmed dry milk<br>1x TST<br>1 hour, RT | 1:10,000 α-rabbit IgG HRP<br>3% skimmed dry milk<br>1x TST<br>1 hour, RT |
| Anti-FLAG M2-Peroxidase (HRP) (Sigma) | 10% skimmed dry milk<br>1x TST<br>1 hour, RT | 1:5000<br>5% skimmed dry milk<br>1x TST<br>1 hour, RT | not necessary |
| Anti-FLAG M2 (Sigma) | 10% skimmed dry milk<br>1x TST<br>1 hour, RT | 1:5000<br>5% skimmed dry milk<br>1x TST<br>1 hour, RT | 1:10,000 α-mouse HRP<br>3% skimmed dry milk<br>1x TST<br>1 hour, RT |
| Anti-β-Actin (Santa Cruz) | 10% skimmed dry milk<br>1x TST<br>1 hour, RT | 1:1000<br>3% skimmed dry milk<br>1x TST<br>1 hour, RT | 1:10,000 α-mouse HRP<br>3% skimmed dry milk<br>1x TST<br>1 hour, RT |

## 3.15 Plasmids

### 3.15.1 pcDNA4_HisMaxC

For molecular cloning of target genes and transient overexpression of recombinant proteins in mammalian cell lines, the pcDNA4_HisMaxC vector (Invitrogen) was used. A vector map of pcDNA4_HisMax A, B and C is shown in Figure 3.7.

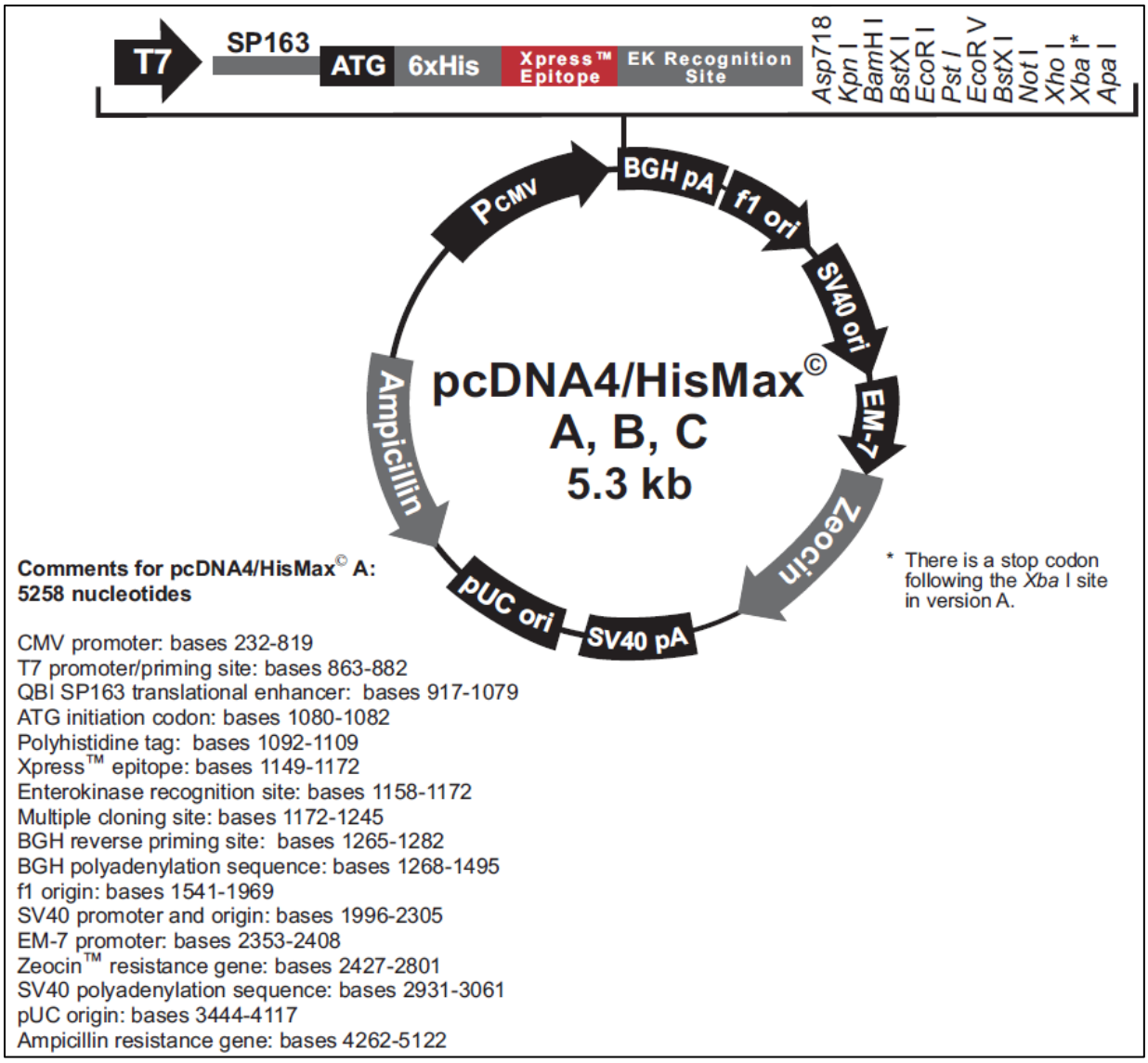


**Figure 3.7: Vector map of mammalian expression vector pcDNA4_HisMax A, B and C[23].** The three different versions slightly vary in their multiple cloning sites (MCS). In this study, only version C was used. The vector contains an ampicillin resistance gene for positive selection of bacteria (e.g. *E.coli*) and a zeocin resistance gene for positive selection of mammalian cells carrying the plasmid. A human cytomegalovirus immediate-early (CMV) promoter allows high-level expression of target genes in a wide range of mammalian cells. Recombinant proteins expressed with this vector are fused with an N-terminal hexahistidine tag, which allows immunodetection and purification.

[23] https://tools.thermofisher.com/content/sfs/manuals/pcdna4hismax_man.pdf ; March 2017

### 3.15.2 pLVX_Tight_Puro

The tetracycline (Tet)-inducible, lentiviral expression vector pLVX_Tight_Puro was provided with the Lenti-X Tet-Off Advanced Inducible Expression System (Clontech) and was used for the construction of bicistronic vectors. A vector map and the multiple cloning site (MCS) of pLVX_Tight_Puro are shown in Figure 3.8.

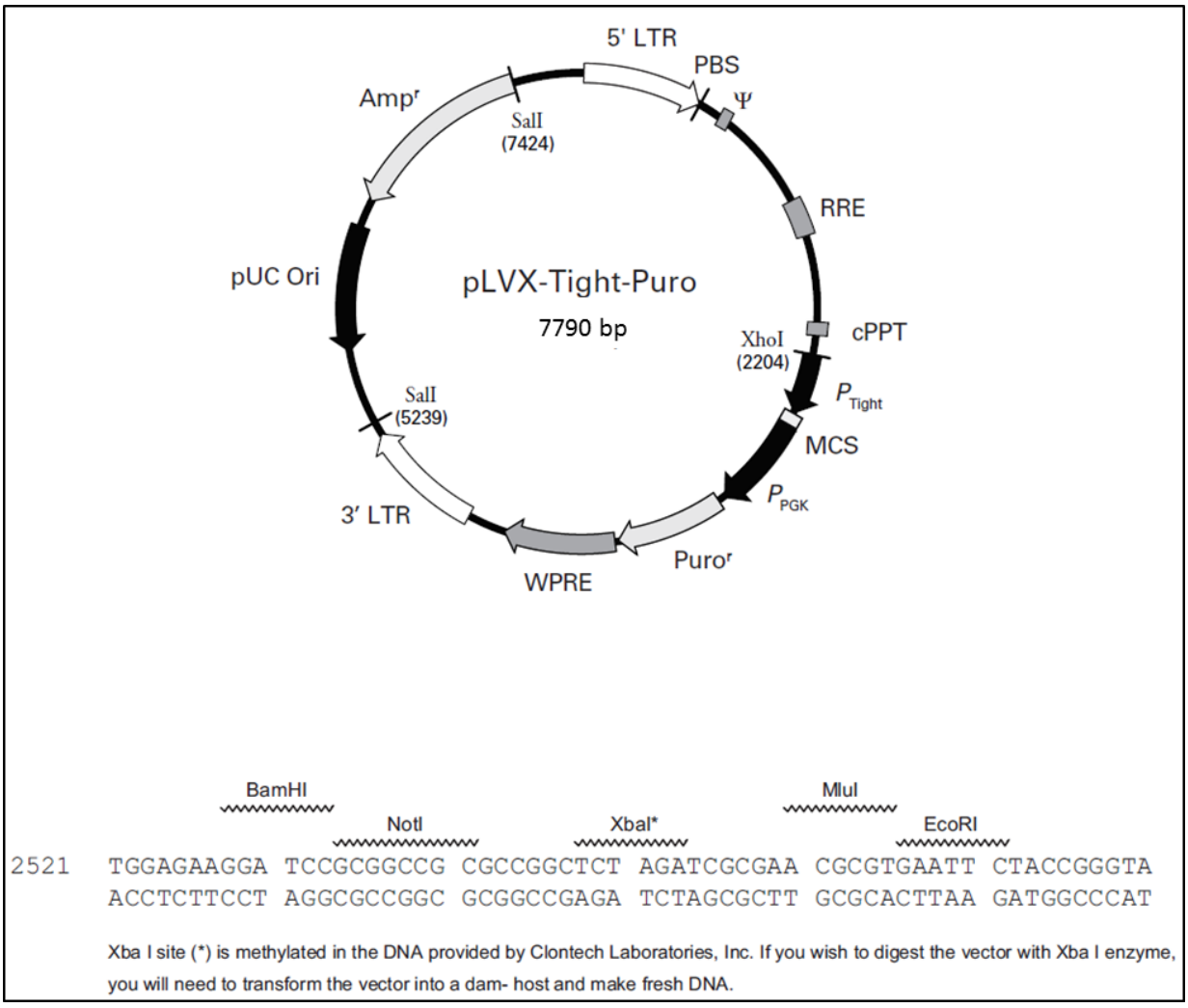


**Figure 3.8: Vector map and MCS of tetracycline (Tet)-inducible, lentiviral expression vector pLVX_Tight_Puro[24].** The vector contains an ampicillin resistance gene (Ampʳ) for positive selection of bacteria (e.g. *E.coli*) carrying the plasmid and allows production of infectious lentiviral particles. The region between the 5' and 3' LTR of the plasmid can be stably integrated into the genome of transduced mammalian cells and a puromycin resistance gene (Puroʳ) enables positive selection. The $P_{Tight}$ promoter only allows expression of a downstream gene, when a specific transactivator (tTA-Advanced) binds to the promoters tetracycline response element. The gene for tTA-Advanced is encoded on the pLVX_Tet-Off_ Advanced plasmid (Clontech, not shown). By adding doxycycline to the cell culture growth medium expression of genes under control of the tTA-$P_{Tight}$ complex can be switched off ("Tet-Off system").

[24] http://www.clontech.com/xxclt_ibcGetAttachment.jsp?cItemId=43886&minisite=10024&secItmId=21621 ; March 2017

### 3.15.3 pLVX_IRES_Puro

The bicistronic lentiviral expression vector pLVX_IRES_Puro (Clontech) was used as a template for amplification of the constitutively active human cytomegalovirus immediate early promoter ($P_{CMV\ IE}$) and an internal ribosomal entry site (IRES). A vector map and the MCS of pLVX_IRES_Puro are shown in Figure 3.9.

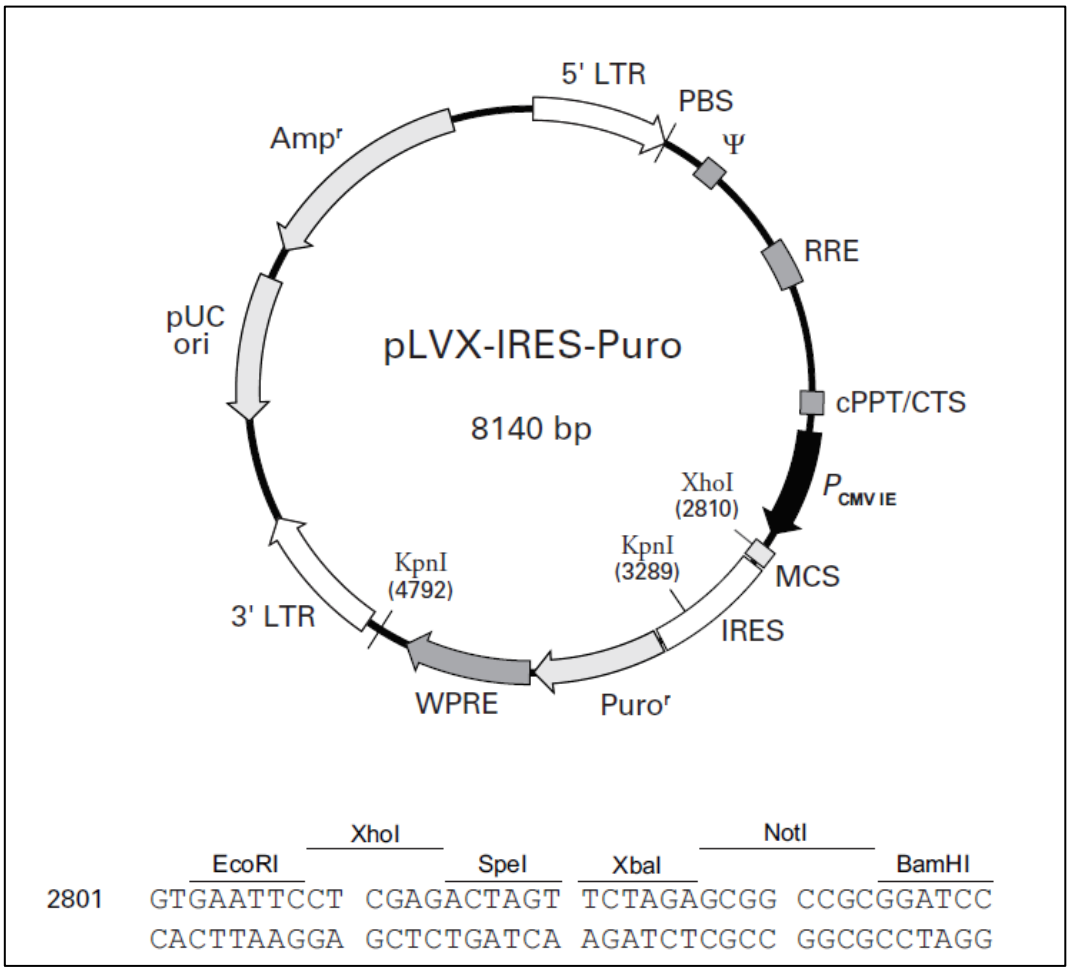


**Figure 3.9: Vector map and MCS of bicistronic lentiviral expression vector pLVX_IRES_Puro (Clontech)[25].** The vector contains an ampicillin resistance gene (Ampʳ) for positive selection of bacteria (e.g. *E.coli*) and a puromycin resistance gene (Puroʳ) for positive selection of mammalian cells carrying the plasmid. As the $P_{CMV\ IE}$ promoter is constitutively active, the plasmid is suitable for transient overexpression of recombinant proteins.

[25] http://www.clontech.com/xxclt_ibcGetAttachment.jsp?cItemId=46006 ; March 2017

### 3.15.4 pBK-CMV

The phagemid expression vector pBK-CMV (Agilent Technologies) was used as a template for amplification of the SV40 promoter and the combined neomycin/kanamycin resistance gene cassette. A vector map and the MCS of pBK-CMV are shown in Figure 3.10.

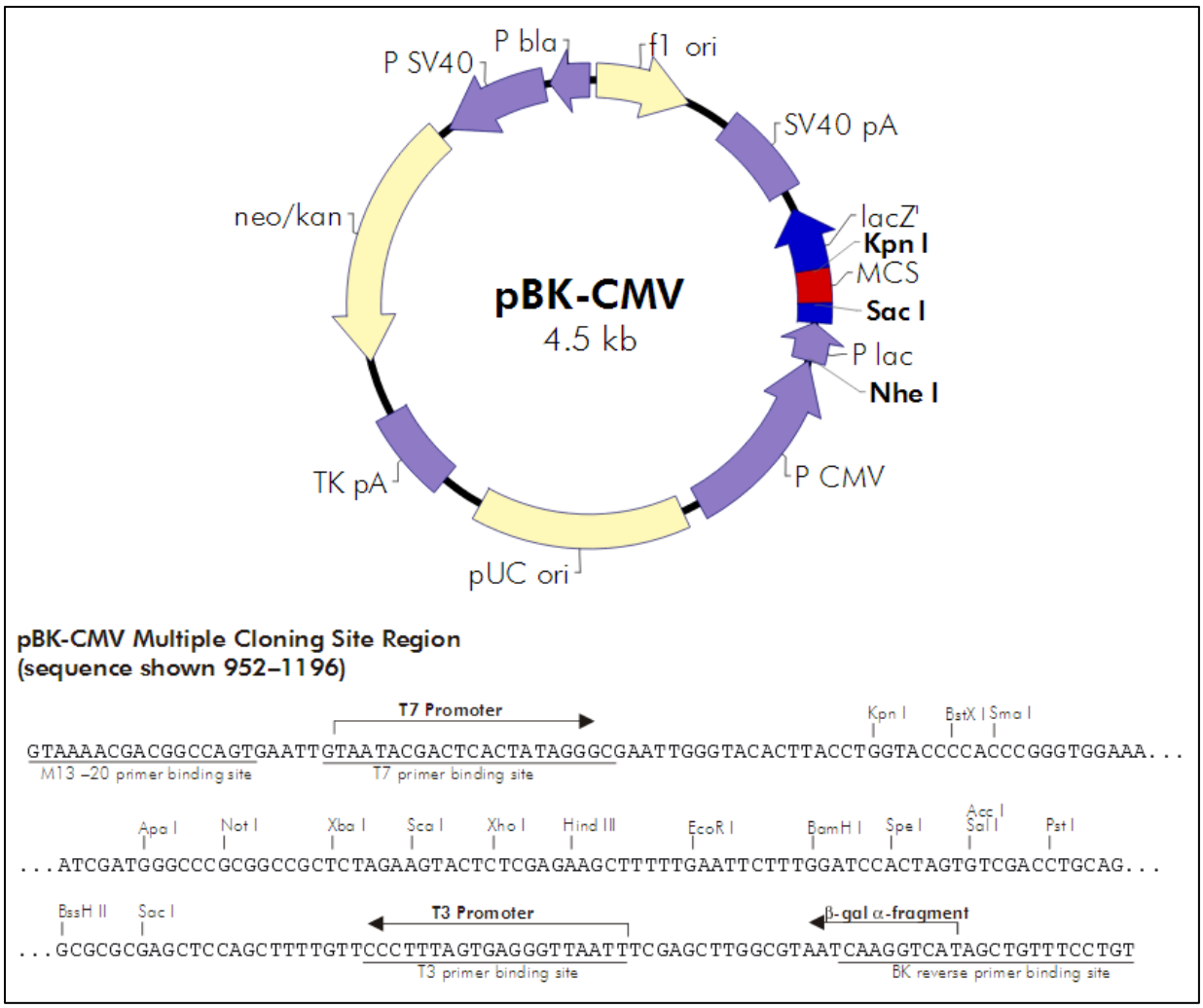


**Figure 3.10: Vector map and MCS of phagemid expression vector pBK-CMV (Agilent Technologies)[26].** The vector contains a combined neomycin/kanamycin resistance gene that allows positive selection of prokaryotic and eukaryotic cells carrying the plasmid. The vector is suitable for overexpression of recombinant proteins in both prokaryotic and eukaryotic cells.

[26] http://www.chem-agilent.com/pdf/strata/212209.pdf ; March 2017

# 4 Methods

## 4.1 Molecular cloning

### 4.1.1 Agarose gel electrophoresis and extraction of DNA fragments

For separation of DNA fragments by size and preparation of DNA fragments for ligation, agarose gel electrophoresis was performed. Depending on the expected size of the DNA fragments, gels consisted of 1% or 2% (w/v) UltraPure Agarose (Thermo Fisher Scientific, Waltham, MA, USA) in 1x TAE buffer. For detection of DNA fragments under UV-light, the gels contained 0.5 µg/ml ethidium bromide (EtBr). Samples were loaded onto the gels using 6x Purple Gel Loading Dye (New England Biolabs, Ipswich, MA, USA). Used molecular weight standards are listed in section 0. 1x TAE containing 0.25 µg/ml EtBr was used as running buffer. Electrophoresis was performed at 90 V for 30-45 minutes. For documentation, an UV-transilluminator (ImageQuant 300 Imager, GE Healthcare) was used. Desired DNA fragments were sliced from the gel with a sterile razor blade and purified by using the E.Z.N.A. MicroElute Gel Extraction Kit (Omega Biotek, Norcross, GA, USA) according to the manufacturer's instructions.

### 4.1.2 Site-directed mutagenesis

DNA sequences were point-mutated using the Q5 Site-Directed Mutagenesis Kit and Q5 Hot Start High-Fidelity DNA Polymerase (both New England Biolabs) according to the manufacturer's instructions. Primers for mutagenesis were designed using the NEBaseChanger online tool [27]. The temperature program and reaction conditions for site-directed mutagenesis are shown in Table 4.1 and Table 4.2. Circularized PCR products were transformed into chemically competent *E. coli* as described in section 4.1.8.

**Table 4.1: Temperature program for site-directed mutagenesis by PCR using Q5 Hot Start High-Fidelity DNA Polymerase.** For optimal product yield and primer specificity, multiple PCR reactions at different annealing temperatures were performed simultaneously. Tested annealing temperatures included 61.7°C / 63.0°C / 65.0°C / 67.4°C / 69.4°C and 70.5°C. In total 30 thermal cycles were performed.

| PCR temperature program | | |
|---|---|---|
| Initial Denaturing | 98°C | 30 seconds |
| Denaturing<br>Annealing<br>Extension | 98°C<br>61-71°C<br>72°C | 10 seconds<br>25 seconds<br>25 seconds/kb |
| Final Extension<br>Cooling | 72°C<br>8°C | 2 minutes<br>forever |

[27] http://nebasechanger.neb.com/ - May 2016

**Table 4.2: Reaction conditions for site-directed mutagenesis by PCR using Q5 Hot Start High-Fidelity DNA Polymerase.**

| Components | 25 µl Reaction | Final Concentration |
|---|---|---|
| Nuclease-free $H_2O$ | 10.75 µl | - |
| 5x Q5 Reaction Buffer | 5.00 µl | 1x |
| 5x Q5 High GC Enhancer | 5.00 µl | 1x |
| 10 mM dNTPs | 1.00 µl | 0.4 mM |
| 20 µM Forward Primer | 1.00 µl | 0.8 µM |
| 20 µM Reverse Primer | 1.00 µl | 0.8 µM |
| Template Plasmid (5 ng/µl) | 1.00 µl | 0.2 ng/µl |
| Q5 DNA Polymerase (2 U/µl) | 0.25 µl | 0.02 U/µl |
| Total Volume | 25.00 µl | - |

### 4.1.3 Polymerase chain reaction (PCR)

DNA fragments for molecular cloning were amplified by PCR using Phusion High-Fidelity DNA Polymerase (Thermo Fisher Scientific, Waltham, MA, USA). Specific primers with flanking restriction enzyme recognition sites were designed using Serial Cloner 2.6 software[28]. Primer annealing temperatures were calculated using the NEB Tm Calculator online tool[29]. The reaction conditions and temperature program for PCR are shown in Table 4.3 and Table 4.4. PCR products were analyzed by agarose gel electrophoresis and extracted as described in section 4.1.1.

**Table 4.3: Reaction conditions for PCR with Phusion High-Fidelity DNA Polymerase.**

| Components | 30 µl Reaction | Final Concentration |
|---|---|---|
| Nuclease-free $H_2O$ | 15.70 µl | - |
| 5x GC Buffer | 6.00 µl | 1x |
| 10 mM dNTPs | 2.00 µl | 0.67 mM |
| 25 mM $MgCl_2$ | 1.00 µl | 0.83 mM |
| 20 µM Forward Primer | 2.00 µl | 1.33 µM |
| 20 µM Reverse Primer | 2.00 µl | 1.33 µM |
| Template Plasmid (5 ng/µl) or cDNA | 1.00 µl | 0.17 ng/µl |
| Phusion DNA Polymerase (2 U/µl) | 0,30 µl | 0.02 U/µl |
| Total Volume | 30.00 µl | - |

[28] http://serialbasics.free.fr/Serial_Cloner.html - May 2016
[29] http://tmcalculator.neb.com/#!/ - May 2016

**Table 4.4: Temperature program for PCR using Phusion High-Fidelity DNA Polymerase.**
To ensure optimal product yield and primer specificity, multiple PCR reactions at different annealing temperatures were performed simultaneously. Tested annealing temperatures included 60.7°C / 62.0°C / 64.0°C / 66.4°C / 68.4°C and 69.5°C. In total 35 thermal cycles were performed.

| PCR temperature program | | |
|---|---|---|
| Initial Denaturing | 98°C | 2 minutes |
| Denaturing<br>Annealing<br>Extension | 98°C<br>60-70°C<br>72°C | 30 seconds<br>30 seconds<br>25 seconds/kb |
| Final Extension<br>Cooling | 72°C<br>8°C | 5 minutes<br>forever |

### 4.1.4 Hybridization of oligonucleotides

For generation of double stranded DNA fragments (>80 bp), equal volumes of complementary single stranded oligonucleotides (20 µM each) were mixed and denatured in a heat block at 95°C for 5 minutes. Then the heat block was removed from its basis and the DNA solution was allowed to slowly cool down to room temperature.

### 4.1.5 Restriction enzyme digestion

For preparation of DNA fragments for ligation or verification of successful molecular cloning restriction enzyme (RE) digestion with sticky end-producing type II REs was performed. REs and respective buffers were purchased from New England Biolabs (see section 0). Optimal buffer conditions for co-digestion with two REs and conditions for heat inactivation were determined using the Double Digest Finder online tool[30]. To prevent re-circularization of digested vector DNA during ligation, 5'-phosphate groups were removed by incubation with calf intestinal alkaline phosphatase (CIP). Reaction conditions for digestion of vector DNA or PCR products are shown in Table 4.5 and Table 4.6.

**Table 4.5: Reaction conditions for RE digestion and dephosphorylation of vector DNA.** For single-digestions the second RE was omitted and the volume of $H_2O$ adapted accordingly. The reaction mix was incubated at 37°C for 2 hours. Next, REs were heat-inactivated at 65 or 80°C for 20 minutes. For removal of 5' phosphates 0.16 U/µl CIP were added and the mixture was incubated at 37°C for 1 h. Digested DNA was separated by agarose gel electrophoresis and purified using the MicroElute Gel Extraction Kit (Omega Biotek, Norcross, GA, USA) according to the manufacturer's instructions.

| Components | 60 µl Reaction |
|---|---|
| Nuclease-free $H_2O$ | 46.00 µl |
| 10x NEBuffer 3.1, 2.1 or CutSmart | 6.00 µl |
| Plasmid (500 ng/µl) | 4.00 µl |
| Restriction Enzyme #1 (2 U/µl) | 2.00 µl |
| Restriction Enzyme #2 (2 U/µl) | 2.00 µl |
| Total Volume | 60.00 µl |

[30] https://www.neb.com/tools-and-resources/interactive-tools/double-digest-finder - May 2016

**Table 4.6: Reaction conditions for RE digestion of PCR products and oligonucleotides.** The reaction mix was incubated at 37°C for 2 hours. Next, REs were heat-inactivated at 65 or 80°C for 20 minutes. Digested DNA was purified with the MicroElute Gel Extraction Kit (Omega Biotek, Norcross, GA, USA) according to the manufacturer's instructions.

| Components | 30 µl Reaction |
|---|---|
| Nuclease-free $H_2O$ | 5.00 µl |
| 10x NEBuffer 3.1, 2.1 or CutSmart | 3.00 µl |
| PCR product or hybridized oligo | 20.00 µl |
| Restriction Enzyme #1 (2 U/µl) | 1.00 µl |
| Restriction Enzyme #2 (2 U/µl) | 1.00 µl |
| Total Volume | 30.00 µl |

Methylation of DNA by Dam methylase or Dcm methyltransferase can prevent recognition of some RE sequences (e.g. SexAI, ClaI, …) [55–58]. To allow cleavage of such sites, vector DNA was transformed into *dam-/dcm-* Competent *E. Coli* (New England Biolabs) and isolated by Miniprep (see sections 4.1.8 and 4.1.9).

### 4.1.6 Blunting of sticky end overhangs

To delete unique RE sites vector DNA was digested with the respective RE (see section 4.1.5) to generate linearized DNA with 3' or 5' overhangs. The overhangs were either removed or filled in by the 3'→ 5' exonuclease activity or the DNA polymerase activity of DNA Polymerase I, Large (Klenow) Fragment (New England Biolabs). Conditions for the reaction are shown in Table 4.7. Subsequently, the blunted plasmid DNA was circularized by ligation with T4 DNA ligase, transformed into chemically competent *E. coli* and extracted by Miniprep (see sections 4.1.8 - 4.1.9).

**Table 4.7: Reaction conditions for blunting of linearized plasmid DNA with sticky end overhangs.** The reaction mix was incubated at 25°C and 350 rpm for 15 minutes. The reaction was stopped by adding EDTA to a final concentration of 10 mM and heating at 75°C for 20 minutes. Resulting blunted vector DNA was purified by preparative agarose gel electrophoresis before ligation and transformation into *E. coli.*

| Components | 70 µl Reaction |
|---|---|
| 2 µg linearized & heat inactivated plasmid (see Table 4.5) | 60.00 µl |
| 10x NEBuffer 3.1, 2.1 or CutSmart | 1.00 µl |
| 10 mM dNTPs | 1.00 µl |
| DNA Pol. I, Large Klenow Frag. (5 U /µl) | 1.00 µl |
| Total Volume | 70.00 µl |

### 4.1.7 Ligation of DNA fragments

For circularization of linearized blunt-end vector DNA and ligation of DNA fragments with complementary overhangs T4 DNA Ligase (New England Biolabs) was used. For efficient ligation a molar vector DNA:insert DNA ratio of approximately 1:3 was used. Reaction conditions for ligation of DNA fragments are shown in Table 4.8. After ligation, the plasmid DNA was transformed into chemically competent *E. coli* (see section 4.1.8).

**Table 4.8: Reaction conditions for ligation of DNA fragments.** For circularization of blunt-ended plasmids insert DNA was omitted and $H_2O$ volume was adapted accordingly. The reaction mixture was incubated at 25°C and 350 rpm for 3 hours. For heat inactivation of T4 DNA Ligase, the reaction mixture was incubated at 65°C for 10 minutes.

| Components | 15 µl Reaction |
|---|---|
| Nuclease-free $H_2O$ | 9.50 µl |
| 10x T4 DNA Ligase Reaction Buffer | 1.50 µl |
| Vector DNA | 2.00 µl |
| Insert DNA | 1.00 µl |
| T4 DNA Ligase (400 U/µl) | 1.00 µl |
| Total Volume | 15.00 µl |

### 4.1.8 Transformation of NEB 5-alpha or *dam-/dcm-* competent *E. coli*

For amplification plasmid DNA or ligated DNA fragments, DNA was transformed into NEB 5-alpha Competent *E. coli* (New England Biolabs, catalog nr. C2987H). To obtain unmethylated DNA, plasmid DNA was transformed into *dam-/dcm-* Competent *E. coli* (New England Biolabs, catalog nr. C2925H). Transformation was performed according to the manufacturer's instructions, except the volumes of competent cells and DNA solutions were downscaled by a factor of 4. For positive selection, transformed cells were plated on LB agar plates containing the appropriate antibiotic (100 µg/ml ampicillin or 50 µg/ml kanamycin) and incubated at 37°C overnight. For molecular cloning of *ELOVL4*, plated cells were incubated at 25°C for 72 hours, until single colonies were visible.

### 4.1.9 Colony picking and plasmid preparation

To obtain plasmid DNA from *E. coli* clones, single colonies were picked with a sterile pipette tip. The cells were streaked out on a LB agar plate and the tip was used to inoculate 3 ml of LB medium. For positive selection, LB agar plates and liquid LB medium cultures contained the appropriate antibiotic (100 µg/ml ampicillin or 50 µg/ml kanamycin). Cells on agar plates were incubated at 37°C overnight. Agar plates with cells carrying *ELOVL4*-constructs were incubated at 25°C for 72 hours, until colonies were visible. Inoculated liquid LB cultures were incubated at 37°C and 180 rpm overnight and used for plasmid preparation with the QIAprep Spin Miniprep Kit (Qiagen, Venlo, Netherlands) or the NucleoBond Xtra Midi Kit (Macherey-Nagel, Dueren, Germany), according to the manufacturer's instructions. For plasmid

preparation of *E. coli* carrying *ELOVL4*-constructs the inoculated liquid cultures were incubated at 25°C and 180 rpm for 72 hours. The concentration of purified plasmid DNA was determined by differential A260/A280 spectrophotometry with a NanoDrop ND-1000 (Peqlab, Erlangen, Germany).

### 4.1.10 Colony PCR

To verify successful cloning of oligonucleotides (>80 bp) colony PCR with FIREPol DNA Polymerase (Solis Biodyne, Tartu, Estonia) was performed. Therefore, single colonies of *E. coli* clones were picked with sterile pipette tips and streaked out on LB agar plates containing 100 µg/ml ampicillin. The remaining cells on the tips were resuspended in 50 µl nuclease free $H_2O$ and the tips were further used for inoculation of 3 ml LB overnight cultures (ONCs) containing 100 µg/ml ampicillin. The resuspended cells were denatured at 95°C for 10 minutes, cell debris was removed by short centrifugation and the supernatants were used as templates for PCR with specific primers. Positive clones were identified by a size shift of the resulting PCR product and the respective ONCs were used for plasmid preparation (see section 4.1.9). Reaction conditions and temperature program for colony PCR are shown in Table 4.9 and Table 4.10.

**Table 4.9: Reaction conditions for colony PCR using FIREPol DNA Polymerase.**

| Components | 25 µl Reaction | Final Concentration |
|---|---|---|
| Nuclease-free $H_2O$ | 12.60 µl | - |
| 10x Buffer 511 | 2.50 µl | 1x |
| 10 mM dNTPs | 1.00 µl | 0.40 mM |
| 25 mM $MgCl_2$ | 1.50 µl | 1.50 mM |
| 20 µM Forward Primer | 2.00 µl | 1.60 µM |
| 20 µM Reverse Primer | 2.00 µl | 1.60 µM |
| Template (supernatant) | 3.00 µl | - |
| FIREPol DNA Polymerase (5 U/µl) | 0,40 µl | 0.08 U/µl |
| Total Volume | 25.00 µl | - |

**Table 4.10: Temperature program for colony PCR using FIREPol DNA Polymerase.** The optimal annealing temperatures of used primers were determined in a pre-experiment by performing multiple colony PCR reactions at different annealing temperatures. Tested annealing temperatures included 56.7°C / 58.0°C / 60.0°C / 62.4°C / 64.3°C and 65.5°C. For the actual experiments, the determined optimal annealing temperature was used. In total 30 thermal cycles were performed.

| PCR temperature program | | |
|---|---|---|
| Initial Denaturing | 95°C | 3 minutes |
| Denaturing<br>Annealing<br>Extension | 95°C<br>56-66°C<br>72°C | 30 seconds<br>60 seconds<br>30 seconds |
| Final Extension<br>Cooling | 72°C<br>8°C | 5 minutes<br>forever |

### 4.1.11 DNA sequencing

Cloned DNA fragments that were confirmed by RE digestion (see section 4.1.5) or colony PCR (see section 4.1.10) were further verified by DNA sequencing at Microsynth AG (Wien, Austria). The sequencing reactions were prepared according to the service providers instructions. Used primers for sequencing are listed in Table 3.3. Results were evaluated using Serial Cloner 2.6[31] and Chromas 2.5.0 software[32].

### 4.1.12 Preparation of bacterial glycerol stocks

For long time storage of *E. coli* clones carrying verified plasmids bacterial glycerol stocks were prepared. Therefore single colonies were picked and used for inoculation of 3 ml LB medium ONCs (containing 100 µg/ml ampicillin or 50 µg/ml kanamycin). The cells were incubated at 37°C and 180 rpm for 18 hours. The bacterial suspensions were then transferred to cryovials and mixed with sterile 40% (v/v) glycerol, to a final concentration of 15% glycerol. The bacterial glycerol stocks were immediately frozen at -80°C.

## 4.2 Cell culture

Mammalian cell lines were purchased from ATCC and CLS GmbH (see section 0). The cells were cultivated in 25 cm², 75 cm² or 175 cm² cell culture flasks (Greiner Bio-One GmbH, Frickenhausen, Germany) at 37°C, 5% $CO_2$ and 95% air humidity. As standard growth medium Dulbecco's Modified Eagle's Medium - high glucose (Gibco/Thermo Fisher Scientific) supplemented with 10% fetal calf serum (FCS), 100 µg/ml Penicillin and 100 µg/ml Streptomycin (DMEM +/+) was used. For passaging the cells were washed with 1x PBS and dissociated with 0.05% Trypsin-EDTA (Gibco/Thermo Fisher Scientific, Waltham, MA, USA) by incubation at 37°C for 3 – 8 minutes (depending on the cell line). For assessment of cell viability and cell counting a CASY-1 cell counter (Schärfe System, Reutlingen, Germany) was used.

**Long time storage:** For long time storage, the cells were grown to 80% confluency, split at a 1:4 ratio, resuspended in 1x Freeze Medium (DMEM supplemented with 10% DMSO, 15% FCS, 100 µg/ml Penicillin and 100 µg/ml Streptomycin) and transferred to cryogenic vials. The vials were placed in a freezing container and put at -80°C for 24 hours. The frozen cell stocks were then cryopreserved by immersion in liquid nitrogen.

**Metafectene mediated transfection:** For transfection of mammalian cells, Metafectene (Biontex Laboratories GmbH, München/Laim, Germany) was used according to the

[31] http://serialbasics.free.fr/Serial_Cloner.html - May 2016
[32] http://technelysium.com.au/wp/chromas/ - May 2016

manufacturer's instructions[33]. Depending on the cell line, 150,000 or 300,000 cells per 6-well were cultivated overnight and the medium was replaced with 1 ml fresh DMEM +/+. Depending on the expected expression levels, 0.5 µg – 2.5 µg of plasmid DNA in a total volume of 110 µl DMEM without additives (DMEM -/-) containing 4.54% (v/v) Metafectene were added to the cells. To prevent toxicity, the transfection mixture was removed 4 hours post-transfection and replaced with fresh DMEM +/+.

**Preparation of samples for Western blot analysis:** To obtain cell lysates for Western blot analysis, cell pellets were washed three times with 1x PBS (4°C), suspended in RIPA buffer (containing 1x protease inhibitor mix; "+Pi", see section 3.1) or HSL buffer (+Pi), lysed by sonication on ice (2 times for 15 seconds, amplitude 2) and centrifuged (1000 g, 4°C, 15 minutes) for removal of cell debris. Alternatively, adherent cells in 6-well cell culture plates were washed three times with 1x PBS (4°C) and harvested in 1x SDS loading buffer (see section 3.1) by scraping with a pipette tip.

## 4.3 Lentiviral transduction

Cell lines stably overexpressing target genes were established using the Lenti-X Tet-Off Advanced Inducible Expression System (Takara Bio Europe, Saint-Germain-en-Laye, France) according to the manufacturer's instructions. For production of infectious lentiviral particles in HEK-293T cells, the manufacturer's protocol was scaled down by a factor of 6 and performed in 6-well culture dishes. For transduction of target cells with a single lentivirus, 1 ml of infectious virus-supernatant and 2 ml DMEM +/+ (containing 12 µg/ml Polybrene, final concentration 8 µg/ml) were used per 6-well. For co-transduction with two lentiviruses, 500 µl of each infectious virus-supernatant were used accordingly. To enhance transduction efficiency, the cells were centrifuged at 32°C and 1200 g for 1 hour ("spinocculation"). 24 hours post-transduction the medium was replaced with fresh DMEM +/+, containing antibiotics for positive selection of transduced cells (see Table 4.11). To avoid loss of expression, established stable cell lines were cultivated in DMEM +/+ containing the respective antibiotic(s).

**Table 4.11: Antibiotic concentrations of growth medium for positive selection of transduced cells.**

| Cell line | Selection of single-transduced cells: | Selection of co-transduced cells: |
|---|---|---|
| **HEK-293** | 1.5 µg/ml puromycin | 1.5 µg/ml puromycin<br>800 µg/ml G418 |
| **HaCaT** | 1.0 µg/ml puromycin | 1.0 µg/ml puromycin<br>1.0 mg/ml G418 |

[33] http://www.biontex.com/con_4_6_4/cms/upload/pdf/Manual_METAFECTENE_en.pdf, November 2016.

## 4.4 Quantification of protein concentration

To determine the protein concentration of cell lysates that were prepared with detergent-containing buffers (e.g. RIPA buffer), the BCA Protein Assay (Thermo Fisher Scientific) was used according to the manufacturer's instructions. As a protein standard, bovine serum albumin (BSA) was used. Samples were measured in technical replicates, using a Biotrak II Plate Reader (Amersham plc, Amersham, UK). For protein quantification of cell lysates that were prepared with non-detergent buffers (e.g. HSL buffer), the Bradford Protein Assay (Bio-Rad Laboratories, Hercules, CA, USA) was used accordingly.

## 4.5 SDS-PAGE and Western blot analysis

**SDS-PAGE:** Proteins of cell lysates were separated according to their molecular size by discontinuous denaturing sodium dodecyl sulfate polyacrylamide gel electrophoresis (SDS-PAGE) with resolving gels containing 10% acrylamide/bis and 1x Tris-Glycine buffer. To load samples onto gels, cell lysates were mixed with 4x SDS-PAGE loading dye to a final concentration of 1x and denatured at 95°C for 10 minutes. Gel electrophoresis was performed at 25 mA per gel for 70 minutes. Used protein size standards are listed in section 3.8.

**Western blot analysis:** After electrophoresis the proteins were transferred onto a polyvinylidene difluoride membrane (Roti-PVDF, pore size 0.45 µm; Roth GmbH, Karlsruhe, Germany) by wet electroblotting with CAPS buffer at 200 mA for 70 minutes. For blocking of unspecific epitopes the membrane was incubated with 10% (w/v) skimmed dry milk (Roth) in 1x TST at room temperature for 1 hour. For immunodetection of specific proteins the blocked membrane was then incubated with different primary antibodies and HRP-conjugated secondary antibodies (see section 3.14 for details). To increase specificity the membrane was washed with 1x TST after incubation with the primary and secondary antibody respectively. For analysis, the membrane was incubated with Pierce ECL Substrate (Thermo Fisher Scientific, see section 3.12) for 1 minute and immune-labeled proteins were detected either by exposure to a light sensitive film or by using a ChemiDoc Touch Imaging System (BioRad).

## 4.6 ß-gal assay and fluorescence microscopy

The ß-gal assay is based on the ß-galactosidase-catalyzed hydrolysis of X-gal (5-bromo-4-chloro-3-indolyl-β-D-galactopyranoside) to galactose and 5-bromo-4-chloro-3-hydroxyindole. The subsequent dimerization and oxidation of 5-bromo-4-chloro-3-hydroxyindole results in the formation of 5,5'-dibromo-4,4'-dichloro-indigo, an insoluble, bright blue colored product. A schematic of this reaction is shown in Figure 4.1.

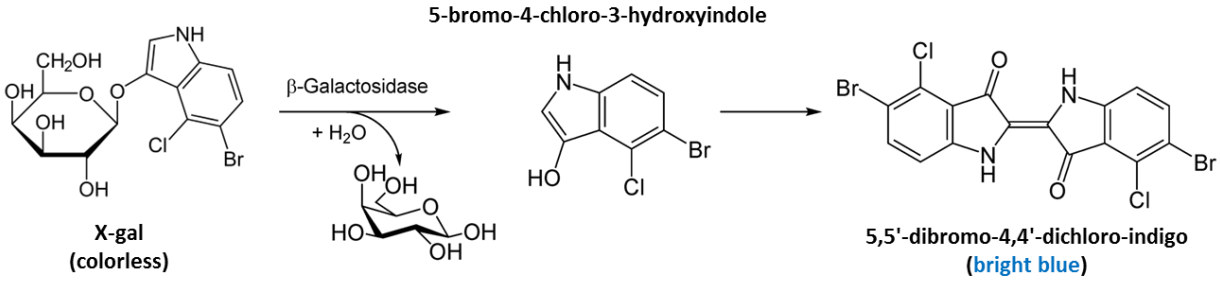


**Figure 4.1: Enzymatic hydrolysis of X-gal by ß-galactosidase.** The reaction yields 5,5'-dibromo-4,4'-dichloro-indigo, an insoluble compound with a bright blue color.

For the ß-gal assay 250,000 cells stably overexpressing both LacZ and YFP were seeded in 6-well culture dishes. After 24 hours the cells were washed with 1x PBS, fixed with 0.5% (v/v) glutaraldehyde in 1x PBS for 5 minutes, washed again and then incubated with β-gal staining solution B (see section 3.1) until staining of cells was visible. To verify expression of YFP, the cells were analyzed by fluorescence microscopy with blue light excitation at 450-490 nm using an Eclipse TE300 microscope (Nikon CEE GmbH, Wien, Austria).

## 4.7 Radiolabeling of cellular lipids

To trace sphingolipids in cells transiently or stably overexpressing multiple target enzymes radiolabeling experiments with either [$^{14}$C]linoleic acid, [$^{14}$C]palmitic acid or [3-$^{3}$H]D-erythro-sphingosine C-18 were performed. For experiments with transiently overexpressing cells 150,000 COS-7 or 1x10$^{6}$ HEK-293T were grown in 6-well cell culture dishes and co-transfected with the desired plasmids, using metafectene (see section 4.2). For experiments with stably overexpressing HaCaT, 150,000 cells were grown in 6-well culture dishes for 24 hours.

To promote lipid synthesis (especially ω-O-AcylCer synthesis), cells were cultivated in DMEM +/+ containing the following additives for 24 hours:

- 10 µM palmitic acid (PA) bound to delipidated BSA at a molar FA/BSA ratio of 3:1
- 10 µM oleic acid (OA) bound to delipidated BSA at a molar FA/BSA ratio of 3:1
- 10 µM linoleic acid (LA) bound to delipidated BSA at a molar FA/BSA ratio of 3:1
- 10 µM lignoceric acid (C24:0) in EtOH
- 10 µM nervonic acid (C24:1) in EtOH
- 10 µM cerotic acid (C26:0) in EtOH
- 1 µM sphingosine in DMSO (omitted for [$^{3}$H]sphingosine labeling experiments)

Next, radiolabeling of lipids was performed by incubating the cells with DMEM +/+ containing either 20 µM [$^{14}$C]linoleic acid or 20 µM [$^{14}$C]palmitic acid (both Hartmann Analytic GmbH, 55 mCi/mmol, bound to 0.135 mM fatty acid free BSA, resulting activity = 1.1 µCi/ml), or 50 nM [3-$^{3}$H]D-erythro-sphingosine C-18 (American Radiolabeled Chemicals, 20 Ci/mmol, resulting activity = 1.0 µCi/ml) for 24 hours. For radiolabeling, the culture medium furthermore contained all above listed additives except non-labeled LA during for [$^{14}$C]LA labeling experiments or non-labeled PA and sphingosine for [$^{14}$C]PA labeling experiments. Prior to subsequent lipid extraction the cells were washed with 1x PBS.

Total lipids from [$^{14}$C]LA or [$^{14}$C]PA labeled cells were extracted twice with ice cold (-20°C) methanol/isopropanol/glacial acetic acid (66:33:1, v/v/v), dried under nitrogen stream, reconstituted in chloroform and spotted onto a Silica Gel 60 plate (Merck). As epidermis-specific *Cgi-58* knockout mice (*Cgi-58*$^{epid}$-/-) lack ω-O-AcylCer [59], [$^{14}$C]LA labeled epidermal lipid extracts from wild-type and *Cgi-58*$^{epid}$-/- mice were used as standards for ω-O-AcylCer migration. Ceramides were separated twice by thin layer chromatography (TLC) with the solvent system chloroform/methanol/glacial acetic acid (190:9:1 v/v/v) [60]. Autoradiography signals were obtained by exposure to a PhosphorImager Screen (ApBiotech) and analyzed using a Storm-scanner and Storm-associated software (Molecular Dynamics).

Total lipids from [$^{3}$H]sphingosine labeled cells were extracted twice with chloroform/methanol/glacial acetic acid (66:33:1, v/v/v). After addition of 1/5 volume of $H_2O$ and phase separation by centrifugation at 3,000×g for 10 minutes the lipids were collected from the organic phase and dried under nitrogen stream. The remaining protein pellet from the aqueous phase was solubilized in 0.3 N NaOH, 0.1% (w/v) SDS at 65°C overnight and the protein content was determined using the BCA Protein Assay (see section 4.4). The dried lipids were normalized to the protein content, reconstituted in chloroform, spotted onto a Silica Gel 60 plate (Merck) and separated by TLC as described above. Radioactively labeled lipids were detected by spraying the TLC plate with a mixture of scintillation cocktail (Roth)/methanol/$H_2O$ (4:1:1, v/v/v) and exposing the dried plate to a light sensitive film at -80°C for 72 hours.

# 5 Results

## 5.1 Construction of bicistronic lentiviral expression vectors

To ensure transient or stable co-expression of multiple target proteins in mammalian cells, a bicistronic lentiviral expression system based on pLVX_Tight_Puro was constructed and tested. Infectious lentiviral particles that are generated using this expression system enable transduction of cell lines (such as HaCaT or HEKα), which cannot be transfected using standard methods (e.g. Metafectene-mediated lipofection). The bicistronic expression system was subsequently used to co-express four proteins (ELOVL4, CYP4F22, CERS3 and PNPLA1) in COS7, HaCaT and HEK-293T cells, to investigate a hypothetic pathway for ω-O-AcylCer synthesis.

### 5.1.1 Deletion of an interfering unique ClaI recognition site in pLVX_Tight_Puro

For subsequent cloning of an MCS containing a ClaI site (see section 5.1.3), a unique ClaI site in pLVX_Tight_Puro was deleted as described in section 4.1.6 using ClaI restriction enzyme and DNA Polymerase I, Large (Klenow) Fragment. To verify the deletion of the ClaI site, isolated plasmid DNA from four single *E. coli* colonies was co-digested with ClaI/NcoI-HF and analyzed by gel electrophoresis. All four tested plasmids displayed the expected linearization, which confirmed the deletion of the ClaI recognition site (Figure 5.1). The resulting plasmid was named pLVX_Tight_Puro_ClaI-Fill (7792 bp).

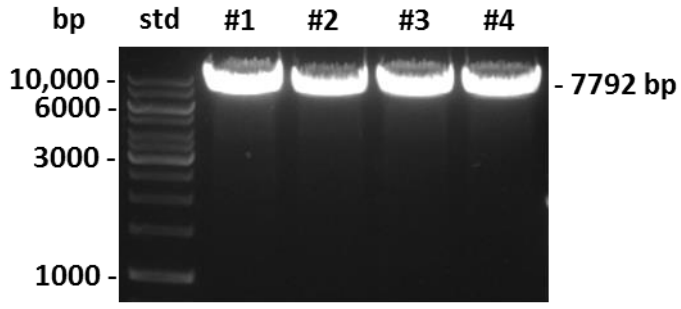


**Figure 5.1: Deletion of a unique ClaI site in pLVX_Tight_Puro using DNA Polymerase I, Large (Klenow) Fragment.** To verify successful deletion of ClaI ist in pLVX_Tight_Puro, plasmid DNA was digested with ClaI/NcoI-HF and analyzed by gel electrophoresis. Linearization of plasmid DNA confirmed deletion of the unique ClaI recognition site, whereas unsuccessful deletion would have resulted in 5849 bp and 1941 bp-sized DNA fragments.

### 5.1.2 Promoter-replacement of $P_{Tight}$ with $P_{CMV\ IE}$

As the original $P_{Tight}$ promoter of pLVX_Tight_Puro_ClaI-Fill requires a transactivator for expression of target genes (see section 0) it was replaced with the constitutively active human cytomegalovirus immediate early promoter ($P_{CMV\ IE}$). For amplification of $P_{CMV\ IE}$ insert DNA a gradient PCR with primer pair PCMV_SalI_fw/PCMV_BamHI_rv and pLVX_IRES_Puro plasmid DNA as template was performed, which yielded specific 621 bp-sized PCR product for cloning (Figure 5.2A).

In the following, purified $P_{CMV\ IE}$ insert DNA was cloned into pLVX_Tight_Puro_ClaI-Fill as previously described, using SalI-HF/BamHI-HF for co-digestion of insert DNA and XhoI/BamHI-HF for co-digestion of vector DNA. Sticky end overhangs produced by SalI are compatible with overhangs generated by XhoI and ligation of the compatible overhangs resulted in a `5′CTCGAC 3′` sequence, which was no longer recognized by either SalI or XhoI. This allowed the subsequent introduction of a MCS containing an unique XhoI site (see section 5.1.3).

To verify successful ligation of vector and insert DNA isolated recombinant plasmid DNA from three different clones were co-digested with NdeI/Acc65I and analyzed by gel electrophoresis. Plasmid DNA from clone #2 and #3 displayed the expected fragment sizes of 5753 bp and 2323 bp (Figure 5.2B) and were further confirmed by DNA sequencing using primer pLVX_Tight_Puro_rv. The verified plasmid was named pLVX_PCMV_Puro (8076 bp).

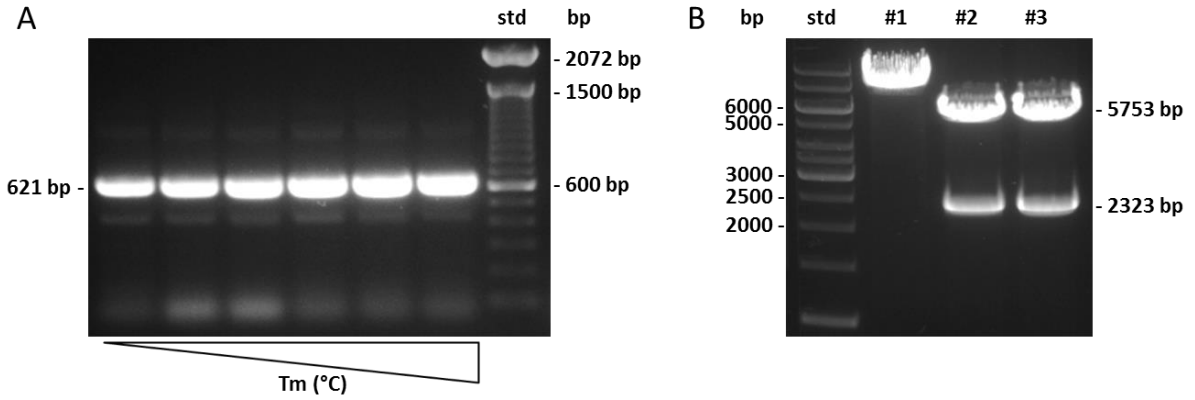


**Figure 5.2: Construction of pLVX_PCMV_Puro. A)** $P_{CMV\ IE}$ insert DNA was amplified by gradient PCR and products were analyzed by gel electrophoresis. Sufficient amounts of specific product with the expected size of 621 bp were detected and purified from the agarose gel. **B)** To verify successful ligation of $P_{CMV\ IE}$ insert DNA and pLVX_Tight_Puro_ClaI-Fill vector DNA isolated recombinant plasmids from three clones were co-digested with NdeI/Acc65I. Clone #2 and #3 displayed the expected 5753 bp and 2323 bp-sized DNA fragments, which confirmed successful cloning of $P_{CMV\ IE}$ insert DNA.

### 5.1.3 Introduction of a second MCS and an IRES into pLVX_PCMV_Puro

To create a bicistronic construct, an IRES with multiple flanking RE recognition sites (Figure 5.3A) was cloned into pLVX_PCMV_Puro. IRES insert DNA (625 bp) was generated by gradient PCR with primer pair IRES2_fw/IRES2_rv and pLVX_IRES_Puro plasmid DNA as template (Figure 5.3B), purified and cloned into pLVX_PCMV_Puro using NotI and MluI.

KpnI-HF control digest of recombinant plasmid DNA from a selected clone led to detection of the expected 6636 bp and 2025 bp-sized DNA fragments (Figure 5.3C), which verified successful introduction of the IRES into pLVX_PCMV_Puro. The resulting plasmid was further confirmed by by DNA sequencing (using primer pLVX_Tight_Puro_rv) and named pLVX_PCMV_IRES_Puro (8661 bp). A vector map and a schematic of the bicistronic MCS of the construct are depicted in Figure 5.4.

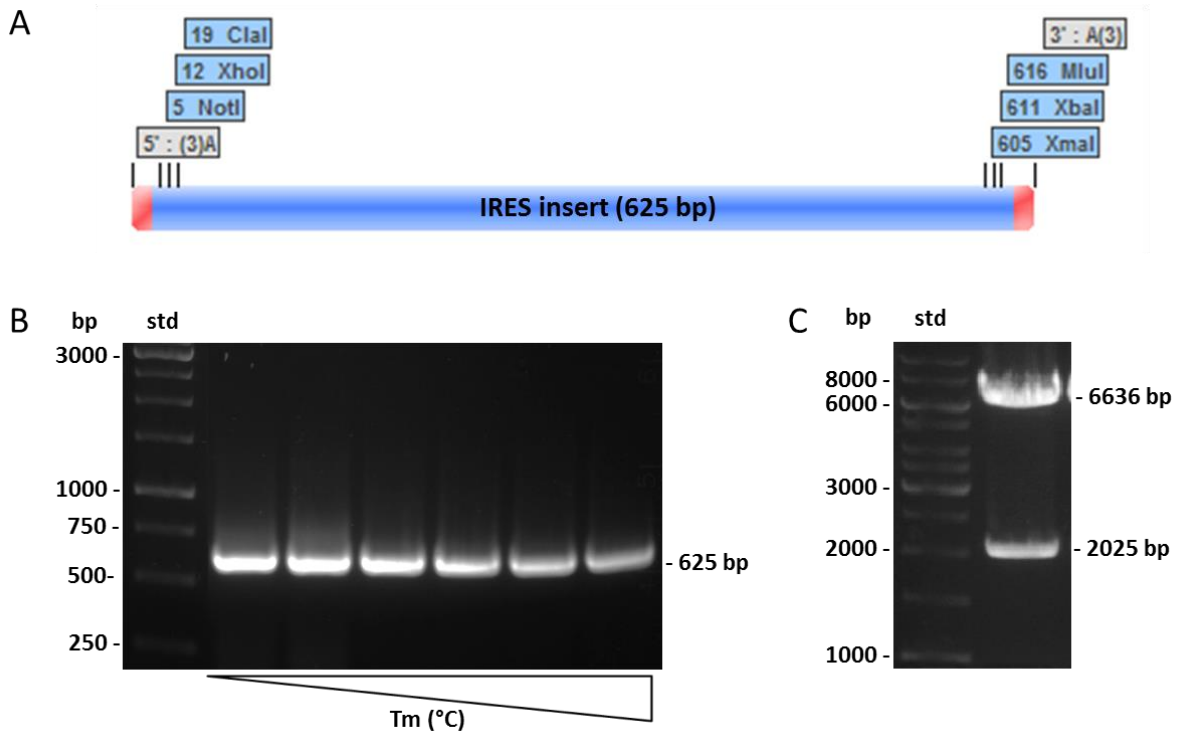


**Figure 5.3: Construction of pLVX_PCMV_IRES_Puro. A)** Schematic of IRES insert DNA**.** Flanking RE recognition sites were added by PCR using primers with specific overhangs for PCR. Cloning of the insert DNA into pLVX_PCMV_Puro created two independent MCS that were linked by the IRES. **B)** For amplification of IRES insert DNA a gradient PCR was performed. Expected 625 bp-sized PCR product was detected by gel electrophoresis and extracted from the gel. **C) T**o verify successful ligation of IRES insert DNA and pLVX_PCMV_Puro vector DNA, isolated recombinant plasmid DNA was digested with KpnI-HF. Detection of the expected 6636 bp and 2025 bp-sized DNA fragments confirmed successful cloning.

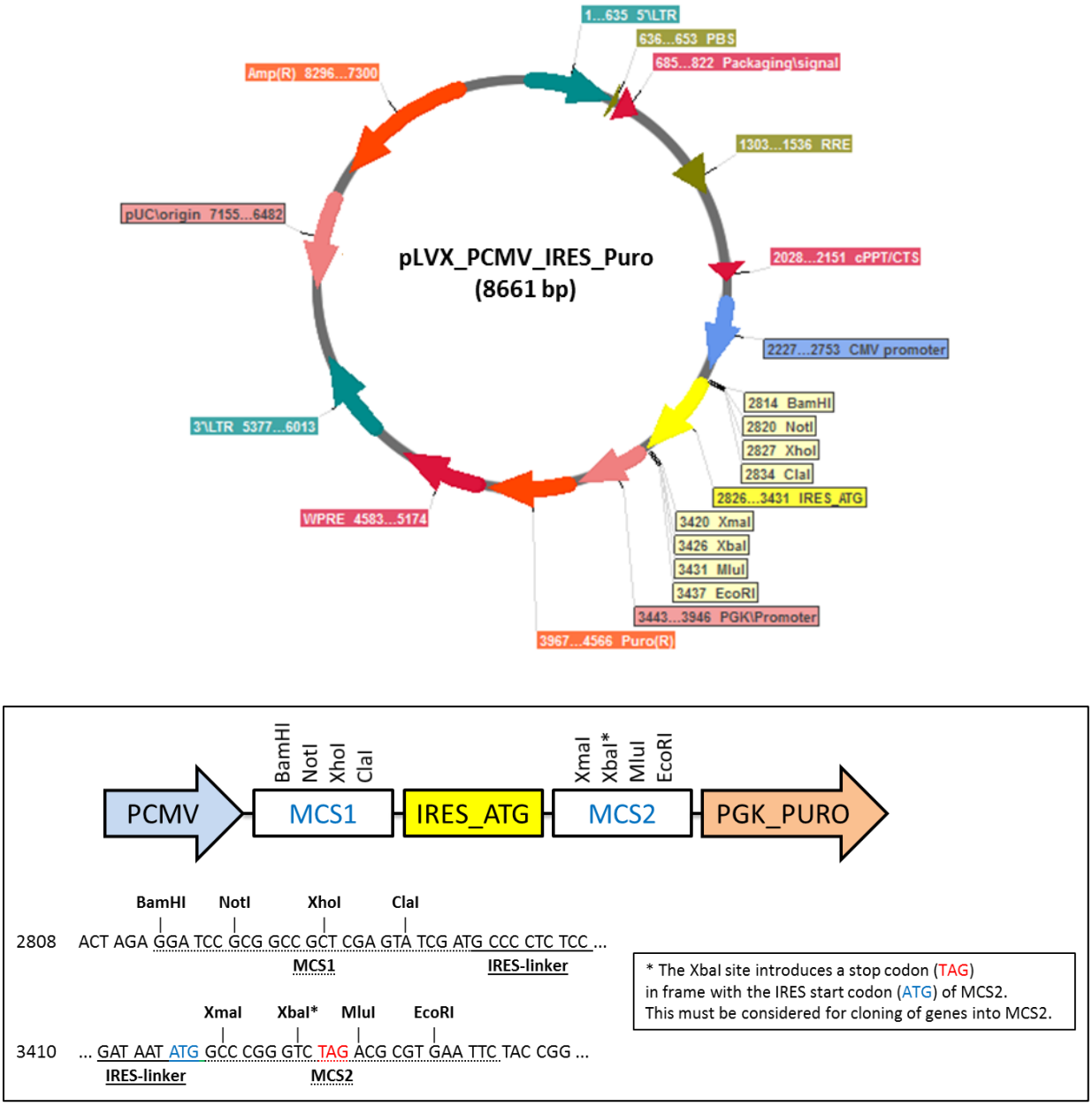


**Figure 5.4: Vector map and schematic of the bicistronic MCS of pLVX_PCMV_IRES_Puro.** The construct allows transient and stable un-coupled co-expression of two target genes using IRES. For efficient initiation of translation, it is recommended that genes cloned into MCS1 are flanked with the Kozak consensus sequence (CCACC) upstream of the genes intrinsic start codon. Genes cloned into MCS1 or MCS2 must contain a stop codon at their respective 3' end. Genes that are cloned into MCS2 must be in frame with a specific start codon at the 3' end of the IRES linker (ATG, indicated in blue), as translation of the downstream gene is exclusively initiated by this start codon.

### 5.1.4 Replacement of the IRES with a P2A peptide derived from porcine teschovirus-1

The size of genes that can be cloned into lentiviral constructs is limited by the DNA packaging capacity of the lentiviral particles that are generated by the respective expression system. Therefore, smaller constructs are favorable, as they allow efficient transduction of larger genes, which is especially important for co-expression of two genes with a bicistronic lentiviral vector.

To establish an alternative co-expression system with a smaller vector size, the IRES of pLVX_PCMV_IRES_Puro was replaced with a P2A peptide. For generation of P2A insert DNA two complementary oligonucleotides (P2A_ClaI_fw/P2A_XmaI_rv) were hybridized (see section 4.1.4) and cloned into pLVX_PCMV_IRES_Puro using ClaI/XmaI. As the synthetic dsP2A oligonucleotide was not 5' phosphorylated, the pLVX_PCMV_IRES_Puro vector backbone was not dephosphorylated, to allow ligation of the DNA fragments (see section 4.1.5). Optimal amounts of vector and insert DNA for ligation were estimated by performing gel electrophoresis and assessing the observed DNA signal intensities (Figure 5.5A).

To verify successful ligation, selected *E. coli* colonies carrying recombinant plasmid DNA were subjected to colony PCR (see section 4.1.10) using primer pair Seq_PCMV_fw and pLVX_Tight_Puro_rv. A colony carrying pLVX_PCMV_Puro was used as a negative control. Clones #9, #10, #11 and #12 displayed the expected PCR product size shift towards 430 bp compared to the 356 bp sized PCR product of the negative control (Figure 5.5B). Recombinant plasmid DNA from clone #9 was further confirmed by DNA sequencing (using primer pLVX_Tight_Puro_rv) and named pLVX_PCMV_P2A_Puro (8150 bp, Figure 5.6.)

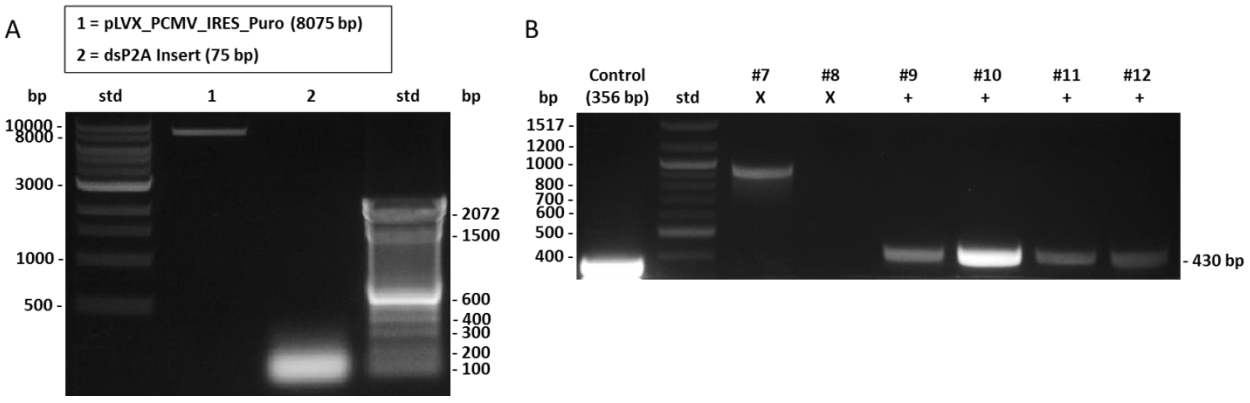


**Figure 5.5: Construction of pLVX_PCMV_P2A_Puro. A)** To estimate an optimal amount of vector and insert DNA for ligation, gel electrophoresis using an 1% agarose gel was performed and observed DNA signal intensities were assessed. **B)** To verify successful cloning, selected *E. coli* colonies carrying recombinant plasmid DNA were subjected to colony PCR and resulting PCR products were separated on a 2% agarose gel. Clones #9, #10, #11 and #12 displayed the expected product size shift towards 430 bp compared to the 356 bp-sized PCR product of the negative control.

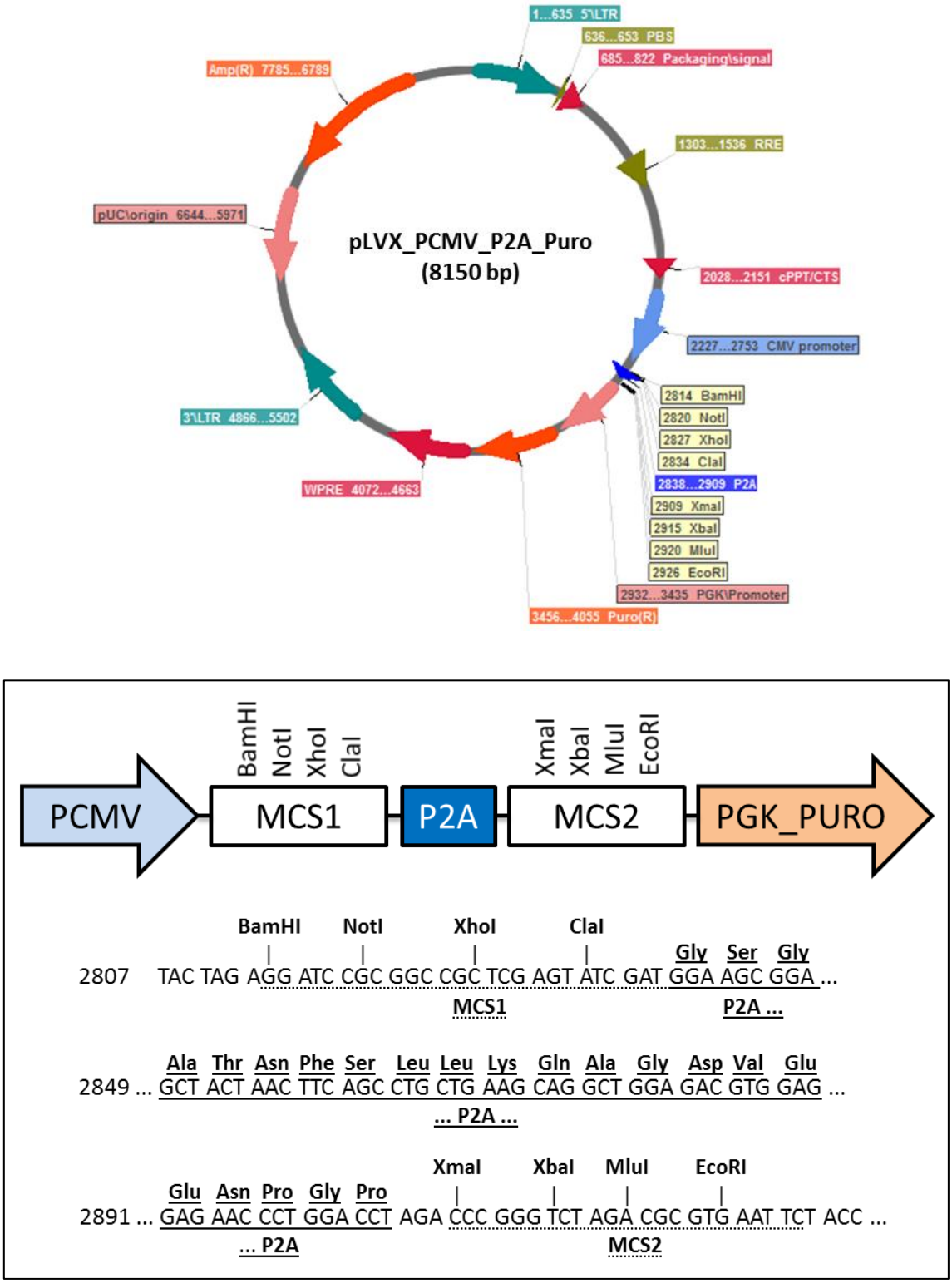


**Figure 5.6: Vector map and schematic of the bicistronic MCS of pLVX_PCMV_P2A_Puro.** The construct allows transient and stable un-coupled co-expression of two target genes using the P2A-linker. For efficient initiation of translation, it is recommended that genes cloned into MCS1 are flanked with the Kozak consensus sequence (CCACC) upstream of the genes intrinsic start codon. Genes cloned into MCS1 must not possess a stop codon and must be cloned in frame with the P2A-linker. To allow co-expression, genes cloned into MCS2 must be cloned in frame with the P2A-linker.

### 5.1.5 Introduction of a P2A-linker with flanking triple FLAG tags (3xFLAG)

To allow simultaneous immuno-detection of co-expressed proteins with a single antibody a P2A-linker with flanking 3xFLAG tags was cloned into pLVX_PCMV_P2A_Puro. For generation of insert DNA a synthetic pEX-A2 construct containing the 3FP2A3F insert (see section 0) was purchased from Eurofins Genomics and amplified by transformation into *E. coli* cells. The 3FP2A3F insert DNA was then obtained by digesting of the purified pEX-A2 construct with ClaI/XmaI, followed by preparative gel electrophoresis (Figure 5.7A). Purified 3FP2A3F insert DNA was cloned into pLVX_PCMV_P2A_Puro as previously described, using ClaI and XmaI.

To verify successful ligation, single *E. coli* colonies carrying recombinant plasmids were subjected to colony PCR (see section 4.1.10) using primer pair Seq_PCMV_fw/pLVX_Tight_Puro_rv. A colony carrying pLVX_PCMV_P2A_Puro was used as a negative control. All tested clones (#1-6) displayed the expected product size shift towards 559 bp compared to the 430 bp-sized PCR product from the negative control (Figure 5.7B). Plasmid DNA from clone #3 was confirmed by DNA sequencing with primer Seq_PCMV_fw and named pLVX_PCMV_3FP2A3F_Puro (8279 bp). A vector map and a schematic of the bicistronic MCS of the construct are depicted in Figure 5.8.

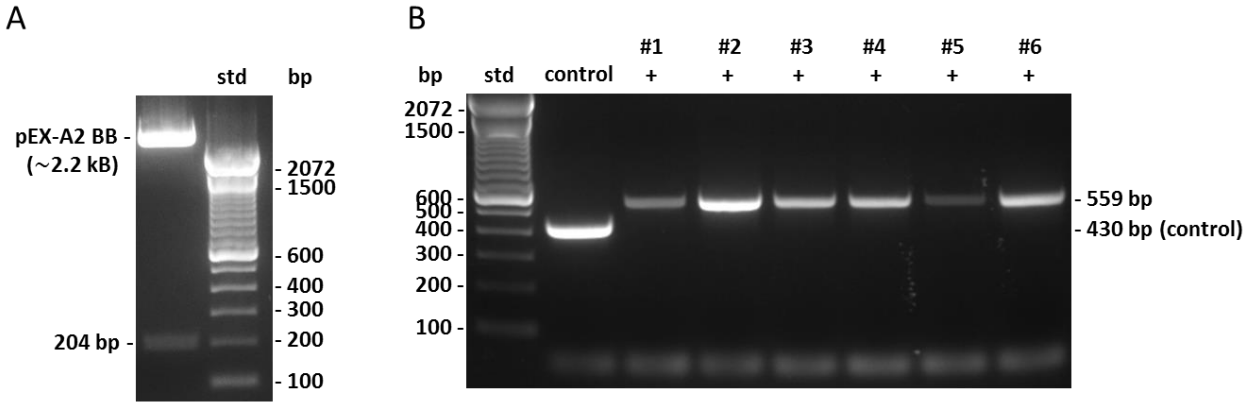


**Figure 5.7: Construction of pLVX_PCMV_3FP2A3F_Puro. A)** For subcloning, 3FP2A3F insert DNA (204 bp) was excised from a synthetic pEX-A2 construct by co-digestion with ClaI/XmaI and purified by preparative gel electrophoresis using a 2% agarose gel. **B)** To verify successful cloning, *E. coli* colonies carrying recombinant plasmid DNA were subjected to colony PCR and resulting PCR products were separated on a 2% agarose gel. All tested clones (#1-6) displayed the expected product size shift towards 559 bp compared to the 430 bp-sized PCR product of the negative control..

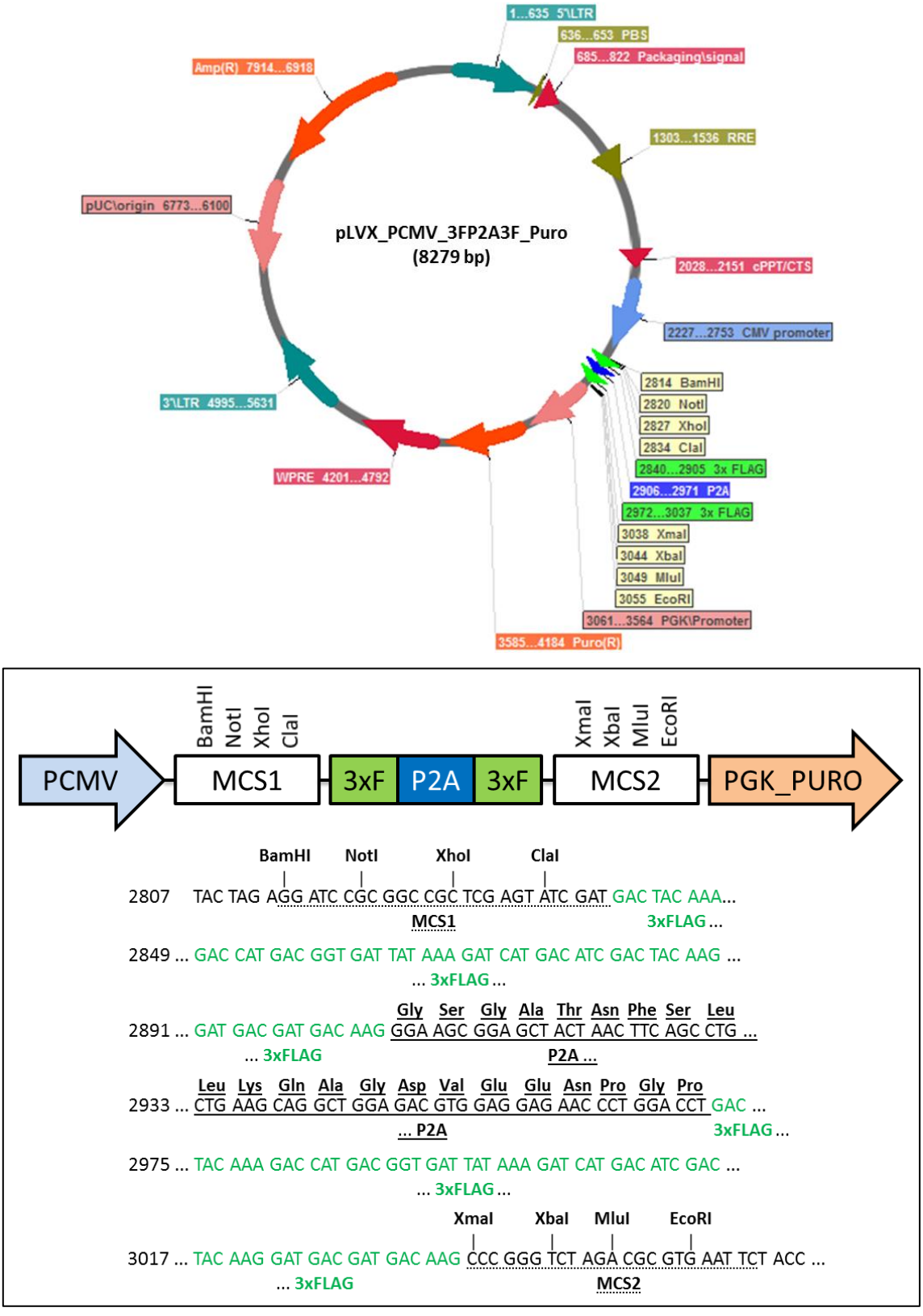


**Figure 5.8: Vector map and schematic of the bicistronic MCS of pLVX_PCMV_3FP2A3F_Puro.** The construct allows transient and stable un-coupled co-expression of two target genes using the P2A-linker. For efficient initiation of translation, it is recommended that genes cloned into MCS1 are flanked with the Kozak consensus sequence (CCACC) upstream of the genes intrinsic start codon. Genes cloned into MCS1 must not possess a stop codon and must be cloned in frame with the P2A-linker. To allow co-expression, genes cloned into MCS2 must be cloned in frame with the P2A-linker.

### 5.1.6 Introduction of a neomycin resistance gene controlled by a SV40 early promoter

For co-transduction of mammalian cells with two different bicistronic lentiviruses carrying different antibiotic selection markers, the phosphoglycerate kinase promoter (PGK) and puromycin resistance gene of pLVX_PCMV_3FP2A3F_Puro were replaced with a SV40 promoter and a neomycin resistance gene.

#### 5.1.6.1 Site-directed mutagenesis of a SexAI site in pBK_CMV_FloxNeo

For replacement of the PGK promoter and the puromycin resistance gene cassette of pLVX_PCMV_3FP2A3F_Puro with a SV40 promoter and a neomycin resistance gene, the vector DNA was digested with EcoRI/SexAI. For subsequent generation of SV40_Neo insert DNA with compatible overhangs, an interfering SexAI recognition site in the SV40 promoter enhancer region of pBK_CMV_FloxNeo was deleted by introducing a 4278C>G (ACCTGGT>AGCTGGT) point mutation. Therefore, a gradient PCR with primer pair pBK_4278CG_fw/pBK_4278CG_rv and pBK_CMV_FloxNeo as template was performed, using Q5 Hot Start High-Fidelity DNA Polymerase. Expected 5.7 kb-sized PCR product was detected at all tested Tm (Figure 5.9A) and subsequent cloning steps were performed as described in section 4.1.2. To confirm successful site-directed mutagenesis, obtained plasmid DNA from single *E. coli* colonies was sequenced using primer Neo_EcoRI_rv. A plasmid with the specific point mutation was identified (Figure 5.9B) and the resulting vector was named pBK_CMV_FloxNeo_SexAImut.

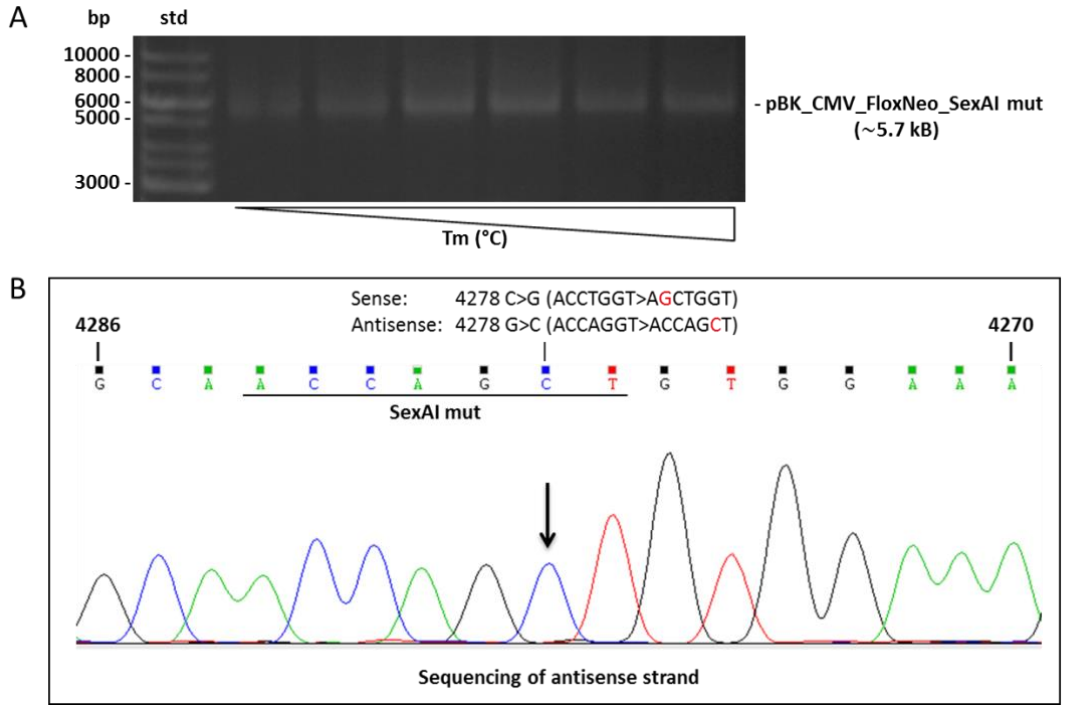


**Figure 5.9: Site-directed mutagenesis of a SexAI site in pBK_CMV_FloxNeo. A)** The interfering SexAI site (nucleotides 4277-4283) was deleted by introducing a 4278C>G point mutation by gradient PCR with Q5 Hot Start High-Fidelity DNA Polymerase. Expected 5.7 kb-sized PCR products were detected by gel electrophoresis at all tested Tm. **B)** Sanger sequencing of purified plasmid DNA after site-directed mutagenesis confirmed successful introduction of the specific point mutation (indicated by a black arrow in the chromatogram).

### 5.1.6.2 Cloning of SV40_NeoR insert into pLVX_PCMV_3FP2A3F_Puro

For amplification of SV40_NeoR insert DNA (lacking the polyadenylation signal) a gradient PCR with primer pair Neo_EcoRI_rv/Neo_SexAI_fw and pBK_CMV_FloxNeo_SexAImut plasmid DNA as template was performed, which yielded expected 1201 bp-sized PCR product (Figure 5.10A).

Purified SV40_NeoR insert DNA was cloned into pLVX_PCMV_3FP2A3F_Puro as previously described, using SexAI and EcoRI. As SexAI RE only digests DNA with a non-methylated recognition site[34], pLVX_PCMV_3FP2A3F_Puro plasmid DNA was prepared from a *dam-/dcm-* Competent *E. coli* strain (lacking Dcm methyltransferase).

To verify successful ligation of vector and insert DNA isolated recombinant plasmids from four different clones were co-digested with BamHI-HF/KpnI-HF and analyzed by gel electrophoresis. All clones displayed the expected DNA fragment sizes of 6168 and 2205 bp (Figure 5.10B) and the plasmid DNA from clone #3 was further confirmed by DNA sequencing, using primers Neo_EcoRI_rv, Neo_SexAI_fw and Neo1493_fw. The resulting plasmid was named pLVX_PCMV_3FP2A3F_Neo (8373 bp). A vector map and a schematic of the bicistronic MCS of the construct are depicted in Figure 5.11.

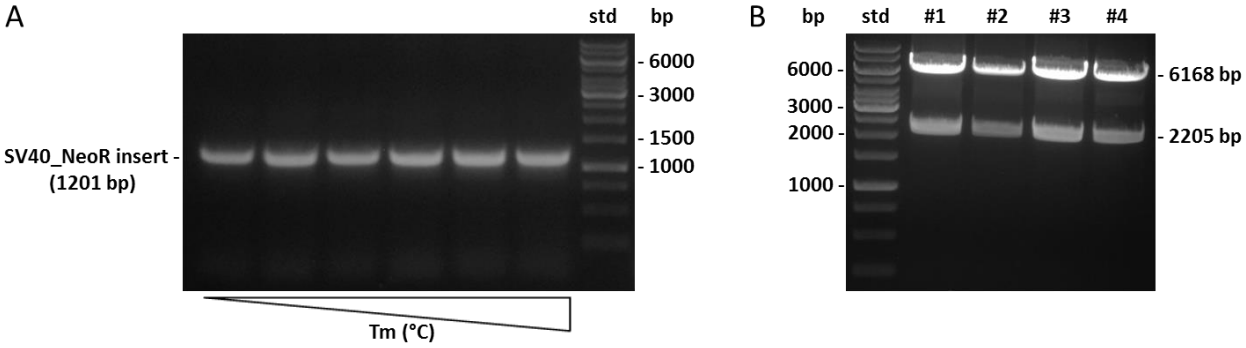


**Figure 5.10: Construction of pLVX_PCMV_3FP2A3F_Neo. A)** SV40_NeoR insert DNA was amplified by gradient PCR and products were analyzed by gel electrophoresis. Specific PCR product with the expected size of 1201 bp was detected and purified from the agarose gel. **B)** To verify successful ligation of SV40_NeoR insert DNA and pLVX_PCMV_3FP2A3F_Puro vector DNA isolated recombinant plasmids from four different clones were co-digested with BamHI-HF/KpnI-HF. All clones displayed the expected 6168 bp and 2205 bp-sized DNA fragments.

[34] https://www.neb.com/tools-and-resources/selection-charts/dam-dcm-and-cpg-methylation ; July 2016

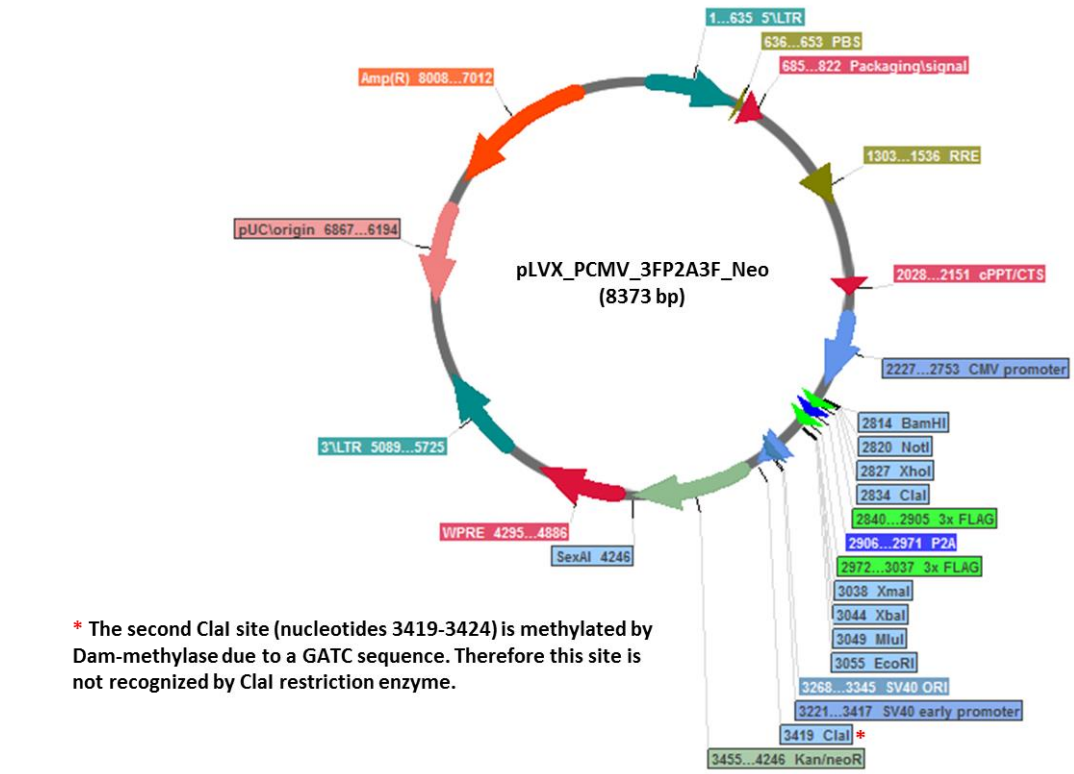


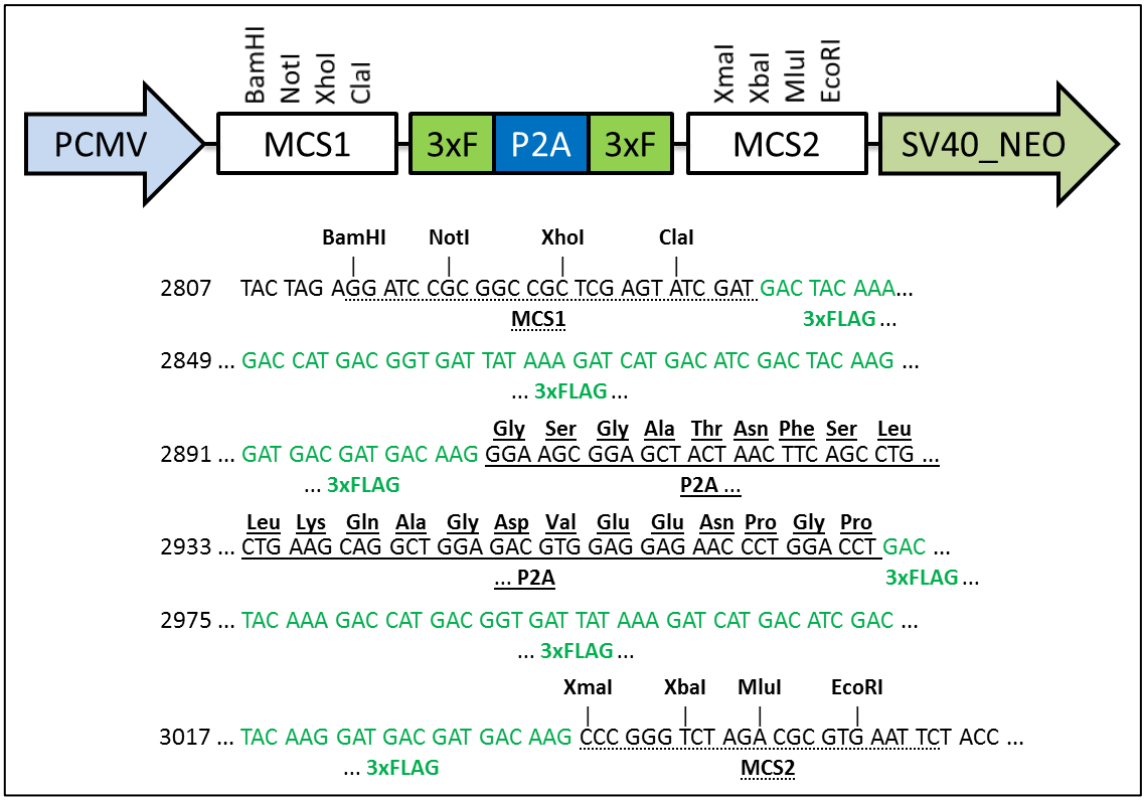


**Figure 5.11: Vector map and schematic of the bicistronic MCS of pLVX_PCMV_3FP2A3F_Puro.** The construct allows transient and stable un-coupled co-expression of two target genes using the P2A-linker. For efficient initiation of translation, it is recommended that genes cloned into MCS1 are flanked with the Kozak consensus sequence (CCACC) upstream of the genes intrinsic start codon. Genes cloned into MCS1 must not possess a stop codon and must be cloned in frame with the P2A-linker. To allow co-expression, genes cloned into MCS2 must be cloned in frame with the P2A-linker.

## 5.2 Molecular cloning of *CERS3* into pcDNA4_HisMaxC

For transient expression in mammalian cells and subsequent sub-cloning the coding sequence (CDS) of human ceramide synthase 3 (*CERS3*) isoform 1 (Accession: NM_001290341.2) was cloned into pcDNA4_HisMaxC. For generation of insert DNA, a gradient PCR with the primer pair hCERS3_BamHI_fw/hCERS3_EcoRI_rv and complementary DNA (cDNA) from human primary keratinocytes (HEKα) as template was performed. Formation of expected 1200 bp-sized PCR product increased with higher primer annealing temperatures (Tm) and maximum yield was observed at Tm=69.5°C (Figure 5.12A). To obtain large amounts of insert DNA for cloning the PCR was repeated with the determined optimal Tm, using purified insert DNA from the gradient PCR as template (Figure 5.12B). The resulting 1200 bp PCR product was extracted from the gel.

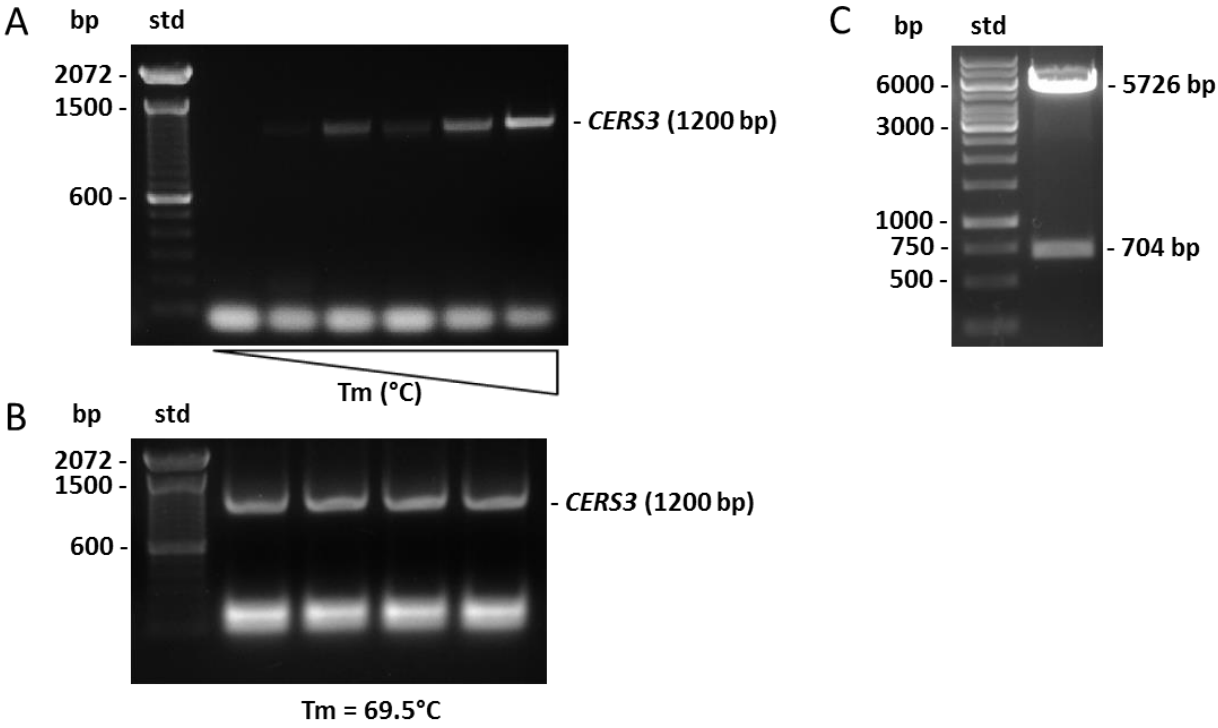


**Figure 5.12: Construction of pcDNA4_HisMaxC_hCERS3. A)** Human *CERS3* (isoform1) insert DNA was amplified by gradient PCR and the expected 1200 bp-sized PCR product was detected by gel electrophoresis. As indicated by the different signal intensities, PCR product formation increased with higher Tm and the optimal yield was observed at Tm=69.5°C. **B)** To obtain large amounts of *CERS3* insert DNA for cloning a second PCR with the determined optimal Tm (69.5°C) was performed using purified PCR product from the previous PCR as template. *CERS3* CDS DNA was detected at the expected size of 1200 bp and extracted from the gel. **C)** HindIII-HF control digest of HisMaxC_hCERS3 plasmid DNA from a selected clone lead to detection of the expected 5726 bp and 704 bp DNA fragments, which confirmed successful cloning of *CERS3* CDS.

To produce compatible sticky end overhangs, purified *CERS3* insert DNA and pcDNA4_HisMaxC vector DNA were co-digested with BamHI-HF/EcoRI-HF. Subsequent cloning steps (vector dephosphorylation, fragment ligation, transformation into competent *E. coli* DH5α, colony picking and plasmid preparation) were performed as described in section 4.1.

To verify successful ligation of vector and insert DNA isolated recombinant plasmids were digested with HindIII-HF and analyzed by gel electrophoresis. Plasmid DNA from one positive clone displayed the expected fragment sizes of 5726 bp and 704 bp (Figure 5.12C) and was further confirmed by DNA sequencing (Microsynth AG Austria, Wien), using primers T7_fw and BGH_rv.

Sequencing revealed that *CERS3* was successfully cloned in frame with the start codon and N-terminal His-tag of pcDNA4_HisMaxC, but contained an annotated missense single nucleotide polymorphism (SNP) c.1141A>G (AGG>GGG, rs2439928); p.381Arg>Gly[35]. As the clinical significance of this variation is not known[36], it could possibly alter the enzymatic activity of CERS3. The constructed plasmid was named pcDNA4_HisMaxC_hCERS3 (6430 bp). Highly concentrated plasmid DNA for further experiments was obtained by Maxiprep (see section 4.1.9).

[35] http://www.ncbi.nlm.nih.gov/projects/SNP/snp_ref.cgi?rs=2439928 , July 2016
[36] http://www.ncbi.nlm.nih.gov/projects/SNP/snp_ref.cgi?rs=2439928 , July 2016

## 5.3 Molecular cloning of *ELOVL4* into pcDNA4_HisMaxC

For transient expression in mammalian cells and subsequent sub-cloning the CDS of human fatty acid elongase 4 (*ELOVL4*; Accession: AF277094.1) was cloned into pcDNA4_HisMaxC. For generation of insert DNA, a gradient PCR with the primer pair hELOVL4_BamHI_fw/hELOVL4_XhoI_rv and HEKα cDNA as template was performed (Figure 5.13A). Low amounts of the expected 960 bp-sized PCR product were detected at the highest two Tm with maximum yield at Tm=67.5°C. To obtain larger amounts of insert DNA for cloning the PCR was repeated with the determined optimal Tm using purified insert DNA from the gradient PCR as template (Figure 5.13B).

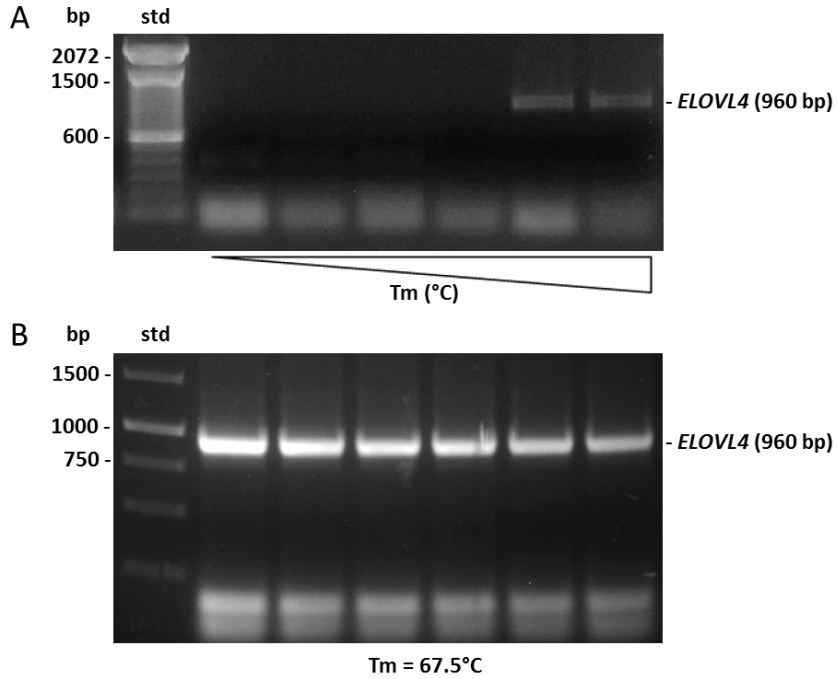


**Figure 5.13: Generation of *ELOVL4* CDS insert DNA. A)** Human *ELOVL4* insert DNA was amplified by gradient PCR and products were analyzed by gel electrophoresis. Formation of specific PCR product with the expected size of 960 bp was only observed at the two highest Tm, with maximum product yield at Tm=67.5°C. **B)** To obtain large amounts of *ELOVL4* insert DNA for cloning a second PCR with the determined optimal Tm (67.5°C) and purified product from the previous PCR as template was performed. *ELOVL4* DNA was detected at the expected size of 960 bp and extracted from the gel.

To produce compatible sticky end overhangs, purified *ELOVL4* insert DNA and pcDNA4_HisMaxC vector DNA were co-digested with BamHI/XhoI and subsequent cloning steps were performed as previously described. To verify successful ligation of vector and insert DNA isolated recombinant plasmids were co-digested with BamHI-HF/EcoRI-HF and analyzed by gel electrophoresis. However, instead of the expected DNA fragments (5594 bp and 563 bp), only linearized DNA was observed (data not shown). To further check for the presence of *ELOVL4* insert DNA, the recombinant plasmids were co-digested with BamHI/XhoI, revealing that two plasmids (#3 and #4) indeed contained insert DNA, but with a smaller DNA fragment size than the expected 948 bp (Figure 5.14).

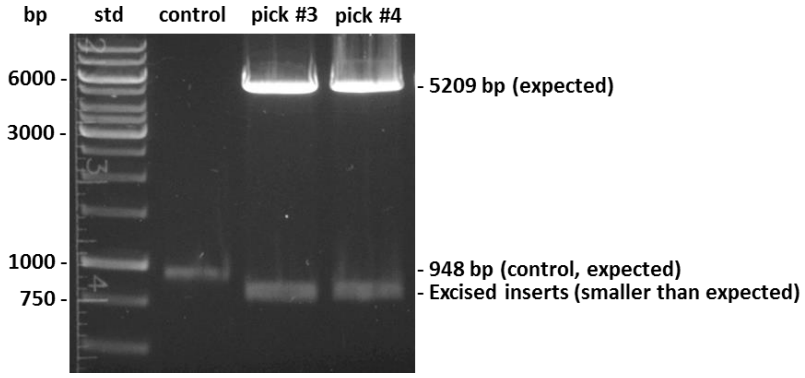


**Figure 5.14: Control digest of recombinant HisMaxC_hELOVL4 constructs with BamHI/XhoI.** As a control for the correct DNA fragment size, RE digested *ELOVL4* insert DNA (948 bp) that was used for cloning was loaded to the first lane of the gel. The excised insert DNA from recombinant plasmids #3 and #4 displayed a shift towards a smaller fragment size in comparison to the control, indicating a deletion in the cloned *ELOVL4* CDS.

To investigate this finding, recombinant plasmid #4 was sequenced (Microsynth AG Austria, Wien), using primer T7_fw. Sequencing revealed that *ELOVL4* CDS was cloned in frame with the start codon of pcDNA4_HisMaxC but contained a 127 bp deletion (c.542_669del), explaining the observed size shift of BamHI/XhoI-excised insert DNA (Figure 5.14). Due to this deletion, the insert DNA lacks the unique EcoRI site of *ELOVL4*, which explains the linearization of recombinant plasmid DNA by co-digestion with BamHI HF/EcoRI-HF. The obtained recombinant plasmid #4 was named pcDNA4_HisMaxC_hELOVL4(c.542_669del).

Several re-attempts to clone *ELOVL4* CDS into pcDNA4_HisMaxC using the standard method did not succeed (data not shown). Interestingly, the specific 127 bp deletion (c.542_669del) in cloned *ELOVL4* CDS was observed for multiple times and confirmed by DNA sequencing. The use of One Shot Stbl3 chemically competent *E. coli* cells (Invitrogen), which are optimized for cloning of unstable inserts, instead of *E. coli* DH5α also did not succeed (data not shown). Therefore a different cloning strategy was applied. In brief, two fragments of *ELOVL4* CDS were cloned consecutively into HisMaxC using the unique internal EcoRI site of *ELOVL4* CDS.

Fragment 1 included nucleotides 4 to 566 of *ELOVL4* CDS and was amplified by performing gradient PCR with primer pair hELOVL4_BamHI_2_fw/hELOVL4_EcoRI_rv and pcDNA4_HisMaxC_hELOVL4(c.542_669del) as template (Figure 5.15A). The resulting 575 bp PCR product was extracted and cloned into pcDNA4_HisMaxC, as previously described, using BamHI-HF and EcoRI-HF. Co-digestion of obtained recombinant plasmid DNA with BamHI-HF/EcoRI-HF resulted in 5242 bp and 563 bp-sized DNA fragment and verified ligation of vector and insert DNA (Figure 5.16). The construct was further verified by sequencing using primers T7_fw/BGH_rv and was named pcDNA4_HisMaxC_hELOVL4-Frag1.

Fragment 2 included nucleotides 553 to 945 of *ELOVL4* CDS and was amplified by performing gradient PCR with primer pair hELOVL4_EcoRI_fw/hELOVL4_XhoI_2_rv and HEKα cDNA as

template (Figure 5.15B). Low amounts of 402 bp PCR product were detected at the lowest two Tm with maximum yield at Tm=61.0°C. To obtain larger amounts of insert DNA for cloning the PCR was repeated with the determined optimal Tm using purified insert DNA from the gradient PCR as template (Figure 5.15C) and resulting PCR product was extracted from the gel.

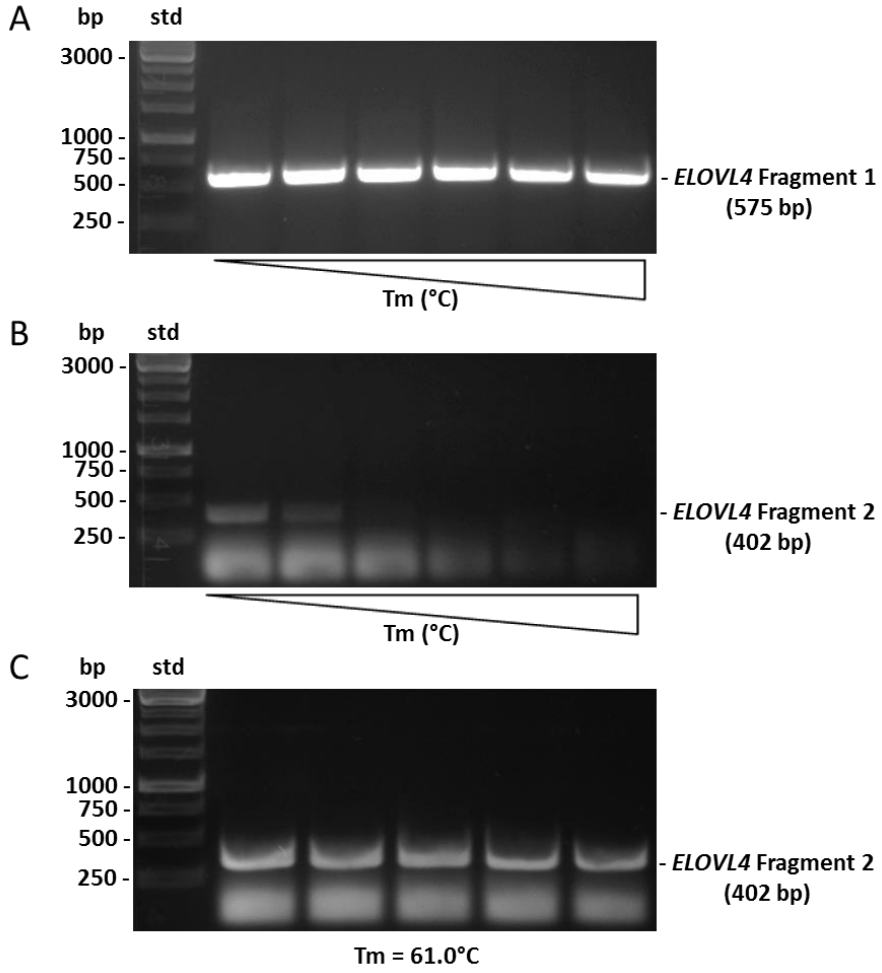


**Figure 5.15: Generation of *ELVOL4* CDS Fragment 1 and Fragment 2 insert DNA. A)** *ELOVL4* Fragment 1 insert DNA was amplified by gradient PCR and products were analyzed by gel electrophoresis. Specific PCR products with the expected size of 575 bp were detected at all Tm and purified from the agarose gel. **B)** *ELOVL4* Fragment 2 insert DNA was amplified by gradient PCR and formation of specific PCR product with the expected size of 402 bp was only observed at the two lowest Tm, with maximum product yield at Tm=61.0°C. **C)** To obtain larger amounts of *ELOVL4* Fragment 2 insert DNA for cloning a second PCR with the determined optimal Tm (61.0°C) and purified PCR product from the previous PCR as template was performed. *ELOVL4* fragment 2 DNA was detected at the expected size of 402 bp and extracted from the gel.

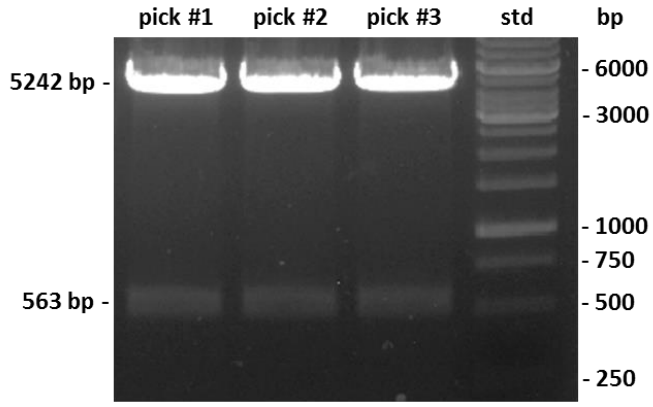


**Figure 5.16: Control digest of recombinant HisMaxC_hELOVL4-Frag1 constructs with BamHI-HF/EcoRI-HF.** The expected 5242 bp and 563 bp-sized DNA fragments were detected in all picks, which indicated successful cloning of *ELOVL4* CDS Fragment1.

Purified *ELOVL4* CDS Fragment 2 insert DNA was cloned into pcDNA4_HisMaxC_hELOVL4-Frag1, as previously described, using EcoRI-HF and XhoI. However, control co-digestion of recombinant plasmid DNA with BamHI-HF/EcoRI-HF indicated that cloning did not succeed, as DNA fragments of the expected sizes (5594 bp and 563 bp) were not detected (Figure 5.17A).

It has been shown that inadvertent expression of cloned genes by a “leaky” eukaryotic promoter can cause toxicity in *E.* coli, which prevents successful cloning[37]. To lower the plasmid copy number and thereby the expression level of the putative toxic gene, incubation of *E. coli* cells at 25°C instead of 37°C has been suggested[38]. In the following, *ELOVL4* CDS Fragment 2 was cloned into pcDNA4_HisMaxC_hELOVL4-Frag1 and *E. coli* cells were incubated at 25°C (see sections 4.1.8 and 4.1.9).

NcoI-HF control digest of a selected recombinant plasmid resulted in the expected 3443 bp, 1307 bp and 719 bp-sized DNA fragments (Figure 5.17B), which confirmed successful cloning of *ELOVL4* CDS. Likely due to the low amount of plasmid DNA used for RE digest, the expected 468 bp and 220 bp-sized DNA fragments were not detectable. For further verification, the recombinant plasmid DNA was sequenced with primers T7_fw, BGH_rv and qRT_ELOVL4_fw, revealing that *ELOVL4 CDS* was cloned in frame with the vector start codon and the N-terminal His-tag. The resulting plasmid was named pcDNA4_HisMaxC_hELOVL4 (6157 bp). Highly concentrated plasmid DNA for further experiments was isolated from *E. coli* [pcDNA4_HisMaxC_hELOVL4] cultivated at 25°C by Maxiprep (see section 4.1.9).

37 https://www.researchgate.net/post/Is_my_gene_toxic_to_the_bacteria_A_mysterious_cloning_problem ; July 2016

38 https://www.neb.com/tools-and-resources/troubleshooting-guides/troubleshooting-guide-for-cloning ; July 2016

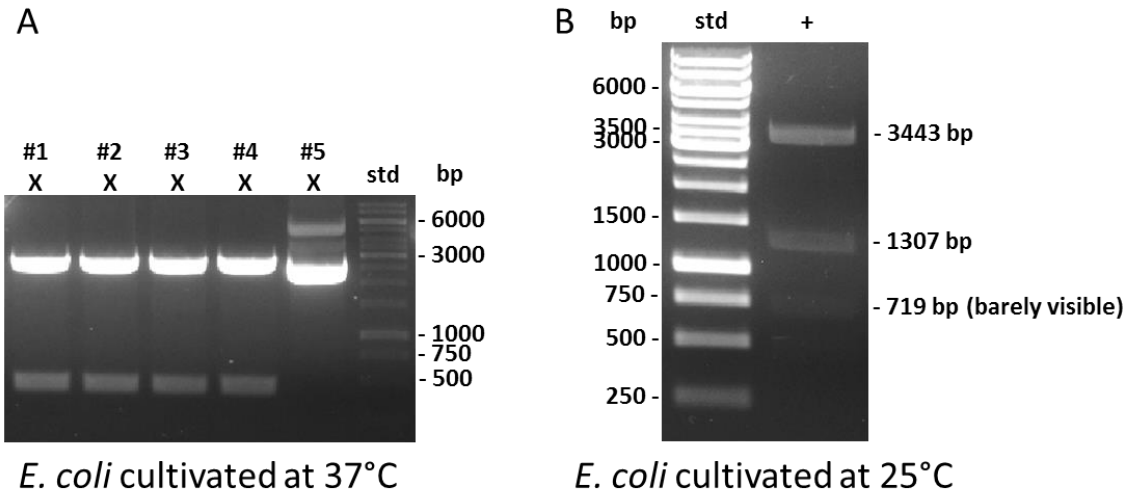


**Figure 5.17: Control digest of recombinant HisMaxC_hELVOL4 constructs from *E. coli* cells cultivated at 37°C using BamHI-HF/ EcoRI-HF (A) or from *E. coli* cultivated at 25°C using NcoI-HF (B).** RE digested plasmid DNA from cells incubated at 37°C did not display the expected 5242 bp and 563 bp DNA fragments, which indicated unsuccessful cloning. In contrast, NcoI-HF digest of plasmid DNA from a selected clone cultivated at 25°C lead to formation of the expected 3443 bp, 1307 bp and 719 bp sized DNA fragments and confirmed successful cloning of *ELVOL4* CDS.

## 5.4 Transient expression of CERS3 and ELOVL4 in COS-7 cells

To confirm transient expression of His-CERS3 and His-ELOVL4, pcDNA4_HisMaxC_hCERS3 and pcDNA4_HisMaxC_hELOVL4 plasmid DNA was transfected into COS-7 cells using metafectene, respectively (see section 4.2). To stimulate lipid synthesis and thereby possibly the up-regulation of target protein expression and/or protein stabilization, transfected cells were cultivated in DMEM +/+ supplemented with the following additives for 48 hours:

- 10 µM PA bound to delipidated BSA at a molar FA/BSA ratio of 3:1
- 10 µM OA bound to delipidated BSA at a molar FA/BSA ratio of 3:1
- 10 µM LA bound to delipidated BSA at a molar FA/BSA ratio of 3:1
- 10 µM C24:0 dissolved in EtOH
- 10 µM C24:1 dissolved in EtOH
- 10 µM C26:0 dissolved in EtOH
- 1 µM sphingosine dissolved in DMSO

Subsequently the cells were harvested in 1x SDS loading buffer and expression of His-CERS3 (51.14 kDa) and His-ELOVL4 (40.40 kDa) was assessed by Western blot analysis with Anti-His (N-term) antibody (Figure 5.18). The molecular weight (MW) of the detected protein bands corresponded to data presented in literature [10,20,21], which confirmed successful expression of the target proteins. The lower His-ELOVL4 band, which is barely visible in Figure 5.18 and indicated by an asterisk, represents the unmodified enzyme, whereas the

upper, pronounced protein band represents the N-glycosylated enzyme. In literature it has been described that ELOVL4 fatty acid elongase activity is independent of the N-glycosylation status [61].

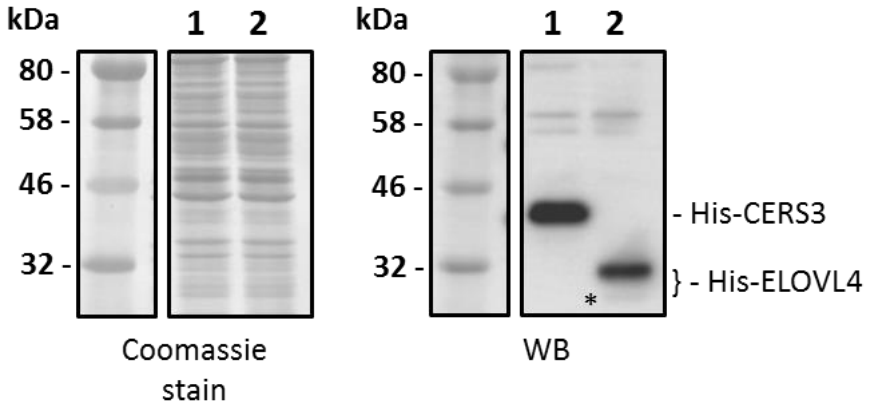


**Figure 5.18: Western blot analysis of COS7 cells transiently expressing human His-CERS3 or His-ELOVL4.** COS-7 cells were either transfected with pcDNA4_HisMaxC_hCERS3 (lane 1) or pcDNA4_HisMaxC_hELOVL4 (lane 2) using metafectene. After harvesting the cells in 1x SDS loading buffer, the expression levels of His-CERS3 and His-ELOVL4 were assessed by Western blot analysis using Anti-His (N-term) antibody. The target proteins were detected at the expected MW, respectively. The barely visible lower His-ELOVL4 band indicated by an asterisk represents the unmodified enzyme, whereas the upper, pronounced band represents the N-glycosylated protein. Coomassie Blue staining of the membrane confirmed successful protein transfer and equal loading of proteins.

## 5.5 Transient and stable co-expression of target proteins using bicistronic lentiviral constructs

To verify the functionality of the generated bicistronic constructs for transient or stable co-expression in mammalian cells, different combinations of target genes (including *Pnpla1/PNPLA1*, *CERS3*, *CYP4F22*, *EYFP* and *LacZ*) were cloned into the different vector constructs. The resulting constructs were subsequently used for metafectene-mediated transfection or generation of stable cell lines by lentiviral transduction. Successful co-expression of the target proteins using the different vector constructs was demonstrated by Western blot analysis.

### 5.5.1 Transient co-expression of murine PNPLA1 and human CYP4F22 in COS-7 cells using pLVX_PCMV_IRES_Puro

Murine *Pnpla1* and human *CYP4F22* (both with a C-terminal 6x His-tag) were cloned into the MCS1 and MCS2, respectively, of pLVX_PCMV_IRES_Puro.

*Pnpla1*-His insert DNA (1843 bp) was amplified by PCR using primer pair mPnpla1_5'_NotI_fw/mPnpla1_5'_ClaI_rv and HisMaxC_mPnpla1 plasmid DNA as template (Figure 5.19A), purified and cloned into MCS1 of pLVX_PCMV_IRES_Puro using NotI-HF/ClaI. Successful cloning was verified by BamHI-HF control digest of recombinant plasmid DNA from three different clones, which all displayed the expected 8709 bp, 1324 bp and 445 bp-sized DNA fragments (Figure 5.19B). Plasmid DNA from clone #1 was further confirmed by DNA sequencing (using primers Seq_PCMV_fw and Seq_IRES_rv) and named pLVX_PCMV_mPnpla1-His_IRES_Puro (10,478 bp).

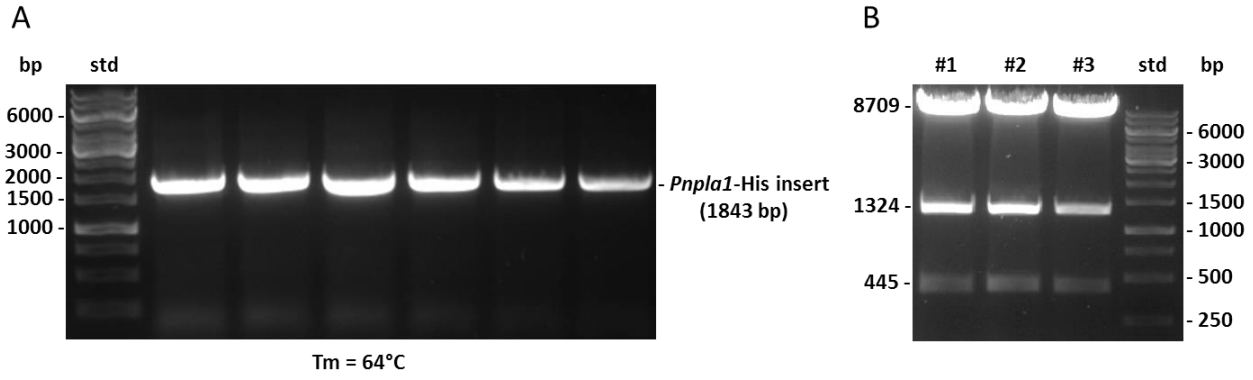


**Figure 5.19: Construction of pLVX_PCMV_mPnpla1-His_IRES_Puro. A)** *Pnpla1*-His insert DNA was amplified by PCR. Expected 1843 bp-sized PCR product was detected by gel electrophoresis and purified from the agarose gel. **B)** To verify successful ligation of *Pnpla1*-His insert DNA and pLVX_PCMV_IRES_Puro vector DNA, isolated recombinant plasmids from three different clones were digested with BamHI-HF. Plasmid DNA of all selected clones displayed the expected 8709 bp, 1324 bp and 445 bp-sized DNA fragment sizes.

Next, specific 1635 bp-sized *CYP4F22*-His insert DNA was generated accordingly by gradient PCR using primer pair CYP_XmaI_fw/CYP_XbaI_rv and HisMaxC_hCYP4F22 plasmid DNA as template (Figure 5.20A). After purification, *CYP4F22*-His insert DNA was cloned into MCS2 of pLVX_PCMV_mPnpla1-His_IRES_Puro using XmaI/XbaI and successful cloning was verified by NcoI-HF control digest. Plasmid DNA of three different selected clones displayed the expected 6196 bp, 3855 bp 1739 bp and 305 bp-sized DNA fragments (Figure 5.20A) and vector DNA from clone #3 was further confirmed by DNA sequencing (using primers pLVX_Tight_Puro_rv and Seq_IRES_fw). The resulting, verified plasmid was named pLVX_PCMV_mPnpla1His_IRES_hCYP4F22His_Puro (12,095 bp).

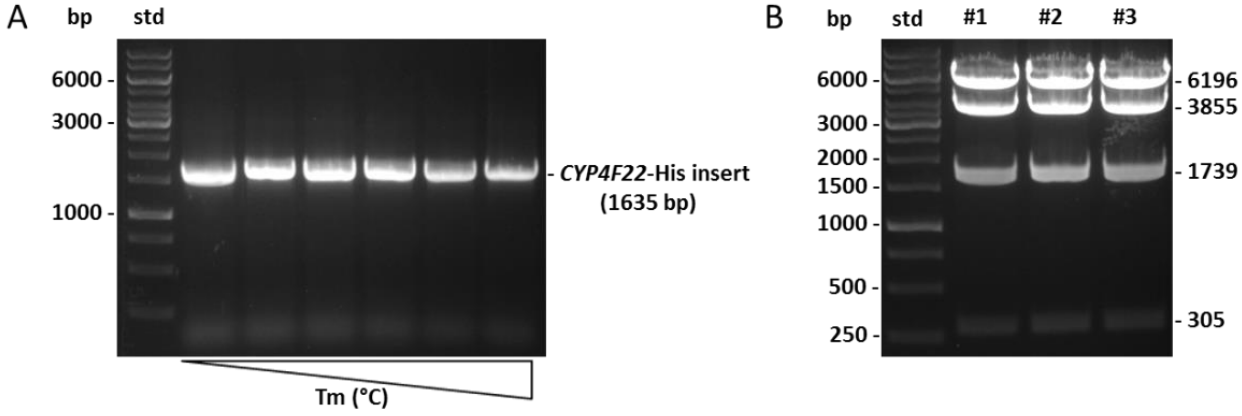


**Figure 5.20: Construction of pLVX_PCMV_mPnpla1His_IRES_hCYP4F22His_Puro. A)** Specific 1635 bp-sized *CYP4F22*-His insert DNA was amplified by gradient PCR and purified from the agarose gel. **B)** NcoI-HF control digest of recombinant plasmid DNA from three different clones resulted in expected 6196 bp, 3855 bp 1739 bp and 305 bp-sized DNA fragments, which confirmed successful cloning of *CYP4F22*-His insert DNA.

In the following, transient co-expression of mPNPLA1-His and hCYPF422-His was assessed by transfecting pLVX_PCMV_mPnpla1His_IRES_hCYP4F22His_Puro plasmid DNA into COS-7 cells (using metafectene). 24 hours post-transfection the cells were harvested in 1x RIPA (+Pi) buffer, disrupted by sonication and protein concentration of resulting cell lysate was determined by BCA protein assay. 20 µg lysate protein were separated by SDS-PAGE and expression of the target proteins was analyzed by Western blot analysis using Anti-His (C-term) antibody. The MW of the detected protein bands corresponded to data presented in literature [10,24], which confirmed successful co-expression of mPNPLA1-His (65.90 kDa) and hCYP4F22-His (63.12 kDa). However, the signal intensity of the hCYP4F22-His band was very weak in comparison to the mPNPLA1-His band, which indicated low expression levels of hCYP4F22-His (Figure 5.21).

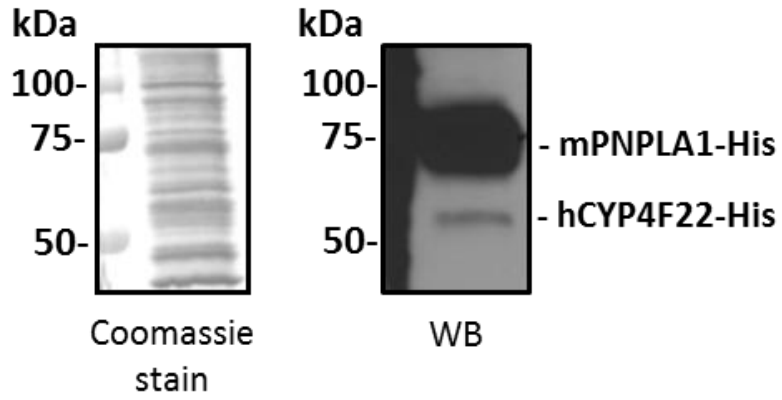


**Figure 5.21: Western blot analysis of COS-7 cells transiently co-expressing mPNPLA1-His and hCYP4F22-His, after metafectene-mediated transfection with pLVX_PCMV_mPnpla1His_IRES_hCYP4F22His_Puro.** 24 hours post-transfection the cells were disrupted in 1x RIPA (+Pi) buffer and resulting cell lysate was analyzed by Western blot analysis using Anti-His (C-term) antibody. Thereby, high expression of mPNPLA1-His, but only very low expression of hCYP4F22-His was observed.

### 5.5.2 Co-expression of target proteins using pLVX_PCMV_P2A_Puro

#### 5.5.2.1 Transient co-expression of human *PNPLA1* and *CERS3* in COS-7 cells

Human *PNPLA1* and *CERS3* (both with a C-terminal 1xFLAG-tag) were cloned into the MCS1 and MCS2, respectively, of pLVX_PCMV_P2A_Puro. *PNPLA1*-1xFLAG insert DNA was generated by a gradient PCR using primer pair 5'hP1_NotI_fw/5'hP1_P2A_XhoI_rv and HisMaxC_hPNPLA1 plasmid DNA as template, yielding specific 1647 bp-sized PCR product (Figure 5.22A). After purification, *PNPLA1*-1xFLAG insert DNA was cloned into MCS1 of pLVX_PCMV_P2A_Puro using NotI-HF and XhoI. Control digest of recombinant plasmid DNA (using EcoRI-HF) confirmed successful cloning by resulting expected 9062 bp and 716 bp-sized DNA fragments (Figure 5.22B). The vector construct was further verified by DNA sequencing (using primers PCMV_fw and pLVX_Tight_Puro_rv) and named pLVX_PCMV_hPNPLA1-1xF_P2A_Puro (9778 bp).

*CERS3*-1xFLAG insert DNA was amplified by a gradient PCR using primer pair hCERS3_XbaI_fw/hCERS3_FLAG_MluI_rev and HisMaxC_hCERS3 plasmid DNA as template. Specific 1227 bp-sized PCR product yield increased at higher Tm and the DNA bands that resulted from PCR at the three highest Tm were extracted from the gel for cloning (Figure 5.22C). Purified *CERS3*-1xFLAG insert DNA was cloned into MCS2 of pLVX_PCMV_hPNPLA1-1xF_P2A_Puro using XbaI/MluI. Control digest of plasmid DNA from three different selected clones (using BamHI-HF/XhoI) resulted in the expected 8338 bp, 1585 bp and 1009 bp-sized DNA fragments (Figure 5.22D). Plasmid DNA from clone #3 was further verified by DNA sequencing (using primers pLVX_Tight_Puro_rv and qRT_CERS3_rv) and named pLVX_PCMV_hPNPLA1-1xF_P2A_hCERS3-1xF_Puro (10,988 bp).

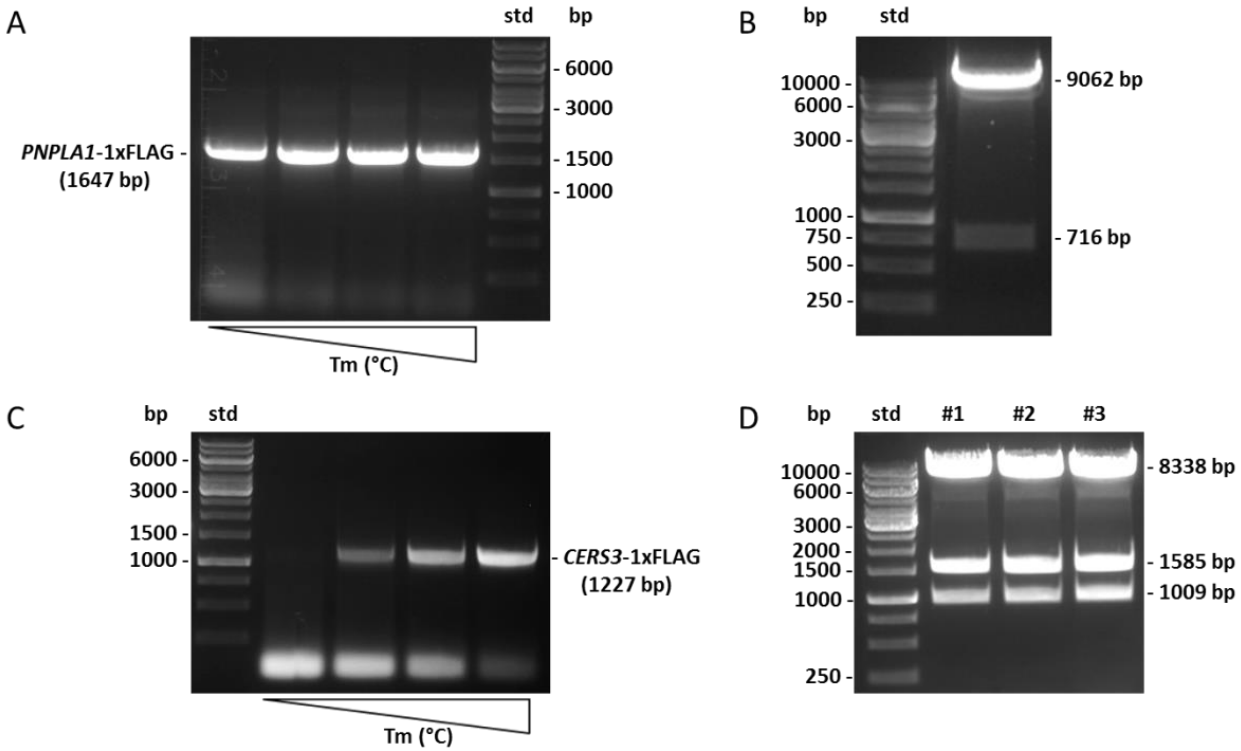


**Figure 5.22: Construction of pLVX_PCMV_hPNPLA1-1xF_P2A_hCERS3-1xF_Puro.** Specific 1647 bp-sized *PNPLA1*-1xFLAG insert DNA was amplified by gradient PCR **(A)**, purified from the agarose gel and successful cloning of the insert DNA into MCS1 of the expression vector was verified by EcoRI-HF control digest of recombinant plasmid DNA, which resulted in expected 9062 bp and 716 bp-sized DNA fragments **(B)**. *CERS3*-1xFLAG insert DNA (1227 bp) was amplified by gradient PCR. Specific PCR product bands with the expected MW were detected at the highest three tested Tm **(C)**, purified from the agarose gel and cloned into MCS2 of pLVX_PCMV_hPNPLA1-1xF_P2A_hCERS3-1xF_Puro. Successful cloning was confirmed by BamHI-HF/XhoI control digest of plasmid DNA from three selected clones and detection of expected 8338 bp, 1585 bp and 1009 bp-sized DNA fragments **(D)**.

In the following, pLVX_PCMV_hPNPLA1-1xF_P2A_hCERS3-1xF_Puro was transfected into COS-7 cells using metafectene. 24 hours post-transfection the cells were harvested in 1x SDS loading buffer and subjected to Western blot analysis (using Anti-FLAG M2-HRP antibody) to verify transient co-expression of the target proteins. Specific PNPLA1-1xFLAG (61.37 kDa) and CERS3-1xFLAG (49.15 kDa) protein bands with the expected respective MW, were detected and similar signal intensities of the protein bands suggested approximately equimolar expression levels of both enzymes (Figure 5.23). Furthermore, no uncleaved PNPLA1/CERS3 fusion-protein was detected, which suggested high P2A-mediated cleavage efficiency.

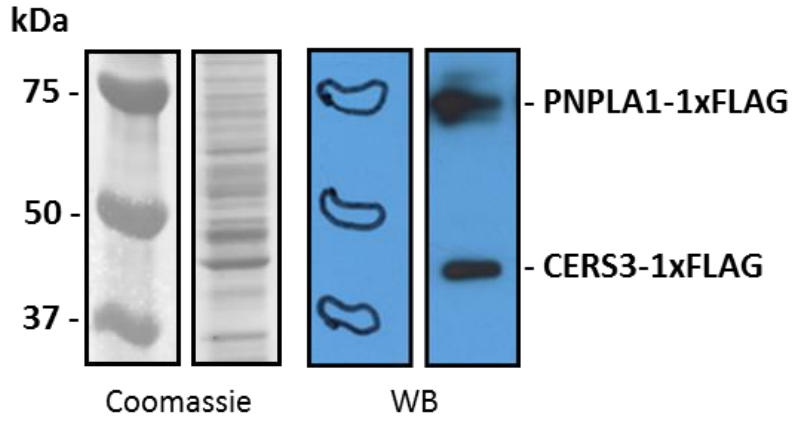


**Figure 5.23: Western blot analysis of COS-7 cells transiently co-expressing human PNPLA1-1xFLAG and CERS-1xFLAG after metafectene-mediated transfection with pLVX_PCMV_hPNPLA1-1xF_P2A_hCERS3-1xF_Puro.** 24 hours post-transfection the cells were harvested in 1x SDS and resulting cell lysate was analyzed by Western blot analysis using Anti-FLAG M2-HRP antibody. This analysis revealed approximately equimolar protein expression of both target enzymes and no expression of uncleaved fusion-protein was observed.

#### 5.5.2.2 Stable co-expression of human *PNPLA1* and *CYP4F22* in HEK-293 cells

Human *PNPLA1* and *CYP4F22* (both with a C-terminal 1xFLAG-tag) were cloned into the MCS1 and MCS2, respectively, of pLVX_PCMV_P2A_Puro. The resulting DNA construct was used for the generation of infectious lentiviral particles, which were subsequently used for lentiviral transduction of HEK-293 cells.

For molecular cloning, specific *CYP4F22*-1xFLAG insert DNA (1638 bp) was generated by gradient PCR using primer pair CYP_XbaI_fw/CYP_FLAG_MluI_rv and HisMaxC_hCYP4F22 plasmid DNA as template (Figure 5.24A). After purification from the gel, *CYP4F22*-1xFLAG insert DNA was cloned into MCS2 of pLVX_PCMV_hPNPLA1_P2A_Puro using XbaI/MluI. Successful ligation of insert- and vector DNA was confirmed by EcoRI-HF control digest of recombinant plasmid DNA from three different clones, which resulted in the expected 9062 bp and 2337 bp-sized DNA fragments (Figure 5.24B). Plasmid DNA from clone #3 was further verified by DNA sequencing (using primers pLVX_Tight_Puro_rv and qRT_CYP4F22_rv) and named pLVX_PCMV_hPNPLA1-1xF_P2A_hCYP4F22-1xF_Puro (11,399 bp).

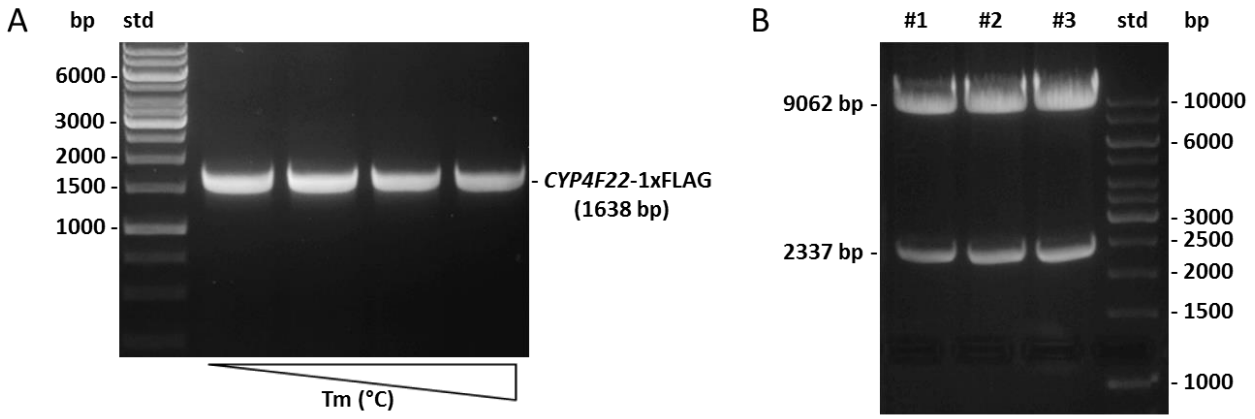


**Figure 5.24: Construction of pLVX_PCMV_hPNPLA1-1xF_P2A_hCYP4F22-1xF_Puro. A)** *CYP4F22*-1xFLAG insert DNA (1638 bp) was generated by gradient PCR and purified from the agarose gel. **B)** To verify successful ligation of *CYP4F22*-1xFLAG insert DNA and pLVX_PCMV_hPNPLA1-1xF_P2A_Puro vector DNA, isolated recombinant plasmid DNA from three clones was digested with EcoRI-HF and the expected 9062 bp and 2337 bp-sized DNA fragments were detected in all three samples.

To establish a cell line stably co-expressing both target proteins, HEK-293 cells were transduced with lentiviral particles that were generated using pLVX_PCMV_hPNPLA1-1xF_P2A_hCYP4F22-1xF_Puro (see section 4.3). To investigate if target protein-expression of stable cell lines could be optimized by adapting the virus concentration, three different volumes of lentiviral supernatant were used for transduction (1 ml, 0.5 ml or 250 µl). After selection with 1.5 µg/ml puromycin for 14 days, the cells were harvested in RIPA (+Pi) buffer, disrupted by sonication and cell lysate protein concentration was determined by BCA protein assay. In the following, 15 µg lysate protein from each generated cell line was separated by SDS-PAGE and expression of the target proteins was assessed by Western blot analysis (using Anti-FLAG M2-HRP antibody). In the following, the membrane was stripped and incubated with an antibody recognizing β-Actin. Detection of specific β-Actin protein-bands with the expected MW and similar signal intensities (Figure 5.25) verified equal loading of proteins and ensured comparability of protein-signals from the first Western blot.

The signal intensities of the detected specific PNPLA1-1xFLAG and human CYP4F22-His protein bands from the different samples were very similar (Figure 5.25), which indicated equimolar expression of target proteins in the different cell lines. Formation of uncleaved fusion proteins was not observed. The results furthermore suggested that efficiency of target protein-expression was not significantly altered by using different virus concentrations for transduction.

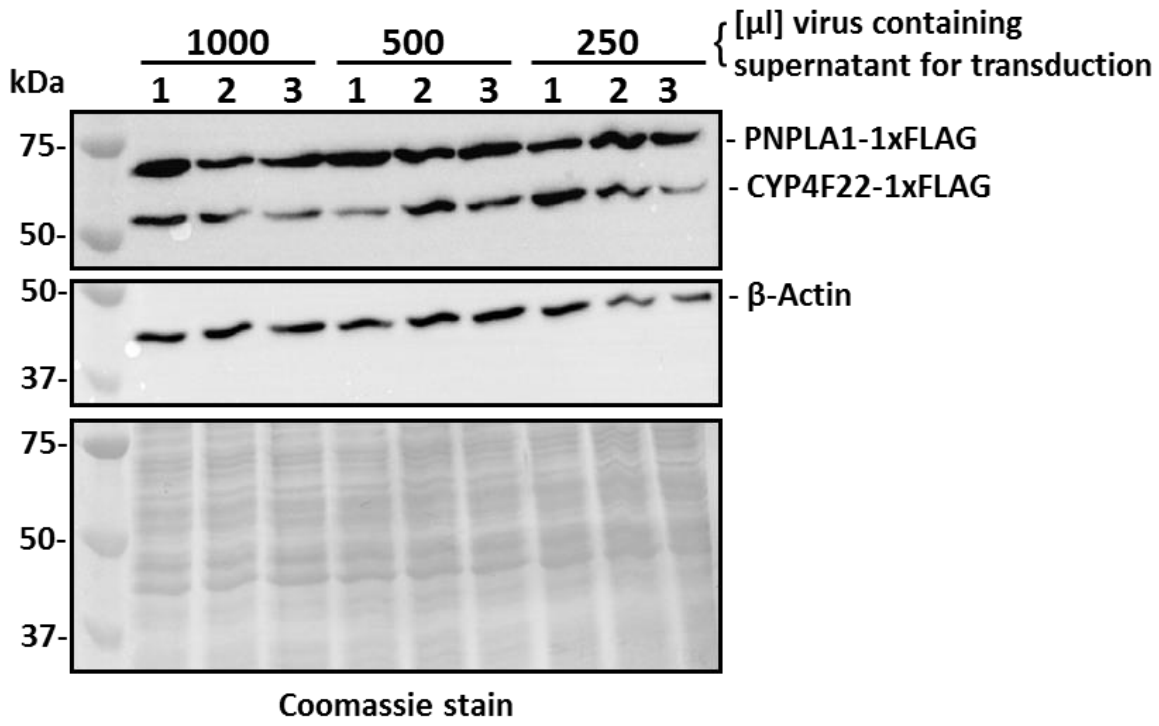


**Figure 5.25: Western blot analysis of HEK-293 cells, stably co-expressing human PNPLA1-1xFLAG and CYP4F22-1xFLAG after transduction with lentiviral particles, which were generated using pLVX_PCMV_hPNPLA1-1xF_P2A_hCYP4F22-1xF_Puro.** Different volumes (1 ml, 0.5 ml or 250 µl) of lentiviral supernatants were used for transduction of HEK-293 cells, to check whether expression-efficiency of the target proteins could be optimized. The stable cells were selected with 1.5 µg/ml puromycin for 14 days, harvested in RIPA (+Pi) buffer and cell lysates were prepared by sonication. Western blot analysis (using Anti-FLAG M2-HRP antibody) revealed approximately equimolar protein expression of the target proteins, but the use of different viral titers for transduction did not appear to alter expression-efficiency. Loading of equal protein amounts was verified by membrane-stripping and incubation with an anti-β-Actin antibody, as well as subsequent coomassie blue staining.

### 5.5.3 Co-expression of EYFP and LacZ using pLVX_PCMV_3FP2A3F_Puro

The genes for yellow fluorescent protein (*EYFP*) and β-galactosidase (*LacZ*) were cloned into the expression vector and the resulting construct was used for generation of HEK-293 cells that expressed the target proteins in a transient or stable fashion. In the following, stable HEK-293 cells were subjected to ß-gal assay and fluorescence microscopy (using blue light excitation), which resulted in blue staining (due to ß-gal activity) and simultaneous yellow fluorescence (due to YFP-expression) of the cells. The results indicated that proteins, which are co-expressed by 2A peptide-mediated self-cleavage, are correctly folded and enzymatically active.

#### 5.5.3.1 Cloning of *EYFP* and *LacZ*

*EYFP* insert DNA (792 bp) was generated by gradient PCR using primer pair YFP_NotI_fw/YFP_ClaI_rv and pEYFP-C1 plasmid DNA as template (Figure 5.26A). Purified *EYFP* insert DNA was cloned into MCS1 of pLVX_PCMV_3FP2A3F_Puro using NotI-HF/ClaI. To verify successful cloning, recombinant plasmid DNA from three selected clones was digested with NcoI-HF. The control digest resulted in the expected 6196 bp, 2545 bp and 304 bp-sized DNA fragments (Figure 5.26B) and plasmid DNA from clone #3 was further confirmed by DNA sequencing (using primer PCMV_fw). The verified construct was named pLVX_PCMV_EYFP_3FP2A3F_Puro (9045 bp).

Another gradient PCR (using primers LacZ_XmaI_fw/BGH_MluI_rv and pcDNA4_HisMax_LacZ plasmid DNA as template) was performed for amplification of 3169 bp-sized *LacZ* insert DNA (Figure 5.26C). After purification, the insert DNA was cloned into MCS2 of pLVX_PCMV_EYFP_3FP2A3F_Puro (using XmaI and XbaI) and recombinant plasmid DNA from three selected clones (#1, #2 and #4) displayed the expected 8803 bp and 3345 bp-sized DNA fragments upon XhoI control digest (Figure 5.26D). The additional high MW DNA bands (annotated as “uncut plasmid” in Figure 5.26D) likely represented nicked open circular plasmid DNA, which resulted from incomplete digestion due to low XhoI activity. The verified construct was named pLVX_PCMV_EYFP_3FP2A3F_LacZ_Puro (12,148 bp).

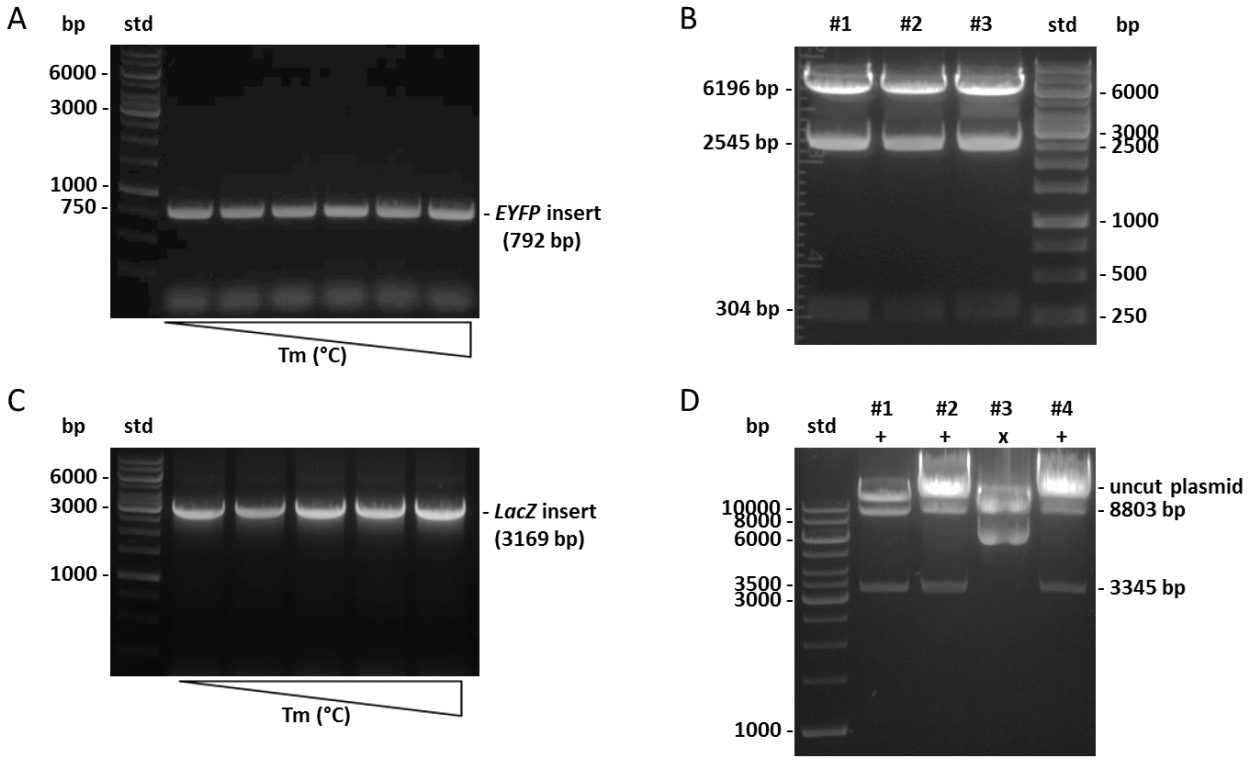


**Figure 5.26: Construction of pLVX_PCMV_EYFP_3FP2A3F_LacZ_Puro.** *EYFP* insert DNA (792 bp) was generated by gradient PCR **(A)** and successful cloning into MCS1 of pLVX_PCMV_3FP2A3F_Puro was verified by NcoI-HF control digest of recombinant plasmid DNA from three selected clones, which resulted in the expected 6196 bp, 2545 bp and 304 bp-sized DNA fragments **(B)**. For amplification of *LacZ* insert DNA (3169 bp) another gradient PCR was performed **(C)** and the purified insert DNA was cloned into MCS2 of pLVX_PCMV_EYFP_3FP2A3F_Puro. XhoI control digest of resulting recombinant plasmid DNA from four selected clones resulted in the expected 8803 bp and 3345 bp-sized DNA fragments from clones #1,#2 and #4 **(D)**. The DNA bands with the highest MW ("uncut plasmid") likely represent nicked open circular plasmid DNA due to incomplete XhoI digestion.

### 5.5.3.2 Transient co-expression of EYFP and LacZ in HEK-293

To assess transient co-expression, pLVX_PCMV_EYFP_3FP2A3F_LacZ_Puro plasmid DNA was transfected into HEK-293 cells using Metafectene. 24 hours post-transfection, the cells were harvested in 1x SDS loading buffer and expression of the target proteins was analyzed by Western blot with Anti-FLAG M2-HRP antibody. Specific EYFP-3xFLAG (33.61 kDa) and 3xFLAG-LacZ (118.68 kDa) protein bands were detected at the expected MW, respectively, and similar signal intensities indicated co-expression of approximately equimolar protein levels (Figure 5.27). Another pronounced band detected at >150 kDa likely represented uncleaved EYFP-3xFLAG_P2A_3xFLAG-LacZ fusion-protein (152.28 kDa), which indicated incomplete P2A-mediated cleavage.

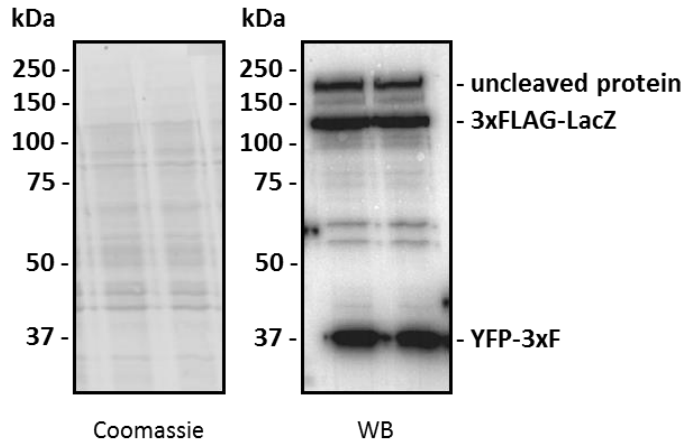


**Figure 5.27: Western blot Analysis of HEK-293 cells transiently co-expressing EYFP-3xFLAG and 3xFLAG-LacZ.** The cells were transfected with pLVX_PCMV_EYFP_3FP2A3F_LacZ_Puro, harvested in 1x SDS loading buffer (24 hours after transfection) and subjected to Western blot analysis using Anti-FLAG M2-HRP antibody. Similar signal intensities of specific EYFP-3xFLAG and 3xFLAG-LacZ protein bands were detected, indicating approximately equimolar expression levels. Another band detected at >150 kDa likely represents uncleaved EYFP-3xFLAG_P2A_3xFLAG-LacZ fusion-protein (152.28 kDa), indicating incomplete P2A-mediated cleavage.

#### 5.5.3.3 Stable co-expression of *EYFP* and *LacZ* in HEK-293

To establish a cell line that stably expressed both EYFP-3xFLAG and 3xFLAG-LacZ, and to investigate correct folding and enzymatic activity of the expressed target proteins, HEK-293 cells were transduced with lentiviral particles that were generated using pLVX_PCMV_EYFP_3FP2A3F_LacZ_Puro (see section 4.3). After selection with 1.5 µg/ml puromycin for 14 days, the cells were harvested in RIPA (+Pi) buffer, disrupted by sonication and the protein content of resulting cell lysates was determined with the BCA protein assay. 15 µg lysate protein per cell line were separated by SDS-PAGE, followed by Western blot analysis with Anti-FLAG M2-HRP antibody. Specific EYFP-3xFLAG (33.61 kDa) and 3xFLAG-LacZ (118.68 kDa) protein bands were detected at the expected MW, respectively (Figure 5.28). The signal intensity of the LacZ band was significantly reduced compared to the EYFP band, which indicated low expression and/or increased degradation of LacZ. The previously observed EYFP-3xFLAG_P2A_3xFLAG-LacZ fusion-protein band (152.28 kDa) was observed again, which indicated incomplete P2A-mediated cleavage.

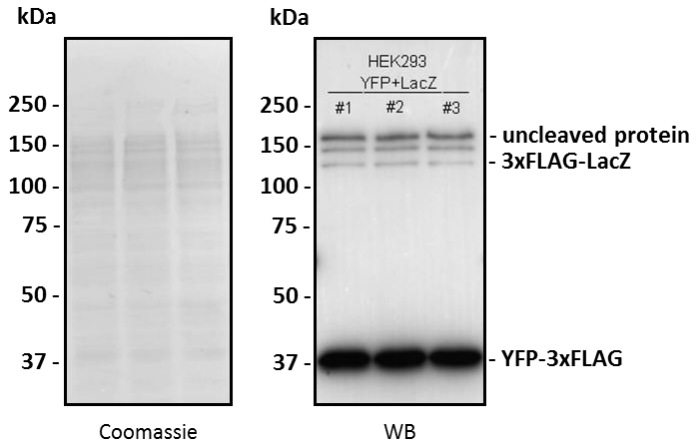


**Figure 5.28: Western blot analysis of HEK-293 cells stably co-expressing EYFP-3xFLAG and 3xFLAG-LacZ.** HEK-293 cells were transduced with lentiviral particles (generated using pLVX_PCMV_EYFP_3FP2A3F_LacZ_Puro), selected with 1.5 µg/ml puromycin for 14 days, harvested in RIPA (+Pi) buffer and analyzed by Western blot analysis using Anti-FLAG M2-HRP antibody, resulting detection of specific EYFP and LacZ protein-bands. Low signal intensity of the LacZ-band indicated low expression and/or increased degradation of LacZ. Furthermore, detection of an EYFP-3xFLAG_P2A_3xFLAG-LacZ fusion-protein band indicated incomplete P2A-mediated cleavage of the expressed target proteins.

#### 5.5.3.4 Treatment of stable HEK-293 cells with proteasome inhibitor MG132

To investigate wether the reduced LacZ expression level in HEK-293 cells stably co-expressing EYFP and LacZ (Figure 5.28) resulted from increased proteasomal degradation of the protein, the cells were treated with the proteasome inhibitor MG132 (Sigma-Aldrich). Therefore, the cells were cultivated in DMEM +/+ containing either 10 µM MG132 (dissolved in DMSO) or vehicle for 24 hours. To promote lipid synthesis and thereby possibly the up-regulation of target protein expression and/or protein stabilization, the growth medium was further supplemented with 30 µM PA, 25 µM OA and 15 µM LA (all bound to delipidated BSA at a molar FA/BSA ratio of 3:1).

After 24 hours the cells were harvested in HSL (+Pi) buffer, disrupted by sonication and the protein content of resulting cell lysates was determined using the Bradford protein assay. 20 µg of lysate protein per cell line were separated by SDS-PAGE, followed by Western blot analysis using Anti-FLAG M2-HRP antibody. In the following, equal protein loading was verified by staining the membrane with coomassie blue. Specific EYFP-3xFLAG and 3xFLAG-LacZ protein bands at the expected MW, respectively, were detected (Figure 5.29). In untreated cells, LacZ-expression levels were significantly reduced compared to YFP (indicated by lower signal intensity of the LacZ protein band). In contrast, the MG132-treated cells displayed similar signal intensities of the LacZ- and YFP protein-bands, which indicated equimolar expression of both target proteins. The results verified that P2A-medatiated co-expression *de facto* yields equimolar protein levels, but suggested that the observed expression levels depend on specific protein stability.

As demonstrated here, treatment of cells with proteasome inhibitor MG132 is a possible method to achieve equimolar protein expression with a 2A peptide-based expression system despite low protein stability (in this case low stability of LacZ).

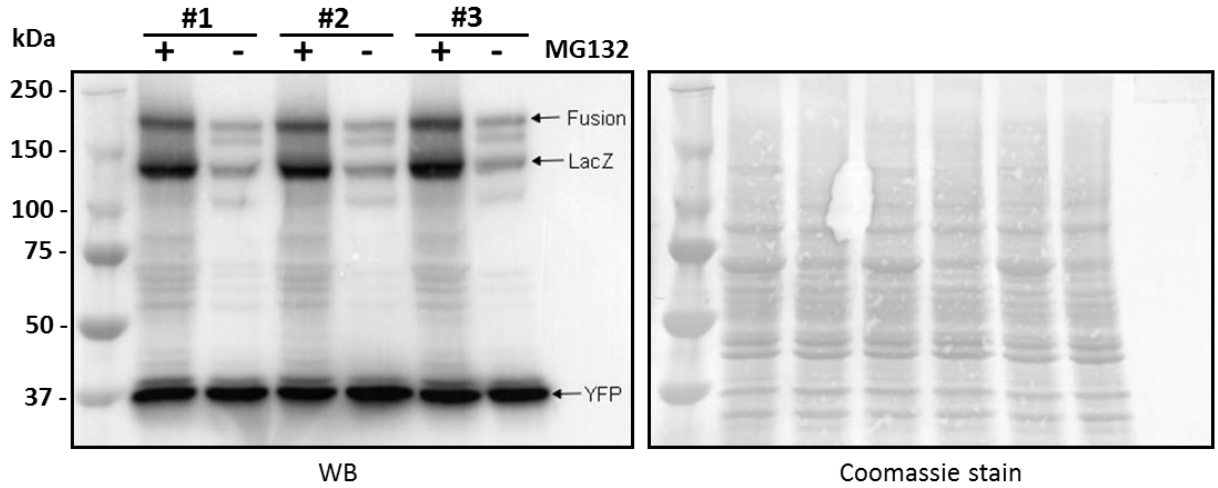


**Figure 5.29: Western blot analysis of HEK-293 cells stably co-expressing EYFP-3xFLAG and 3xFLAG-LacZ, after treatment with proteasome inhibitor MG132 (+) or DMSO (-).** HEK-293 cells from three different stable cell lines (#1-3) were treated with either 10 µM MG132 (dissolved in DMSO) or vehicle for 24 hours, harvested in HSL (+Pi) buffer and subjected to Western blot analysis using Anti-FLAG M2-HRP antibody. In untreated cells, LacZ expression levels were markedly reduced compared to YFP, but MG132-treatmant restored equimolar expression of both target proteins (indicated by similar LacZ and YFP signal intensities of the treated cells). Equal protein loading was verified by subsequent coomassie blue staining of the membrane.

### 5.5.3.5 ß-gal assay and fluorescence microscopy

To demonstrate that P2A-mediated self-cleavage of fusion proteins results correctly folded and enzymatically active enzymes, HEK-293 cells stably co-expressing EYFP-3xFLAG and 3xFLAG-LacZ were subjected to ß-gal assay and fluorescence microscopy (see section 4.6). Approximately 50% of cells displayed blue staining after incubation in β-gal staining solution B at 37°C for 12 hours, which indicated the presence of enzymatically active LacZ. Subsequent fluorescence microscopy with blue light (450-490 nm) excitation revealed uniform yellow-green fluorescence of all cells and thereby suggested strong expression of correctly folded EYFP (Figure 5.30).

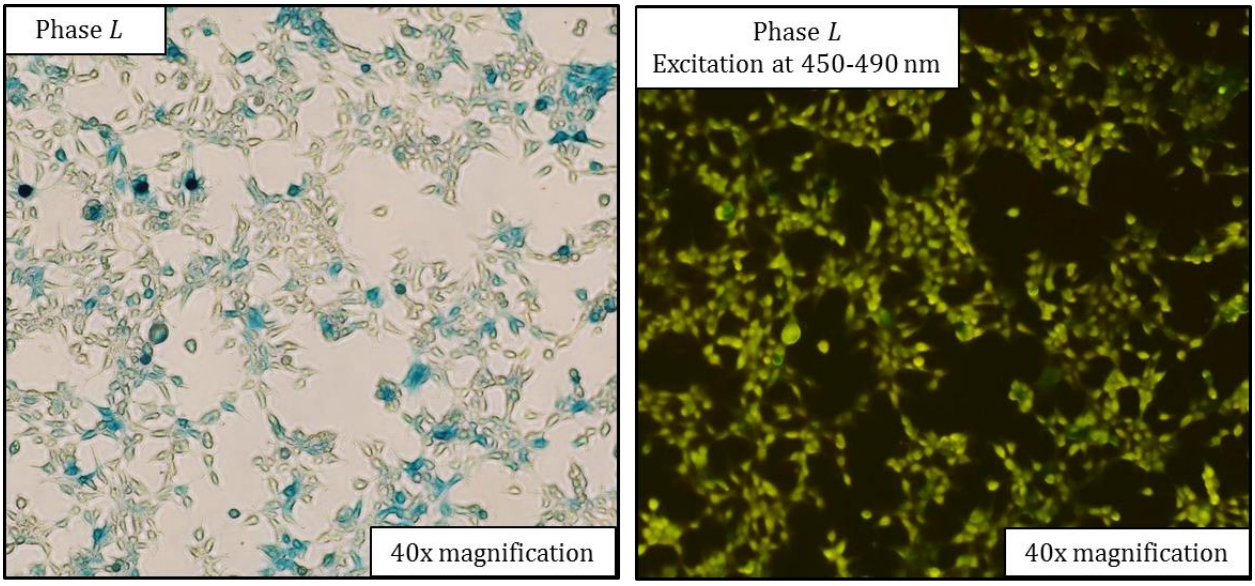


**Figure 5.30: ß-gal assay and fluorescence light microscopy of HEK-293 cells stably co-expressing EYFP and LacZ.** The HEK293-cells were incubated in β-gal staining solution B at 37°C for 12 hours, which resulted in blue staining of ~50% of cells and thereby verified expression of enzymatically active ß-galactosidase (left image). Furthermore, fluorescence microscopy with blue light excitation revealed uniform yellow-green fluorescence of all cells, which verified expression of correctly folded EYFP (right image). “Phase L” indicates the phase ring configuration that was used for microscopy.

## 5.6 Generation of bicistronic lentiviral constructs for co-expression of ELVOL4, CYP4F22, CERS3 and PNPLA1

After verifying that P2A-based expression vectors allow equimolar co-expression of correctly folded and enzymatically active target proteins (see 5.5), bicistronic constructs for co-expression of ELOVL4, CYP4F22, CERS3 and PNPLA1, the four target enzymes of the hypothetic ω-O-AcylCer synthesis pathway, were generated. As a control, two bicistronic constructs for the co-expression of EYFP together with LacZ or hPNPLA1(p.S53A) together with CERS3 were created. The four generated constructs are listed below:

- pLVX_PCMV_hCYP4F22_3FP2A3F_hELOVL4_Puro
- pLVX_PCMV_hPNPLA1_3FP2A3F_hCERS3_Neo
- pLVX_PCMV_hPNPLA1(p.S53A)_3FP2A3F_hCERS3_Neo
- pLVX_PCMV_EYFP_3FP2A3F_LacZ_Neo

### 5.6.1 Generation of pLVX_PCMV_hCYP4F22_3FP2A3F_hELOVL4_Puro

*CYP4F22* insert DNA (1603 bp) was generated by gradient PCR using primer pair hCYP_NotI_fw/hCYP_ 3F2A_XhoI_rv and HisMaxC_hCYP4F22 plasmid DNA as template (Figure 5.31). Three PCR reactions performed at the highest tested Tm (see Table 4.4) yielded specific PCR product with the expected MW. The DNA bands were purified from the agarose gel, cloned into MCS1 of pLVX_PCMV_3FP2A3F_Puro using NotI_HF/XhoI and successful cloning was verified by NcoI-HF control digest of recombinant plasmid DNA from selected clones. Plasmid DNA from clones 3 and #6 resulted in the expected 6196 bp, 1936 bp and 1748 bp-sized DNA fragments (Figure 5.32) and DNA sequencing (using primers PCMV_fw and pLVX_Tight_Puro_rv) confirmed that *CYP4F22* insert DNA was free of mutations. The plasmid was named pLVX_PCMV_hCYP4F22_3FP2A3F_Puro (9880 bp).

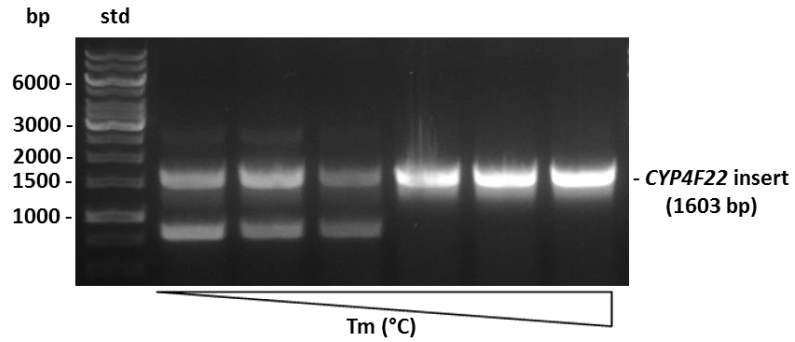


**Figure 5.31: Generation of *CYP4F22* insert DNA.** *CYP4F22* insert DNA was amplified by gradient PCR and products were analyzed by gel electrophoresis. Specific 1603 bp-sized PCR product was generated by reactions with the three highest Tm (66.4°C/68.4°C/69.5°C) and purified from the agarose gel.

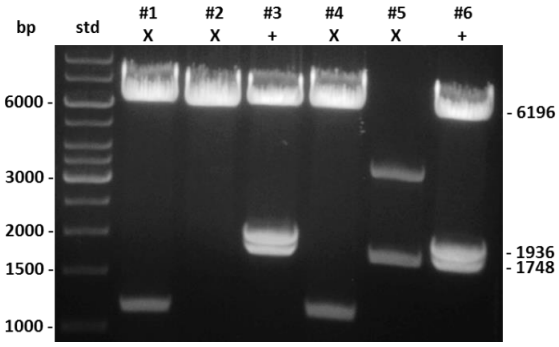


**Figure 5.32: NcoI-HF control digest of recombinant pLVX_PCMV_hCYP4F22_3FP2A3F_Puro constructs from six selected clones.** Digested plasmid DNA from clones #3 and #6 displayed the expected 6196 bp, 1936 bp and 1748 bp-sized DNA fragments.

Next, a gradient PCR (using primer pair hELOVL4_XmaI_fw/BGH_MluI_rv and HisMaxC_hELOVL4 plasmid DNA as template) was performed for amplification of *ELOVL4*-BGH insert DNA (1017 bp, Figure 5.33). The purified insert DNA was cloned into MCS2 of pLVX_PCMV_hCYP4F22_3FP2A3F_Puro (using XmaI/MluI), with incubation of *E. coli* at 25°C. NcoI-HF control digest of recombinant plasmid DNA from six selected clones resulted in the expected 6196 bp, 1944 bp, 1748 bp and 986 bp-sized DNA fragments (Figure 5.34) and DNA sequencing (using primers qRT_ELOVL4_fw and BGH_rv) further verified successful cloning. The plasmid was named pLVX_PCMV_hCYP4F22_3FP2A3F_hELOVL4_Puro (10,874 bp).

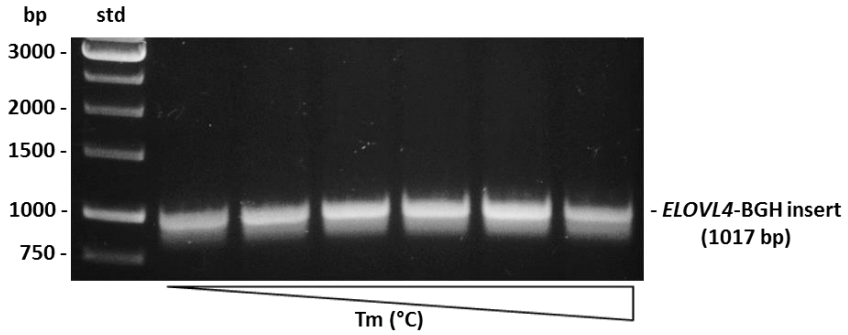


**Figure 5.33: Gradient PCR for generation of *ELOVL4*-BGH insert DNA (1017 bp).** PCR reactions with six different Tm (60.7°C/62.0°C/64.0°/66.4°C/68.4°C and 69.5°C) resulted in specific 1017 bp-sized PCR product, which was purified from the agarose gel and used for molecular cloning.

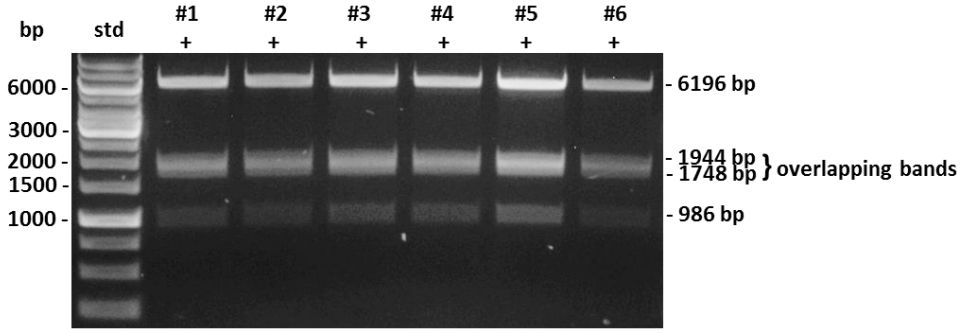


**Figure 5.34: NcoI-HF control digest of recombinant pLVX_PCMV_hCYP4F22_3FP2A3F_hELOVL4_Puro constructs from six selected clones.** Digested plasmid DNA from all different clones displayed the expected 6196 bp, 1944 bp, 1748 bp and 986 bp-sized DNA fragments.

### 5.6.2 Generation of pLVX_PCMV_hPNPLA1_3FP2A3F_hCERS3_Neo

For amplification of *PNPLA1* insert DNA (1623 bp) a gradient PCR using primer pair 5'hP1_NotI_fw/5'hP1_3F2A_XhoI_rv and HisMaxC_hPNPLA1 plasmid DNA as template was performed (Figure 5.35A). Purified *PNPLA1* insert DNA was cloned into MCS1 of pLVX_PCMV_3FP2A3F_Neo (using NotI_HF and XhoI) and recombinant plasmid DNA from selected clones was confirmed by RE digestion (data not shown), followed by DNA sequencing with primer PCMV_fw. The verified plasmid was named pLVX_PCMV_hPNPLA1_3FP2A3F_Neo (10,433 bp).

Next, *CERS3* insert DNA (1203 bp) was generated by gradient PCR (using primer pair hCERS3_XbaI_fw/hCERS3_3F2A_MluI_rev and HisMaxC_hCERS3 plasmid DNA as template, Figure 5.35A), purified and cloned into MCS2 of pLVX_PCMV_hPNPLA1_3FP2A3F_Neo using XbaI and MluI. Resulting recombinant plasmid DNA from three different selected clones displayed the expected 6196 bp, 2298 bp, 970 bp, 703 bp, 691 bp and 305 bp-sized DNA fragments upon NcoI-HF control digest (Figure 5.35B) and was further verified by DNA sequencing (using primers PCMV_fw and qRT_CERS3_rv). The confirmed plasmid was named pLVX_PCMV_hPNPLA1_3FP2A3F_hCERS3_Neo (11,619 bp).

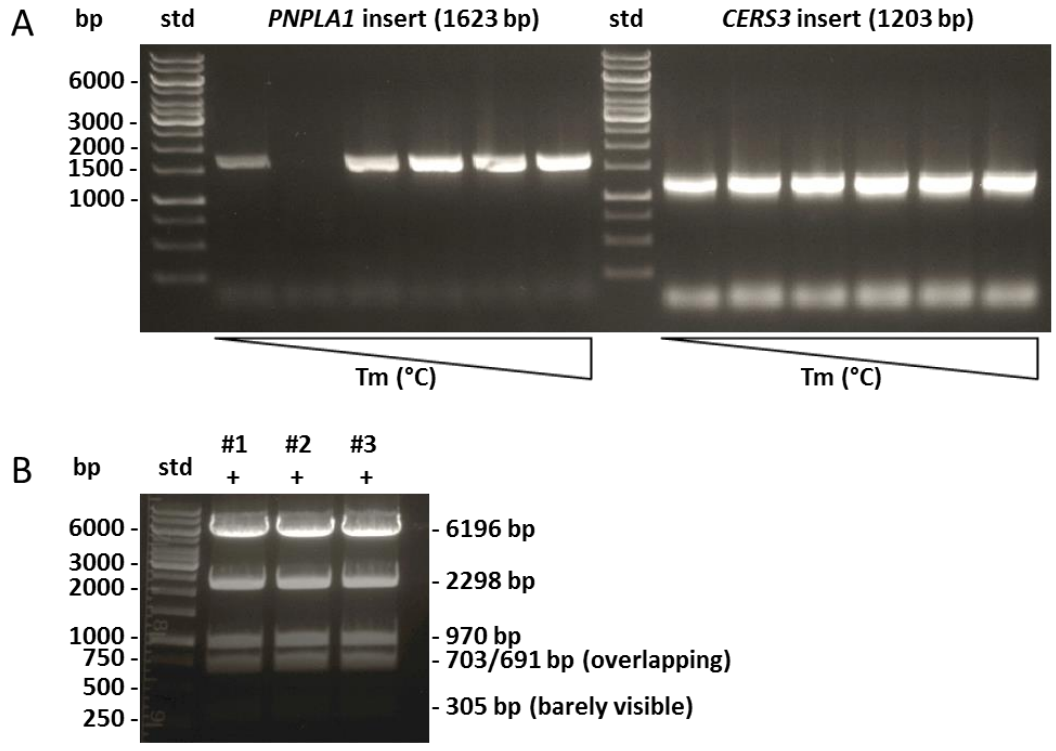


**Figure 5.35: Construction of pLVX_PCMV_hPNPLA1_3FP2A3F_hCERS3_Neo. A)** *PNPLA1* (1623 bp) and *CERS3* (1203 bp) insert DNA was amplified by gradient PCR and resulting specific PCR products with the expected MW, respectively, were purified from the agarose gel. **B)** To verify successful ligation of *CERS3* insert DNA and pLVX_PCMV_hPNPLA1_3FP2A3F_Neo vector DNA, recombinant plasmid DNA from three clones was digested with NcoI-HF. All clones displayed the expected 6196 bp, 2298 bp, 970 bp, 703 bp, 691 bp and 305 bp-sized DNA fragments.

### 5.6.3 Generation of pLVX_PCMV_hPNPLA1(p.S53A)_3FP2A3F_hCERS3_Neo

Human *PNPLA1* with a c.157T>G (TCG>GCG) missense mutation (that results in a p.S53A substitution in the gene products intrinsic catalytic diad) was cloned into MCS1 of pLVX_PCMV_3FP2A3F_Neo, exactly as described in section 5.6.2, except HisMaxC_hPNPLA1(p.S53A) instead of HisMaxC_hPNPLA1 was used as template for PCR amplification of insert DNA (Figure 5.36A). Successful cloning was verified by RE control digest of recombinant plasmid DNA (data not shown) and the c.157T>G (TCG>GCG) missense mutation was confirmed by DNA sequencing using primers PCMV_fw and qRT_P1_fw (Figure 5.36B). The plasmid was named pLVX_PCMV_hPNPLA1(p.S53A)_3FP2A3F_Neo (10,433 bp).

In the following, human *CERS3* insert DNA was cloned into MCS2 of pLVX_PCMV_hPNPLA1(p.S53A)_3FP2A3F_Neo, exactly as described in section 5.6.2. To confirm successful cloning, recombinant plasmid DNA from five different selected clones was subjected to NcoI-HF control digest, which resulted in the expected 6196 bp, 2298 bp, 970 bp, 703 bp, 691 bp and 305 bp-sized DNA fragments (Figure 5.35B). The verified plasmid was named pLVX_PCMV_hPNPLA1(p.S53A)_3FP2A3F_hCERS3_Neo (11,619 bp).

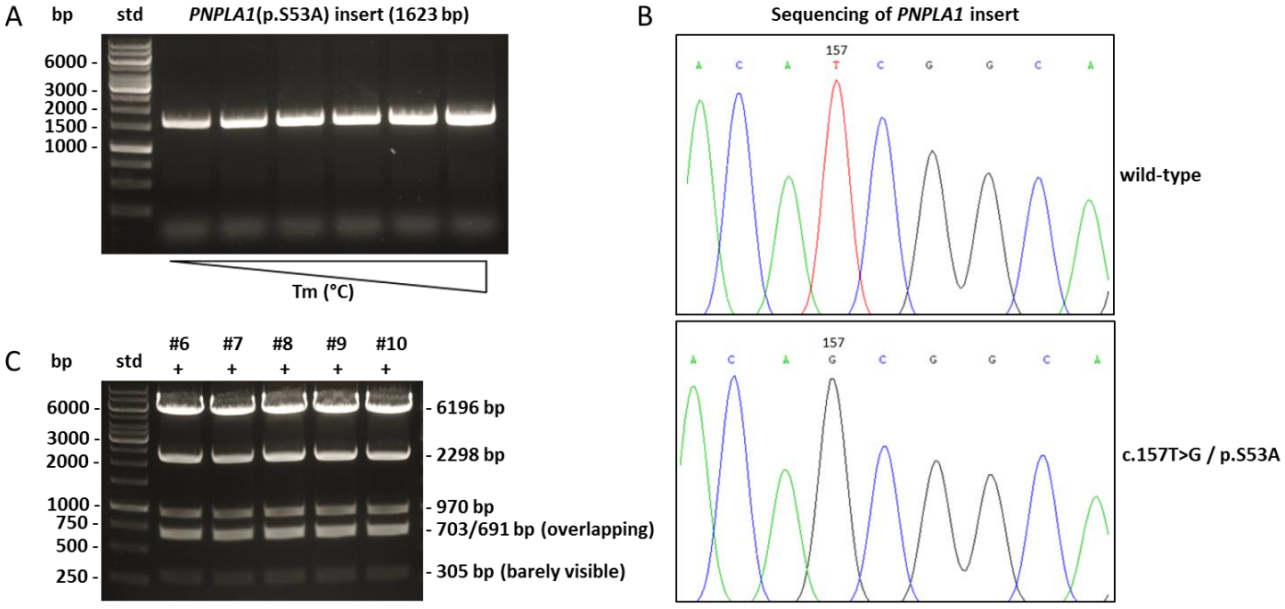


**Figure 5.36: Construction of pLVX_PCMV_hPNPLA1(p.S53A)_3FP2A3F_hCERS3_Neo. A)** Amplification of *PNPLA1*(p.S53A) insert DNA by gradient PCR resulted in expected specific 1623 bp-sized DNA bands. **B)** The c.157T>G (TCG>GCG) missense mutation in *PNPLA1*(p.S53A) insert DNA was confirmed by DNA sequencing of *PNPLA1*(p.S53A) and wild-type *PNPLA1* CDS, followed by chromatogram alignment. **C)** NcoI-HF control digest of recombinant pLVX_PCMV_hPNPLA1(p.S53A)_3FP2A3F_Neo constructs from five different selected clones led to formation of the expected 6196 bp, 2298 bp, 970 bp, 703 bp, 691 bp and 305 bp-sized DNA fragments.

### 5.6.4 Generation of pLVX_PCMV_EYFP_3FP2A3F_LacZ_Neo

*EYFP* and *LacZ* DNA inserts were consecutively cloned into MCS1 and MCS2, respectively, of pLVX_PCMV_3FP2A3F_Neo, exactly as described in section 5.5.3.1. Resulting recombinant pLVX_PCMV_EYFP_3FP2A3F_Neo plasmid DNA (9139 bp) from cloning of the upstream gene was verified by DNA sequencing using primer PCMV_fw.

By subsequent cloning of the downstream gene pLVX_PCMV_EYFP_3FP2A3F_LacZ_Neo plasmid DNA (12,242 bp) was generated. The construct was confirmed by NcoI-HF control digest of recombinant plasmid DNA from three different selected clones, which resulted in the expected 6196 bp, 4348 bp, 703 bp, 691 bp and 304 bp-sized DNA fragments (Figure 5.37). DNA sequencing using primer LacZ_XmaI_fw confirmed that the *LacZ* insert DNA was cloned in frame with the vector start codon and the upstream gene.

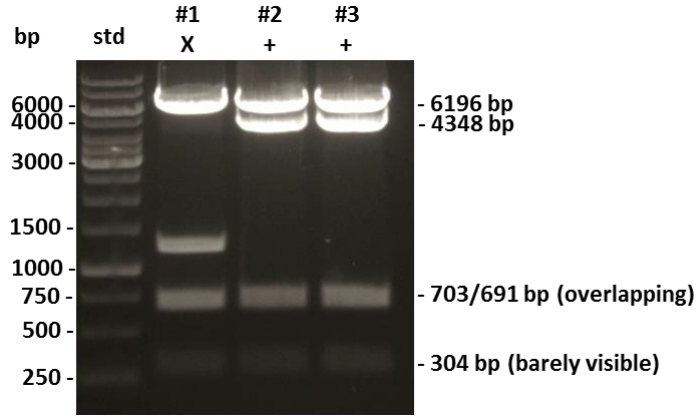


**Figure 5.37: NcoI-HF control digest of recombinant pLVX_PCMV_EYFP_3FP2A3F_LacZ_Neo plasmid DNA from three different selected clones.** Digested vector DNA from clones #2 and #3 displayed expected 6196 bp, 4348 bp, 703 bp, 691 bp and 304 bp-sized DNA fragments, which confirmed successful cloning of *LacZ* insert DNA.

## 5.7 Analysis of ω-O-AcylCer synthesis in COS-7, HaCat or HEK-293T cells co-expressing ELOVL4, CYP4F22, CERS3 and PNPLA1

To investigate the hypothetic pathway for ω-O-AcylCer formation, ELOVL4 (for generation of ULFAs ≥C26), CYP4F22 (for ω-hydroxylation of ULFAs ≥C28), CERS3 (for amide bond linkage of ω-OH-ULFAs and sphingoid bases) and PNPLA1 (the putative transacylase for esterification of ω-OH-CER with LA) were co-expressed in COS-7, HaCaT, or HEK-293T cells. Therefore, the cells were either transfected or transduced with lentiviral particles using different pLVX_PCMV_3FP2A3F_Puro/Neo or pcDNA4_HisMaxC vector constructs. In the following, cellular lipids were traced by radiolabeling using [$^{14}$C]LA, [$^{14}$C]PA or [3-$^{3}$H]D-erythro-sphingosine C-18. To investigate effects on the ceramide metabolism of the overexpressing cells, resulting lipid extracts were then subjected to TLC analysis.

To facilitate readability, the used vector constructs will be abbreviated as following:

- pLVX_PCMV_hCYP4F22_3FP2A3F_hELOVL4_Puro = Y+E_Puro
- pLVX_PCMV_hPNPLA1_3FP2A3F_hCERS3_Neo = P1+C_Neo
- pLVX_PCMV_hPNPLA1(p.S53A)_3FP2A3F_hCERS3_Neo = P1$^{mut}$+C_Neo
- pLVX_PCMV_EYFP_3FP2A3F_LacZ_Neo = YFP+LacZ_Neo

### 5.7.1 Analysis of ω-O-AcylCer synthesis in COS-7 cells transiently co-expressing ELOVL4, CYP4F22, CERS3 and PNPLA1

For transient co-expression of the target enzymes ELOVL4, CYP4F22, CERS3 and PNPLA1, COS-7 cells were co-transfected with Y+E_Puro and P1+C_Neo using metafectene. As a negative control, COS-7 cells were co-transfected with Y+E_Puro and P1$^{mut}$+C_Neo. Twenty-four hours post-transfection, cell samples were harvested in 1x SDS loading buffer and subjected to Western blot analysis using Anti-FLAG M2-HRP antibody. Equal protein loading was confirmed by coomassie blue staining of the membrane. Western blotting verified expression of CYP4F22-3xFLAG (67.16 kDa), 3xFLAG-CERS3 (50.71 kDa) and 3xFLAG-ELOVL4 (39.97 kDa) together with wild-type PNPLA1-3xFLAG or PNPLA1(p.S53A)-3xFLAG (63.09 kDa), respectively (Figure 5.38). In comparison to PNPLA1 and CYP4F22, the expression levels of CERS3 and ELOVL4 were slightly reduced.

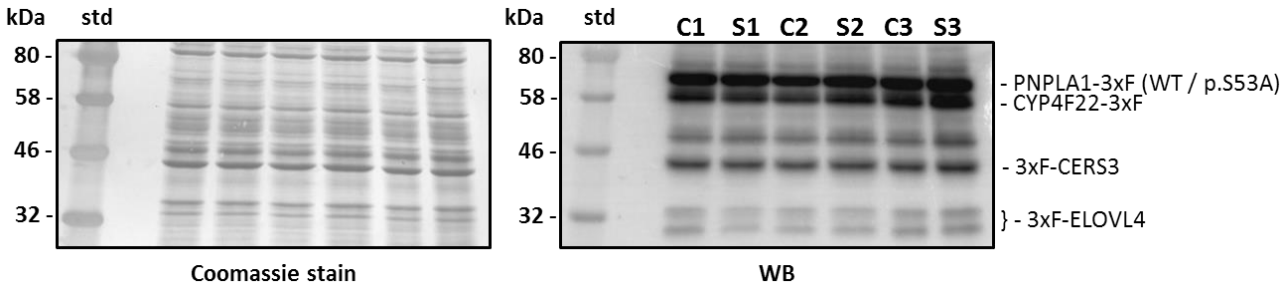


**Figure 5.38: Western blot analysis of COS-7 cells transiently co-expressing four target proteins.** Using metafectene, COS-7 cells were co-transfected with either Y+E_Puro and P1+C_Neo (S1-3) or Y+E_Puro and P1$^{mut}$+C_Neo (C1-3). After 24 hours, cell samples were harvested in 1x SDS loading buffer and target protein expression was assessed by Western blot analysis using Anti-FLAG M2-HRP antibody. The different target protein bands (as indicated) were detected at the expected MWs.

In the following, radiolabeling of cellular lipids for 24 hours using [$^{14}$C]LA, total lipid extraction and TLC separation were performed as described in section 4.7. [$^{14}$C]LA-labeled epidermal lipid extracts from wild-type or *Cgi-58*$^{epid}$-/- mice were used as a standard for ω-O-AcylCer migration. Autoradiography signals were obtained by exposure to a PhosphorImager Screen for 72 hours and analyzed using a Storm-scanner and Storm-associated software.

However, the expected formation of ω-O-AcylCers in cells co-expressing ELVOL4, CYP4F22 and CERS3 together with wild-type PNPLA1 was not observed (Figure 5.39).

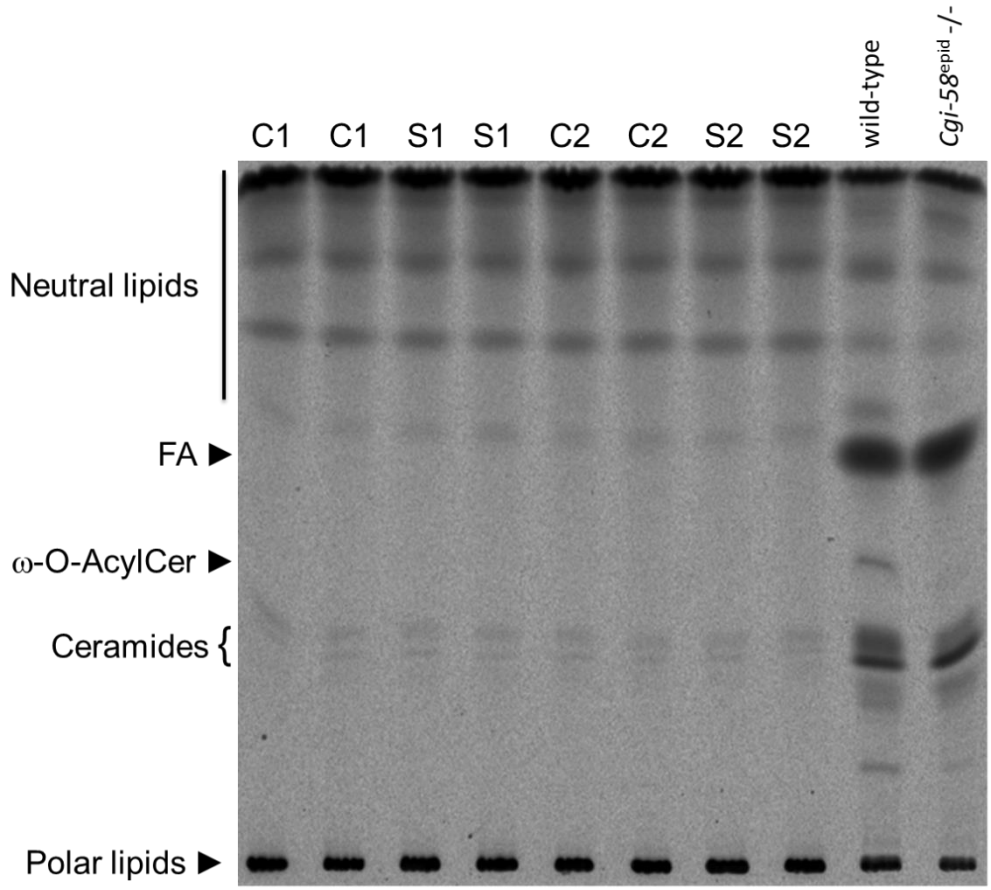


**Figure 5.39: TLC separation of radiolabeled lipids ([$^{14}$C]LA as tracer) from COS-7 cells transiently co-expressing human ELOVL4, CYP4F22, CERS3 together with either wild-type PNPLA1 (samples S1-3) or PNPLA1(p.S53A) (samples C1-3).** Ceramides were separated twice using chloroform/methanol/glacial acetic acid (190:9:1 v/v/v) as the solvent system for TLC and [$^{14}$C]LA labeled epidermal lipid extracts from wild-type or Cgi-58$^{epid-/-}$ mice as a standard for ω–O-AcylCer migration. Specific ω–O-AcylCer autoradiography signals were neither observed in the control or target samples, which indicated absence of detectable amounts of ω–O-AcylCer in the cells. FA, fatty acids; ω-O-AcylCer, ω-O-acylceramides.

### 5.7.2 Analysis of ω-O-AcylCer synthesis in HaCaT cells stably co-expressing ELOVL4, CYP4F22, CERS3 and PNPLA1

For stable co-expression of the target enzymes, HaCaT cells were co-transduced using two different lentiviral suspensions, which were generated using Y+E_Puro and P1+C_Neo (see section 4.3). As a negative control, a second stable HaCaT cell line co-expressing ELOVL4 and CYP4F22 together with EYFP and LacZ was generated using Y+E_Puro and YFP+LacZ_Neo for production of lentiviral particles. For positive selection, the co-transduced HaCaT cells were cultivated in DMEM +/+ containing 1.0 µg/ml puromycin and 1.0 mg/ml G418 for 14 days.

Two weeks post-transduction, cell samples from the two different HaCaT cell lines were harvested in 1x SDS loading buffer and expression of CYP4F22-3xFLAG and 3xFLAG-ELOVL4 together with either EYFP-3xFLAG and 3xFLAG-LacZ or PNPLA1-3xFLAG and 3xFLAG-CERS3 was verified by Western blot analysis using Anti-FLAG M2-HRP antibody (Figure 5.40). This analysis revealed low expression levels of LacZ, CERS3 and EYFP, but strong protein expression of PNPLA1, CYP4F22 and ELOVL4.

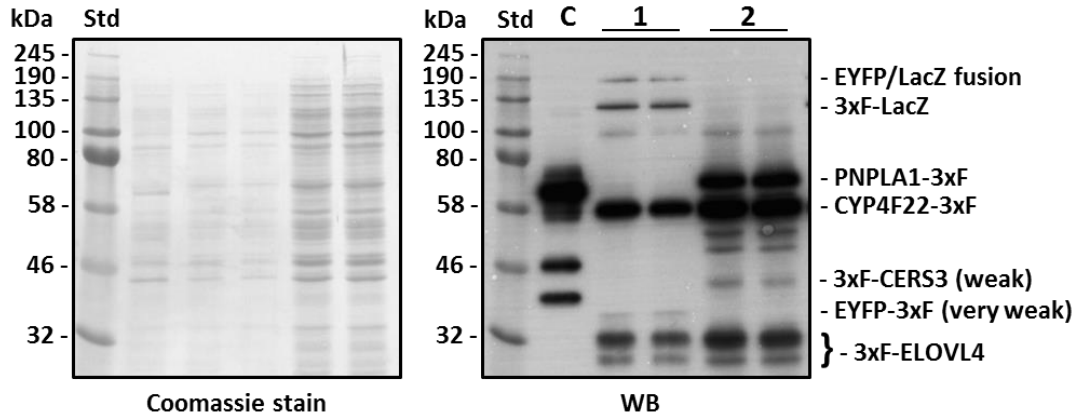


**Figure 5.40: Western blot analysis of HaCaT cells stably co-expressing four target proteins.** The cells were co-transduced with two different bicistronic lentiviral suspensions, which encoded *CYP4F22* and *ELOVL4* together with either *EYFP* and *LacZ* (lane 1) or *PNPLA1* and *CERS3* (lane 2). After 14 days of positive selection with both 1.0 µg/ml puromycin and 1.0 mg/ml G418 samples from the two different cell lines were harvested in 1x SDS loading buffer and expression of the target proteins was assessed by Western blot analysis (using Anti-FLAG M2-HRP antibody). Specific target protein bands were detected at the expected MWs, as indicated. As a MW control for PNPLA1 and CERS3, cellular lysate from HEK-293 cells transiently co-expressing PNPLA1-1xFLAG and 1xFLAG-CERS3 was loaded to lane "C". Due to the smaller 1xFLAG-tag, the detected proteins were shifted towards a smaller MW compared to the corresponding 3xFLAG-tagged proteins.

Next, radiolabeling of cellular lipids for 24 hours using [$^{14}$C]LA or [$^{14}$C]PA, followed by TLC analysis of ceramide metabolism were performed as described in section 4.7. Again, [$^{14}$C]LA-labeled epidermal lipid extracts from wild-type or *Cgi-58*$^{epid}$-/- mice were used as a standard for ω-O-AcylCer migration.

Weak ω-O-AcylCer autoradiography signals were detected in all [$^{14}$C]LA labeled samples, but not in the [$^{14}$C]PA labeled samples. However, the expected accumulation of ω-O-AcylCer in HaCaT cells expressing ELOVL4, CYP4F22, CERS3 and PNPLA1 in comparison to cells expressing ELOVL4 and CYP4F22 together with EYFP and LacZ was not observed (Figure 5.41).

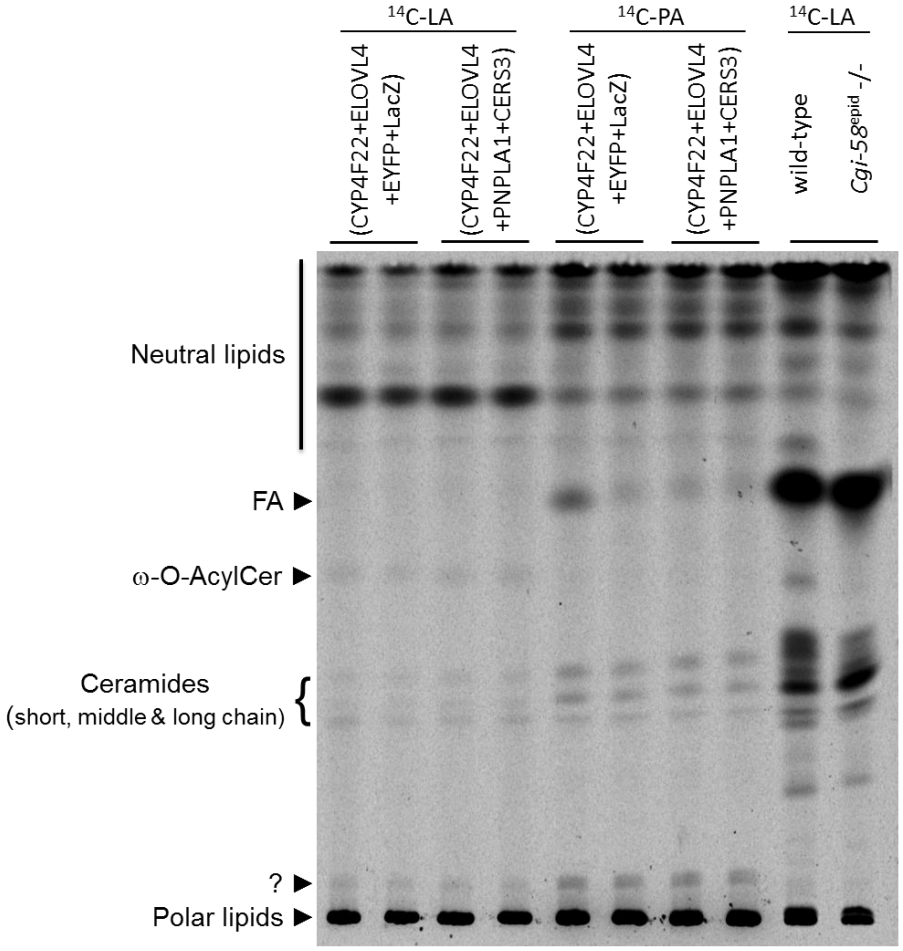


**Figure 5.41: TLC separation of radiolabeled lipids ([$^{14}$C]LA or [14C]PA as tracer) from HaCaT cells stably co-expressing human ELOVL4 and CYP4F22 together with either EYFP and LacZ or PNPLA1 and CERS3.** Ceramides were separated twice using chloroform/methanol/glacial acetic acid (190:9:1 v/v/v) as the solvent system for TLC and [$^{14}$C]LA labeled epidermal lipid extracts from wild-type or Cgi-58$^{epid-/-}$ mice as a standard for ω–O-AcylCer migration. Specific ω-O-AcylCer autoradiography signals were only detected in the [$^{14}$C]LA labeled-, but not the [$^{14}$C]PA labeled samples. The expected ω-O-AcylCer accumulation in cells expressing the target enzymes (including PNPLA1) could not be verified, as the observed ω-O-AcylCer signal intensities were very similar to the corresponding ω-O-AcylCer signals from cells expressing control proteins (CYP4F22 and ELOVL4 together with EYFP and LacZ).

### 5.7.3 Analysis of ω-O-AcylCer synthesis in HEK-293T cells transiently co-expressing ELOVL4, CYP4F22, CERS3 and PNPLA1

For transient co-expression of the target proteins, HEK-293T cells were co-transfected with four different HisMaxC constructs or two different pLVX_PCMV_3FP2A3F_Puro/Neo constructs using metafectene. The used constructs for transfection included: HisMaxC_LacZ, HisMaxC_hPNPLA1, HisMaxC_hPNPLA1(p.S53A), HisMaxC_hCYP4F22, HisMaxC_hCERS3, HisMaxC_hELOVL4, Y+E_Puro, P1+C_Neo and $P1^{mut}$+C_Neo. To verify co-expression, samples of the different transfected cell lines were harvested in 1x SDS loading buffer 24 hours post-transfection, followed by Western blot analysis using Anti-His (N-term) (Figure 5.42A) or Anti-FLAG M2-HRP antibodies (Figure 5.42B). The expected target protein bands were detected at the predicted MWs, as indicated in Figure 5.42. However, the expression levels of His-CERS3, His-ELOVL4, 3xFLAG-CERS3 and 3xFLAG-ELOVL4 were distinctively reduced in the HEK-293T cells, compared to the other expressed proteins.

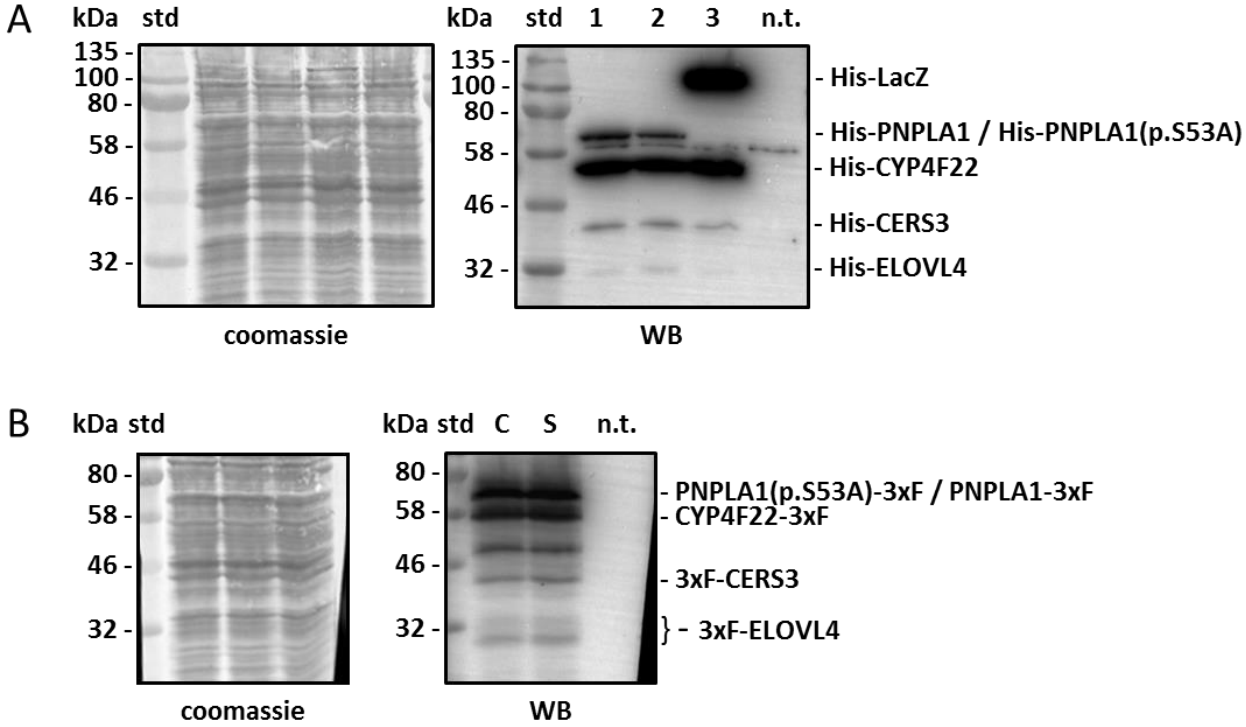


**Figure 5.42: Western blot analysis of HEK-293T cells, transiently co-expressing four target proteins.** Using metafectene, HEK-293T cells were co-transfected with either four different HisMaxC constructs or two different pLVX_PCMV_3FP2A3F_Puro/Neo constructs. 24 hours post-transfection, cell samples from the different cell lines were harvested in 1x SDS loading buffer and resulting cellular lysates were subjected to Western blot analysis using either Anti-His (N-term) antibody **(A)** or Anti-FLAG M2-HRP antibody **(B)**. Detection of specific protein bands (as indicated) at the predicted MW verified co-expression of the different target proteins, but revealed low cellular expression levels of His-CERS3, His-ELOVL4, 3xFLAG-CERS3 and 3xFLAG-ELOVL4 (indicated by low signal intensities of the corresponding protein bands). n.t. = lysate from non-transfected cells (negative control).

Similar to previous experiments, the ceramide metabolism of the different generated cell lines was investigated by radiolabeling of cellular lipids using [3-$^{3}$H]D-erythro-sphingosine C-18 and subsequent TLC-analysis (see section 4.7). [$^{14}$C]PA-labeled Epidermal lipid extracts from wild-type or *Cgi-58*$^{epid}$-/- mice were used as a standard for ω-O-AcylCer migration. In contrast to previous experiments, autoradiography signals were detected by spraying the TLC plate with a mixture of scintillation cocktail (Roth)/methanol/$H_2O$ (4:1:1, v/v/v) and exposing the dried plate to a light sensitive film at -80°C for 72 hours instead of using a PhosphorImager Screen and a Storm-scanner.

Formation of detectable ω-O-AcylCer levels in the HEK-293T cells co-expressing ELOVL4, CYP4F22, CERS3 and PNPLA1 was not observed (Figure 5.43). Furthermore, the lipid profiles of the different cell lines appeared to be very similar, as no apparent signal intensity differences were detected. The lipid species represented by the strong signals annotated as "?" in Figure 5.43 was not identified. However, it likely did not represent ω-O-AcylCer, as it migrated farther than the ω-O-AcylCer standard from wild-type murine epidermal lipid extract.

Taken together, transient or stable co-expression of ELOVL4, CYP4F22 and CERS3 together with PNPLA1 in three different mammalian cell lines (COS-7, HaCat or HEK-293T) did not result in the expected formation of ω-O-AcylCers. These results argue against a putative specific transacylase activity of PNPLA1 for esterification of ω-OH-Cers with linoleic acid.

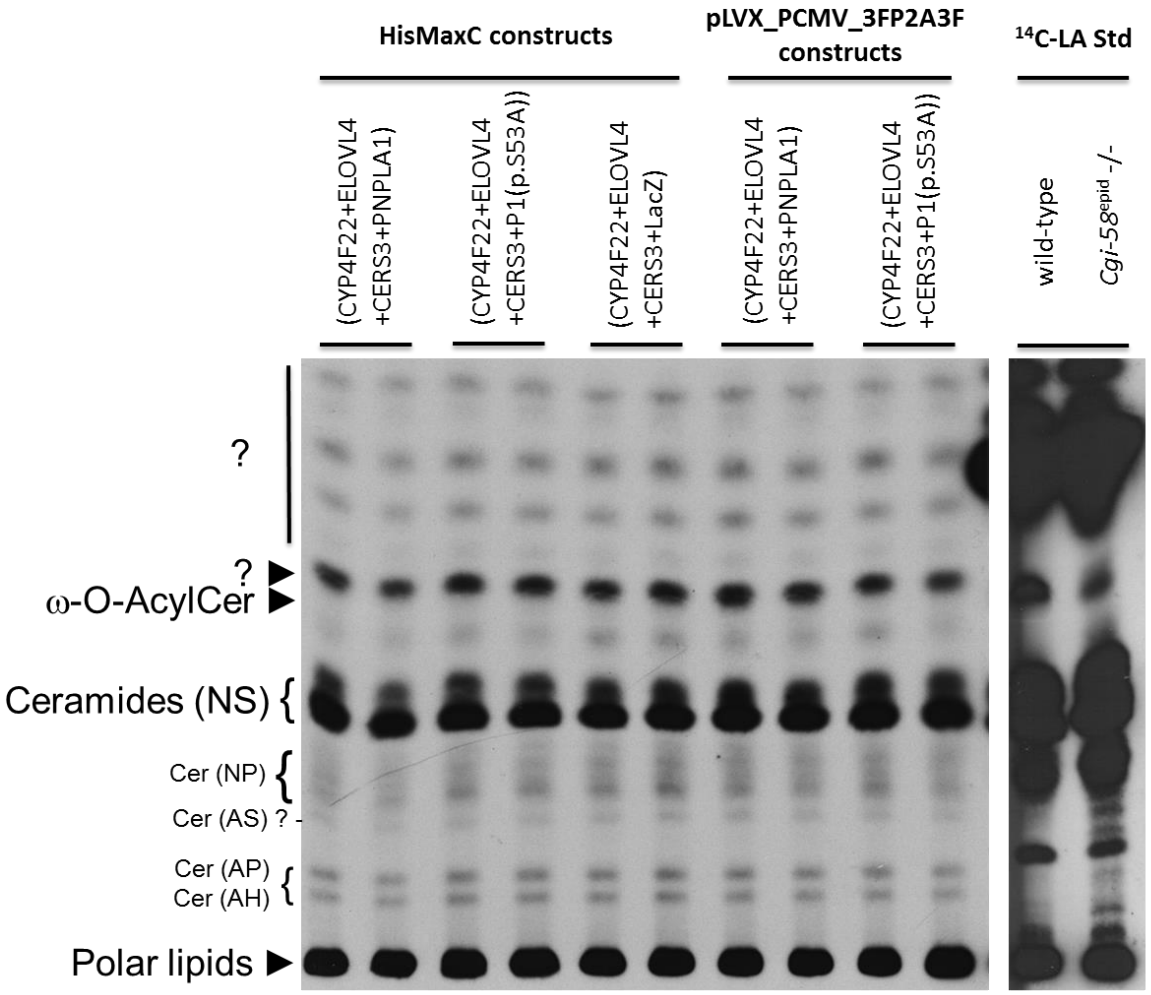


**Figure 5.43: TLC separation of radiolabeled lipids ([3-$^{3}$H]D-erythro-sphingosine C-18 as tracer) from HEK-293T cells transiently co-expressing different combinations of ELOVL4, CYP4F22, CERS3, PNPLA1, PNPLA1(p.S53A) and LacZ.** Ceramides were separated twice using chloroform/methanol/glacial acetic acid (190:9:1 v/v/v) as the solvent system for TLC and [$^{14}$C]PA labeled epidermal lipid extracts from wild-type or Cgi-58$^{epid-/-}$ mice as a standard for ω–O-AcylCer migration. Specific ω–O-AcylCer autoradiography signals were neither observed in the control or target samples, which indicated absence of detectable amounts of ω–O-AcylCer in the cells. In the *Cgi-58*$^{epid}$-/- negative control, residual ω–O-AcylCer was detected due to long exposure time and high sensitivity of the used light sensitive film.

# 6 Discussion

Members of the PNPLA protein family are key enzymes in lipid metabolism and exhibit diverse lipolytic and acyltransferase activities [37]. Until lately, the physiological role and enzymatic activity of PNPLA1 remained unclear. However, in recent publications it was demonstrated that *PNPLA1* mutations are associated with ARCI in humans and Golden Retriever dogs [28,32–36]. Furthermore, the generation of *Pnpla1* knockout mice revealed that such animals display an ichthyosiform skin phenotype and die shortly after birth due to skin barrier dysfunction [24]. It was demonstrated that the barrier defect in *Pnpla1* -/- mice was most probably caused by impaired CLE formation due to the almost complete lack of ω-O-AcylCer in the epidermis, which indicated defective ω-O-AcylCer synthesis. On the other hand, PNPLA1 deficient mice exhibited a distinct accumulation of ω-OH-Cer (the supposed precursor lipids of ω-O-AcylCer) in the epidermis [24].

Based on these results it has been hypothesized that PNPLA1 is the yet unknown acyltransferase/transacylase, which catalyzes the final step of ω-O-AcylCer synthesis (the esterification of ω-OH-Cer with linoleic acid) [4,5,10,24]. To investigate this hypothesis *in vivo*, I decided to perform similar experiments as demonstrated by Ohno *et. al.* [10] identifying the enzymatic function of CYP4F22. In their experiments, Ohno and colleagues co-transfected HEK-293T cells with three different plasmids encoding *3xFLAG-ELOVL4*, *3xFLAG-CERS3* and different *3xFLAG-CYP4F* subfamily members. By radiolabeling cellular lipids with [$^{3}$H]sphingosine and subsequent TLC analysis the authors demonstrated ω-OH-Cers formation in the presence of CYP4F22, which did not occur when another CYP4F subfamily member was co-expressed instead. Thereby they identified CYP4F22 as an ULFA-specific ω-hydroxylase [10].

Similar to this experimental approach, I planned to co-express the three known crucial enzymes of ω-OH-Cer synthesis (ELOVL4, CYP4F22 and CERS3) together with PNPLA1 in HEK-293T, HaCaT or COS-7 cells and analyze the lipid profile accordingly. As a negative control, I planned to express a putative enzymatically inactive mutant variant of PNPLA1 (p.S53A) or an enzymatically inert yellow fluorescent protein (YFP) instead of wild-type PNPLA1.

## 6.1 Generation and evaluation of bicistronic lentiviral expression vectors

As mentioned in the introduction (see section 1.4), co-transfection of multiple single-gene constructs (for instance as conducted by Ohno *et. al.* [10]) is problematic because it cannot be guaranteed that every single cell carries all desired plasmids and therefore expresses all desired gene products. The probability to successfully co-transfect a single cell with multiple DNA constructs decreases with a higher number of different plasmids. Moreover, the cellular uptake of varying amounts of plasmid DNA may result in unequal expression levels of the target proteins. Taken together, these factors may affect the result and reproducibility of experiments and further make it difficult to generate a cell culture model for a multi-gene pathway. To overcome these problems, I generated a bicistronic lentiviral expression system based on the commercially available expression vector pLVX_Tight_Puro. The workflow for generation of the four resulting vector constructs is summarized in Figure 6.1.

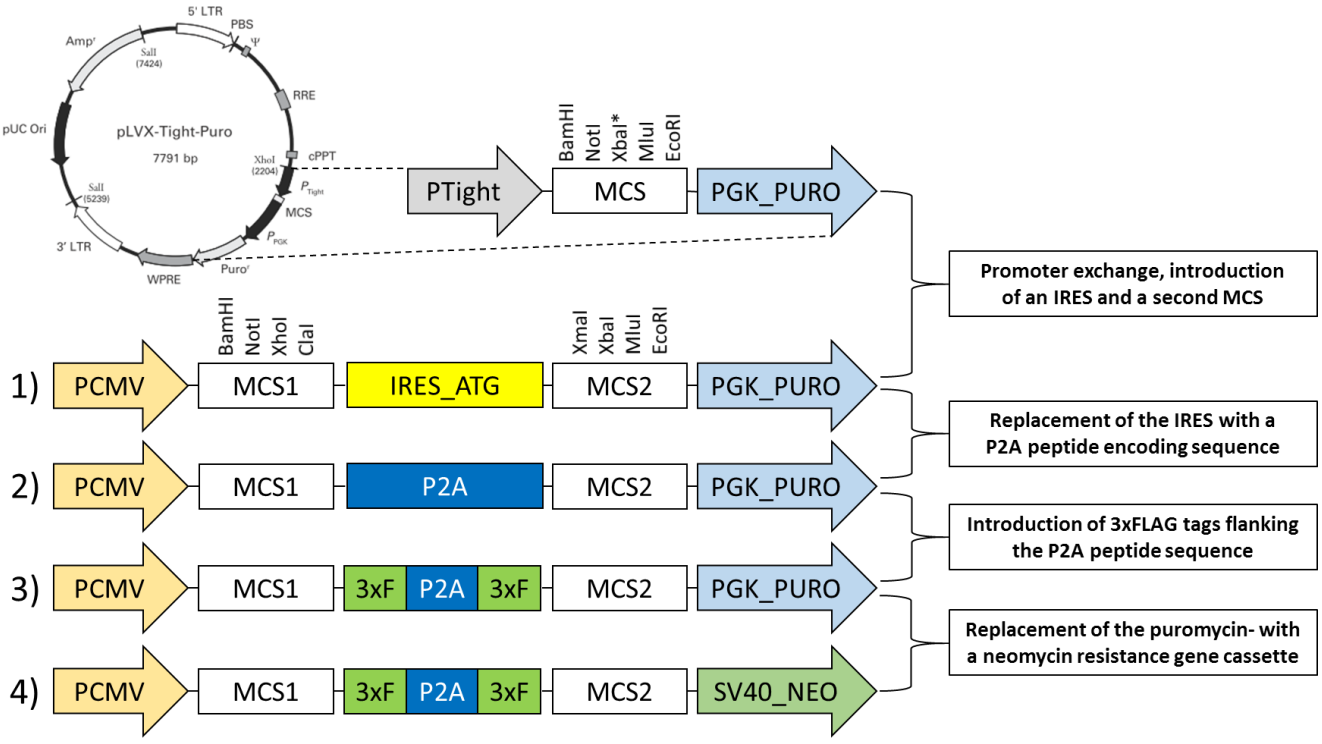


**Figure 6.1: Schematic workflow for the generation of four different bicistronic vector constructs, based on the commercial lentiviral expression vector pLVX-Tight-Puro (Clontech).**

As the original $P_{tight}$ promoter of pLVX-Tight-Puro required the presence of a tetracycline controlled transactivator for transcription-activation, I replaced it with a constitutively active cytomegalovirus promoter ($P_{CMV}$). This strong eukaryotic promoter resulted in high expression levels of target proteins.

Next, I generated an IRES DNA insert with flanking RE recognition sites by PCR and cloned it into the vector construct containing the $P_{CMV}$ promoter. The resulting bicistronic construct (Figure 5.4) was used for successful co-expression of murine *Pnpla1*-His and human *CYP4F22*-His in COS-7 cells (Figure 5.21). However, the expression level of the downstream gene (*CYP4F22*) was significantly reduced compared to the upstream gene (*Pnpla1*) (Figure 5.21). As mentioned in section 1.4, this is a common problem of IRES-mediated co-expression.

To achieve equimolar expression levels of target proteins, I replaced the IRES with a 2A peptide sequence, which has been reported to have very high cleavage efficiency [52]. The resulting P2A vector construct (Figure 5.6) had a significantly smaller size than the IRES-containing construct. As the packaging capacity of lentiviral particles is limited, the P2A-containing vector therefore allowed lentiviral transduction of larger genes.

I further generated a version of the bicistronic vector with a P2A sequence flanked by 3xFLAG tags (Figure 5.8), which enabled C-terminal tagging of the upstream gene and N-terminal tagging of the downstream gene. As the Anti-FLAG M2 antibody recognizes FLAG tags at both termini and even at internal sites, this allowed simultaneous detection of co-expressed proteins as well as uncleaved fusion proteins by Western blot analysis.

At last, I constructed a third version of the P2A construct that encoded a neomycin resistance gene, instead of a puromycin resistance gene (Figure 5.11). Therefore, the expression system could be used for co-transduction of target cells with two different bicistronic lentiviruses (one type mediating a puromycin and the other a neomycin resistance). By treating co-transduced cells with both antibiotics for positive selection, the system enabled generation of cell lines stably co-expressing four target proteins.

Using the generated P2A constructs, I demonstrated equimolar transient or stable co-expression of different target proteins (PNPLA1+CERS3, PNPLA1+CYP4F22 or EYFP+LacZ) in COS-7 or HEK-293 cells. Western blot analysis suggested highly efficient P2A-mediated cleavage of PNPLA1-P2A-CERS3 and PNPLA1-P2A-CYP4F22 fusion proteins, as no uncleaved proteins were detected (Figure 5.23 and Figure 5.25). However, co-expression of EYFP and LacZ resulted in formation of both target proteins as well as uncleaved

EYFP-P2A-LacZ fusion protein (Figure 5.27, Figure 5.28 and Figure 5.29). This indicated that P2A-mediated cleavage efficiency depends on the respective genes *per se*. As 100% cleavage efficiency can therefore not be guaranteed, the generated expression system might not be suitable for certain applications such as subcellular co-localization studies.

I further observed that cells stably co-expressing EYFP and LacZ displayed significantly decreased LacZ expression levels (Figure 5.28). By treating these cells with proteasome inhibitor MG132 equimolar expression levels of EYFP and LacZ were restored (Figure 5.29). This experiment verified that P2A-medatiated co-expression *de facto* yields equimolar protein levels, but suggested that the observed expression levels depend on the specific protein stability. As demonstrated, MG132-treatment of cells is a possibility to achieve equimolar protein expression with a P2A expression vector despite low specific protein stability. However, toxic effects on the cells due to inhibition of proteasomal protein degradation must be taken into account when this method is used.

Finally, HEK-293 cells stably co-expressing EYFP and LacZ were subjected to ß-gal assay and fluorescence microscopy. Resulting blue staining of ~50% of the HEK-293 cells confirmed expression of enzymatically active β-galactosidase (Figure 5.30). The lack of ß-gal activity in the remaining unstained cells might be explained by the low LacZ protein expression level due to increased protein instability (see Figure 5.28). In the following, fluorescence microscopy with blue light (450-490 nm) excitation revealed uniform yellow-green fluorescence of all cells and thereby suggested strong expression of correctly folded EYFP (Figure 5.30). Based on these results I reasoned that also other enzymes that are expressed with the P2A-based expression system are likely to be correctly folded and enzymatically active, despite a C-terminal P2A tail (21 bp) of the upstream- and an additional N-terminal proline of the downstream gene product.

Therefore, I concluded that the generated P2A expression system was suitable for co-expression of enzymatically active ELOVL4, CYP4F22 and CERS3 together with PNPLA1, in order to establish a cell culture model for ω-O-AcylCer synthesis (see section 5.6 and 5.7).

## 6.2 Molecular cloning of *CERS3* and *ELOVL4* into pcDNA4_HisMaxC

Verified HisMaxC constructs encoding *PNPLA1*, *PNPLA1*(p.S53A) (both isoform 1), *CYP4F22*, *YFP* or *LacZ* for sub-cloning and transient expression of N-terminally His-tagged proteins were already available in our laboratory. Using HEKα cDNA as a template for PCR, I generated HisMaxC constructs encoding *CERS3* and *ELOVL4.*

*CERS3* (isoform 1) CDS was successfully cloned into pcDNA4_HisMaxC as described in section 5.1. In contrast to *CERS3*, cloning of *ELOVL4* proved to be unexpectedly difficult (see section 5.3). I was able to amplify full length *ELOVL4* CDS by PCR (Figure 5.13), but several attempts to clone the insert DNA into HisMaxC were unsuccessful. After transformation and overnight incubation at 37°C, plated *E. coli* colonies appeared abnormally small compared to colonies that resulted from the same *E. coli* batch but had been transformed with HisMaxC constructs encoding other genes. Preparation of *ELOVL4* encoding plasmid DNA from these small colonies only yielded ~1.75 µg plasmid DNA, whereas preparation of other HisMaxC constructs resulted in 9-15 µg plasmid DNA.

Interestingly, DNA sequencing revealed that selected recombinant plasmids from multiple cloning attempts frequently contained *ELOVL4* insert DNA with a specific 127 bp deletion, stretching from nucleotide 542 to 669 of *ELVOL4* CDS (Figure 6.2). To investigate if the used insert DNA itself already contained the 127 bp deletion, RE-digested insert DNA used for ligation and insert DNA excised from selected recombinant plasmids after cloning were subjected to gel electrophoresis (Figure 5.14). The insert DNA that had been used for ligation displayed the expected size (948 bp), whereas the excised insert DNA fragments from the recombinant plasmids were shifted towards smaller sizes. This indicated that the specific 127 bp deletion occurred after transformation of ligated HisMaxC_hELOVL4 constructs into competent *E. coli* cells.

BLASTn homology search[39] of *ELOVL4* CDS against the *E. coli* nucleotide collection did not reveal homology of the deleted region, which argued against excision by homologous recombination. However, 158 bp upstream of the deletion site, *ELOVL4* CDS contains a GTGGTGG sequence, which is highly similar to the conserved GCTGGTGG chi recognition sequence of the bacterial RecBCD recombination system (Figure 6.2). Possibly, this sequence is recognized by RecBCD, which would make recombination events in downstream regions much more likely.

[39] https://blast.ncbi.nlm.nih.gov/Blast.cgi ; March 2017


**Figure 6.2: *ELOVL4* CDS contains a sequence with high similarity to a bacterial chi recognition site (indicated in pink).** Recognition of this site might activate the bacterial RecBCD system, thereby creating a recombinational "hotspot". This may explain a frequently observed specific deletion of a 127 bp region in *ELOVL4* CDS (indicated in red) after transformation of *ELOVL4* encoding vector constructs into chemically competent DH5α or One Shot Stbl3 *E. coli*.

The use of One Shot Stbl3 chemically competent *E. coli* (which are optimized for cloning of unstable inserts) instead of *E. coli* DH5-alpha did not lead to successful cloning of *ELOVL4* either. Therefore, I applied a different cloning strategy, which is detailly described in section 5.3. In brief, two fragments of *ELOVL4* CDS were cloned consecutively into HisMaxC using the unique internal EcoRI site of *ELOVL4* CDS. Cloning of the first *ELOVL4* fragment was successful (Figure 5.16B) and selected *E. coli* colonies displayed a normal growth phenotype after transformation with the recombinant vector construct. However, subsequent cloning of the second *ELOVL4* fragment into the fragment 1-encoding construct failed. Selected *E. coli* colonies hosting the resulting recombinant plasmid DNA were abnormally small after incubation at 37°C and control digest of isolated recombinant plasmids confirmed that cloning was unsuccessful (Figure 5.17A).

Although pcDNA4_HisMaxC is a mammalian expression vector, inadvertent expression of cloned genes in bacterial hosts may be possible, as it has been reported that the eukaryotic CMV promoter might be active in *E. coli* [62]. Interestingly, *ELOVL4* CDS also incidentally contains a TATAAT sequence (located at nucleotides 244-249), which is identical to the prokaryotic pribnow box consensus sequence. It is conceivable that transcription could be initiated from this site in *E. coli*. Resulting mRNA would contain an incidental start codon that is in frame with wild-type *ELOVL4* CDS, but would not contain a Shine-Dalgarno sequence (Figure 6.3). However, it has been reported that translation in *E. coli* can be initiated independently of a Shine-Dalgarno sequence [63,64]. The potentially translated N-terminally truncated protein would consist of 216 amino acids, which comprises 69% of wild-type ELOVL4.

Based on these findings I speculated that inadvertent expression of enzymatically active full length or N-terminally truncated ELOVL4 might have caused toxicity in the *E. coli* host. This may explain the observed growth impairment of *E. coli* cells carrying *ELOVL4*-encoding recombinant plasmid DNA and the positive selection of HisMaxC constructs with a specific 127 bp deletion in *ELOVL4* CDS.

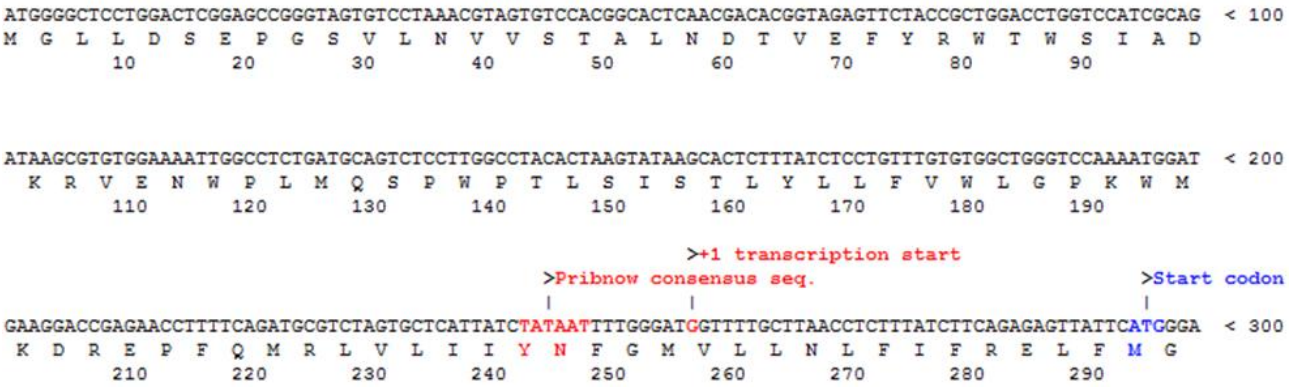


**Figure 6.3: *ELOVL4* CDS contains a coincidental Pribnow box (indicated in red), which might enable transcription in *E. coli*.** The resulting *ELOVL4* mRNA would contain an incidental start codon in frame with wild-type *ELOVL4* CDS (indicated in blue). Shine-Dalgarno independent translation of N-terminally truncated and possibly enzymatically active ELOVL4 may cause toxicity in *E. coli* cells hosting *ELOVL4*-encoding vector constructs.

To lower the plasmid DNA copy number and thereby the expression level of inadvertently expressed and possibly toxic proteins, incubation of *E. coli* cells at 25°C instead of 37°C has been suggested in literature [40, 41] [65]. Based on this recommendation, I further reasoned that incubation of *E. coli* cells at 25°C might also reduce the enzymatic activity of inadvertently expressed ELOVL4 and thereby lower the putative toxicity for *E. coli*.

By incubating *E. coli* cells at 25°C for molecular cloning, I indeed succeeded in generating a HisMaxC vector construct containing unmutated full length *ELOVL4* CDS in frame with the vector start codon (Figure 5.17B). Applying this method, further sub-cloning of *ELOVL4* CDS into other vector constructs was henceforth successful.

Finally, successful transient expression of CERS3 or ELOVL4 with the two different generated vector constructs was verified by metafectene-mediated transfection of COS-7 cells, followed by Western blot analysis (Figure 5.18).

[40] https://www.neb.com/tools-and-resources/troubleshooting-guides/troubleshooting-guide-for-cloning ; 2017

[41] https://www.neb.com/tools-and-resources/feature-articles/bypassing-common-obstacles-in-protein-expression ; 2017

## 6.3 Analysis of ω-O-AcylCer synthesis in COS-7, HaCat or HEK-293T cells co-expressing ELOVL4, CYP4F22, CERS3 and PNPLA1

After verifying that the generated P2A-based bicistronic expression vectors allow equimolar co-expression of correctly folded and enzymatically active target proteins (see 5.5 and 6.1) they were used to investigate the hypothetic pathway for ω-O-AcylCer synthesis. Therefore, the genes encoding ELOVL4 (for generation of ULFAs ≥C26), CYP4F22 (for ω-hydroxylation of ULFAs ≥C28), CERS3 (for amide bond linkage of ω-OH-ULFAs and sphingoid bases) and PNPLA1 (the putative transacylase for esterification of ω-OH-CER with LA) were cloned into P2A expression vectors (see section 5.6). The resulting constructs were then used to transiently or stably co-express these four target enzymes in COS-7, HaCaT, or HEK-293T cells and effects on ω-O-AcylCer formation were examined by radiolabeling of lipids, followed by TLC analysis (see section 0). As a negative control, EYFP, LacZ or a putative inactive PNPLA1(p.S53A) mutant variant were expressed instead of wild-type PNPLA1.

3xFLAG-ELOVL4 and 3xFLAG-CERS3 expressed with the generated P2A constructs were identical to the respective proteins expressed by Ohno *et.al.* [10] in their experiments, except for an additional N-terminal proline originating from the P2A peptide. Although it is not very likely, it cannot be excluded that the enzymatic activities of 3xFLAG-ELOVL4 and 3xFLAG-CERS3 were altered by the respective extra proline.

In contrast to 3xFLAG-CYP4F22 (as expressed by Ohno *et.al.* [10]), CYP4F22 expressed with the generated P2A construct contained a C-terminal 3xFLAG tag, followed by a 21 bp residual P2A tail. Ohno *et.al.* [10] demonstrated that CYP4F22 ω-hydroxylase activity depends on ER-localization mediated by an N-terminal hydrophobic region. Therefore the C-terminal 3xFLAG-P2A tag was not expected to alter CYP4F22 activity, especially as both the 3xFLAG tag and the large C-terminal domain of CYP4F22 containing the active site are hydrophilic[42] [10].

Like CYP4F22, PNPLA1 expressed with the P2A construct also contained a C-terminal 3xFLAG-P2A tag. As PNPLA1 does not possess a C-terminal localization signal[43], this tag was not expected to affect the assumed acyltransferase/transacylase activity of PNPLA1. However, altered enzymatic activity of PNPLA1 due to the 3xFLAG-P2A tag could not be excluded.

To stimulate lipid synthesis (and especially ω-O-AcylCer synthesis), COS-7, HEK-293 and HaCaT cells co-expressing ELOVL4, CYP4F22, CERS3 together with PNPLA1 were cultivated

[42] http://www.sigmaaldrich.com/life-science/molecular-biology/cloning-and-expression/vector-systems/mat-system-vectors/3x-flag.html ; 2017.
[43] http://www.uniprot.org/uniprot/Q8N8W4 ; 2017

in DMEM +/+ containing 10 µM PA, 10 µM OA and 10 µM LA (all bound to delipidated BSA at a molar FA/BSA ratio of 3:1) as well as 1.0 µM sphingosine (dissolved in DMSO). It was unknown if used cells expressed the required fatty acid elongases (ELOVL1-7) for generation of very long chain FAs (VLC-FAs, ≥C18) [4,5,8]. Therefore, the cultivation medium was further supplemented with 10 µM C24:0, 10 µM C24:1 and 10 µM C26:0 (all dissolved in EtOH), which are used as substrates by ELOVL4 to generate ULFAs (≥C26) for ω-O-AcylCer synthesis [4,9–11].

Using metafectene, I was able to transiently co-express 3xFLAG tagged ELOVL4, CYP4F22, CERS3 and PNPLA1 in COS-7 cells and HEK-293T cells (Figure 5.38 & Figure 5.42B), as well as N-terminal His-tagged versions of the enzymes in HEK-293T cells (using single-gene HisMaxC vector constructs, Figure 5.42A). In contrast to COS-7 cells, CERS3 and ELOVL4 expression levels in HEK-293T cells were significantly reduced compared to the other target enzymes (Figure 5.42). Curiously, CERS3 and ELOVL4 expression could not be improved by using higher plasmid DNA concentrations for metafectene-mediated transfection of HEK-293T cells.

Lipid profile analysis of generated COS-7 and HEK-293T cells co-expressing the target enzymes (using [$^{14}$C]LA or [$^{3}$H]sphingosine as tracer) did not provide evidence for the expected synthesis of ω-O-AcylCer, as no specific ω-O-AcylCer autoradiography signals were detected (Figure 5.39 & Figure 5.43). An possible explanation for these results might be that COS-7 and HEK-293T cells were unable to synthesize VLC-FAs by themselves and were further incapable of importing supplied VLC-FAs from the cultivation medium due to a lack of essential FA transport proteins, such as FATP4 [7,10]. As FATP4 also exhibits specific VLC-FA acyl-CoA synthetase activity [66,67], FATP4 deficiency might have prevented CoA-activation of ω-hydroxylated ULFAs, which is crucial for the CERS3-catalyzed amide linkage to a sphingoid base [10]. Yet, the fact that Ohno *et. al.* did not supply any FAs or other additives to HEK-293T cells co-expressing ELOVL4, CERS3 and CYP4F22, but still observed ω-OH-Cer formation, argues against a deficiency of essential acyl-CoA synthetase or fatty acid elongase activities in HEK-293T cells. Although it is not likely, it is also possible that low CERS3 and ELOVL4 expression levels (Figure 5.42) prohibited ω-O-AcylCer formation in HEK-293T cells.

In the following I used generated 2A vector constructs for the production of lentiviral particles and established a HaCaT cell line co-expressing ELOVL4, CYP4F22, CERS3 and PNPLA1 in a stable fashion (Figure 5.40). Radiolabeling of lipids using [$^{14}$C]LA or [$^{14}$C]PA revealed minor ω-O-AcylCer formation, which was however only detected by [$^{14}$C]LA labeling, but not by [$^{14}$C]PA labeling (Figure 5.41). LA is directly used for acylation of ω-O-AcylCers, whereas PA

gets incorporated into ω-O-AcylCers only via *de novo* sphinganine synthesis or when it is used by ELOVLs as substrate for ULFA generation (see section 1.2). Impaired *de novo* sphinganine synthesis and/or fatty acid elongation in used HaCaT cells may therefore explain why ω-O-AcylCers were only detected using [$^{14}$C]LA for radiolabeling, but not when [$^{14}$C]PA was used instead. However, ω-O-AcylCer levels in HaCaT cells expressing ELOVL4 and CYP4F22 together with PNPLA1 and CERS3 or EYFP and LacZ, respectively, was very similar (Figure 5.41). These results therefore argued against the proposed ω-O-AcylCer synthesis pathway and the putative acyltransferase or transacylase activity of PNPLA1.

Recent publications suggest that PNPLA1 (similar as PNPLA2/ATGL) might require a co-activator to exhibit high enzymatic activity, which might offer an explanation for the results of my experiments [24,59]. Due to the significant homology of PNPLA1 and PNPLA2, ABHD5/CGI-58 (the known co-activator of PNPLA2) is a likely candidate protein for co-activation of PNPLA1. This hypothesis if further supported by the fact that global and epidermis-specific CGI-58 knockout mice display an ichthyosifom skin phenotype, resembling the phenotype of *Pnpla1* -/- mice [59,68].

Therefore, future co-expression experiments with the target proteins that were proposed in the present thesis, together with CGI-58 and/or FATP4 have the potential to eventually elucidate the enigmatic activity of PNPLA1, which obviously has a vital function in permeability barrier formation and epidermal ceramide metabolism.

## 6.4 Conclusion

In the course of the present thesis a 2A-peptide based lentiviral expression system for transient or stable co-expression of up to four proteins was established. Evaluation of the generated expression system revealed that it was suitable for equimolar co-expression of correctly folded and enzymatically active proteins. Moreover, it was demonstrated that the specific P2A peptide allows self-cleavage of fusion proteins with up to 100% efficiency, which depended however on the expressed proteins *per se*. The generated P2A expression system therefore serves as a valuable tool for studying multi gene pathways and heteromultimeric proteins.

In the following, the P2A expression system was successfully used for transient or stable co-expression of ELOVL4, CYP4F22, CERS3 and PNPLA1 in COS-7, HaCaT or HEK-293T cells, to generate a complex cell culture model for a proposed ω-O-AcylCer synthesis pathway. However, lipid profile analysis of different established cell lines did not provide sufficient evidence for the hypothesis that PNPLA1 is a specific acyltransferase or transacylase for esterification of ω-OH-Cer with linoleic acid, which indicated the need for further research.

## 6.5 Postscript

Shortly after I have finished writing the present master's thesis, two new publications concerning the physiological role and enzymatic activity of PNPLA1 were published in Nature Communications.

Hirabayashi *et.al.* [69] generated global as well as keratinocyte-specific *Pnpla1* knockout mice (*Pnpla1* -/- and Pnpla1$^{f/f}$ *K14-Cre*, respectively). These PNPLA1 deficient animals exhibited a similar ichthyotic skin phenotype and ω-O-AcylCer synthesis defect as those described in *Pnpla1* -/- mice recently published by Grond *et. al.* [24].

Moreover, Ohno *et.al.* [70] identified PNPLA1 as the enzyme responsible for esterification of ω-OH-Cer with linoleic acid by co-expressing ELOVL4, CYP4F22, CERS3 and PNPLA1 in HEK-293T cells and labeling ω-O-AcylCers using [$^{3}$H]sphingosine (similar to the experiments conducted in the present thesis). Performing an *in vitro* transcription assay using a *PNPLA1* encoding plasmid, Ohno *et. al.* further demonstrated that PNPLA1 uses LA-containing TG rather than linoleoyl-CoA (C18:2-CoA) as substrate for ω-O-AcylCer formation. Therefore, the authors suggested that PNPLA1 likely is a CoA-independent transacylase rather than an acyltransferase.

# 7 Abbreviations

| | |
|---|---|
| APS | ammonium persulfate |
| CAPS | 3-(Cyclohexylamino)-1-propanesulfonic acid |
| AcylCer | acylceramide |
| Amp | ampicillin |
| bp | base pairs |
| BCA assay | bicinchoninic acid assay |
| BSA | bovine serum albumin |
| BHT | butylhydroxytoluol |
| CIP | calf intestinal alkaline phosphatase |
| CERS3 | ceramide synthase 3 |
| Cer | ceramides |
| Chol | cholesterol |
| CDS | coding sequence |
| cDNA | complementary DNA |
| CYP4F22 | cytochrome P450 4F22 |
| DNA | deoxyribonucleic acid |
| dNTPs | deoxyribonucleoside triphosphates |
| DSLR | digital single-lens reflex |
| dd | distilled, deionized |
| DTT | dithiothreitol |
| DNA Pol. | DNA polymerase |
| ds | double strand(ed) |
| Dox | doxycycline |
| ELOVL4 | elongation of very long chain fatty acids 4 |
| *E. coli* | *Escherichia coli* |
| EtOH | ethanol |
| EtBr | ethidium bromide |
| EDTA | ethylenediaminetetraacetic acid |
| FCS | fetal calf serum |
| FFA | free fatty acids |
| GlcCer | glucosylceramide |
| His-tag | hexahistidine-tag |
| HRP | horseradish peroxidase |
| h | hour(s) |
| IRES | internal ribosomal entry site |
| IPA | isopropyl alcohol |
| Kana | kanamycin |
| LB medium | lysogeny broth medium |
| mRNA | messenger ribonucleic acid |
| MeOH | methanol |
| min | minute(s) |
| MCS | multiple cloning site |
| Neo | neomycin |
| NEB | New England Biolabs |
| oligo(s) | oligonucleotide(s) |

| | |
|---|---|
| ODC | overday culture |
| ONC | overnight culture |
| PNPLA1 | patatin like phospholipase domain containing 1 |
| PBS | phosphate buffered saline |
| PolyA | polyadenylation signal |
| PCR | Polymerase chain reaction |
| PVDF | polyvinylidene difluoride |
| Pi | protease inhibitor |
| Puro | puromycin |
| RIPA buffer | radio-immunoprecipitation assay buffer |
| RE | restriction enzyme |
| rpm | revolutions per minute |
| RNA | ribonucleic acid |
| RT | room temperature |
| SNP | single nucleotide polymorphism |
| ss | single strand(ed) |
| SDS | sodium dodecyl sulfate |
| SDS-PAGE | sodium dodecyl sulfate polyacrylamide gel electrophoresis |
| Tet | tetracycline |
| TEMED | tetramethylethylenediamine |
| TLC | thin layer chromatography |
| Triton X-100 | *t*-Octylphenoxypolyethoxyethanol |
| Tris | tris(hydroxymethyl)aminomethane |
| β-gal | β-galactosidase |

# 8 References


1. Wolff K, Goldsmith LA, Katz SI, Gilchrest BA, Paller A, Leffell DJ. Fitzpatrick's Dermatology In General Medicine, Seventh Edition: Two Volumes [Internet]. McGraw-Hill Education; 2007. Available: https://books.google.at/books?id=EF2JAwAAQBAJ

2. Feingold KR, Elias PM. Role of lipids in the formation and maintenance of the cutaneous permeability barrier. Biochim Biophys Acta - Mol Cell Biol Lipids. Elsevier B.V.; 2014;1841: 280–294. doi:10.1016/j.bbalip.2013.11.007

3. Van Smeden J, Janssens M, Gooris GS, Bouwstra JA. The important role of stratum corneum lipids for the cutaneous barrier function. Biochimica et Biophysica Acta - Molecular and Cell Biology of Lipids. 2014. pp. 295–313. doi:10.1016/j.bbalip.2013.11.00

4. Breiden B, Sandhoff K. The role of sphingolipid metabolism in cutaneous permeabilitybarrier formation. Biochimica et Biophysica Acta - Molecular and Cell Biology of Lipids. 2014. pp. 441–452. doi:10.1016/j.bbalip.2013.08.010

5. Uchida Y, Holleran WM. Omega-O-acylceramide, a lipid essential for mammalian survival. J Dermatol Sci. 2008;51: 77–87. doi:10.1016/j.jdermsci.2008.01.002

6. Bikle D, Xie Z, Tu C. Calcium regulation of keratinocyte differentiation. Expert Rev Endocrinol Metab. 2013;7: 461–472. doi:10.1586/eem.12.34.Calcium

7. Khnykin D, Miner JH, Jahnsen F. Role of fatty acid transporters in epidermis. Dermatoendocrinol. Taylor & Francis; 2011;3: 53–61. doi:10.4161/derm.3.2.14816

8. Jakobsson A, Westerberg R, Jacobsson A. Fatty acid elongases in mammals: Their regulation and roles in metabolism. Prog Lipid Res. 2006;45: 237–249. doi:10.1016/j.plipres.2006.01.004

9. Ohno Y, Suto S, Yamanaka M, Mizutani Y, Mitsutake S, Igarashi Y, et al. ELOVL1 production of C24 acyl-CoAs is linked to C24 sphingolipid synthesis. Proc Natl Acad Sci. 2010;107: 18439–18444. doi:10.1073/pnas.1005572107

10. Ohno Y, Nakamichi S, Ohkuni A, Kamiyama N, Naoe A, Tsujimura H, et al. Essential role of the cytochrome P450 CYP4F22 in the production of acylceramide, the key lipid for skin permeability barrier formation. Proc Natl Acad Sci U S A. 2015;112: 7707–12. doi:10.1073/pnas.1503491112

11. Agbaga M-P, Brush RS, Mandal MNA, Henry K, Elliott MH, Anderson RE. Role of Stargardt-3 macular dystrophy protein (ELOVL4) in the biosynthesis of very long chain fatty acids. Proc Natl Acad Sci U S A. 2008;105: 12843–8. doi:10.1073/pnas.0802607105

12. Aldahmesh MA, Mohamed JY, Alkuraya HS, Verma IC, Puri RD, Alaiya AA, et al. Recessive Mutations in ELOVL4 Cause Ichthyosis, Intellectual Disability, and Spastic Quadriplegia. Am J Hum Genet. 2011;89: 745–750. doi:10.1016/j.ajhg.2011.10.011

13. Vasireddy V, Uchida Y, Salem N, Kim SY, Mandal MNA, Reddy GB, et al. Loss of functional ELOVL4 depletes very long-chain fatty acids (???C28) and the unique ??-O-acylceramides in skin leading to neonatal death. Hum Mol Genet. 2007;16: 471–482. doi:10.1093/hmg/ddl480

14. Li W, Sandhoff R, Kono M, Zerfas P, Hoffmann V, Ding BC-H, et al. Depletion of ceramides with very long chain fatty acids causes defective skin permeability barrier function, and neonatal lethality in ELOVL4 deficient mice. Int J Biol Sci. Ivyspring International Publisher; 2007;3: 120–8. Available: http://www.ncbi.nlm.nih.gov/pubmed/17311087

15. Lefèvre C, Bouadjar B, Ferrand V, Tadini G, Mégarbané A, Lathrop M, et al. Mutations in a new cytochrome P450 gene in lamellar ichthyosis type 3. Hum Mol Genet. 2006;15: 767–776. doi:10.1093/hmg/ddi491

16. Lugassy J, Hennies HC, Indelman M, Khamaysi Z, Bergman R, Sprecher E. Rapid detection of homozygous mutations in congenital recessive ichthyosis. Arch Dermatol Res. Springer-Verlag; 2008;300: 81–85. doi:10.1007/s00403-007-0815-0

17. Sugiura K, Takeichi T, Tanahashi K, Ito Y, Kosho T, Saida K, et al. Lamellar ichthyosis in a collodion baby caused by CYP4F22 mutations in a non-consanguineous family outside the Mediterranean. J Dermatol Sci. 2013;72: 193–195. doi:10.1016/j.jdermsci.2013.06.008

18. Rabionet M, Gorgas K, Sandhoff R. Ceramide synthesis in the epidermis. Biochim Biophys Acta - Mol Cell Biol Lipids. Elsevier B.V.; 2014;1841: 422–434. doi:10.1016/j.bbalip.2013.08.011

19. Mizutani Y, Kihara A, Igarashi Y. LASS3 (longevity assurance homologue 3) is a mainly testis-specific (dihydro)ceramide synthase with relatively broad substrate specificity. Biochem J. 2006;398.

20. Radner FPW, Marrakchi S, Kirchmeier P, Kim G-J, Ribierre F, Kamoun B, et al. Mutations in CERS3 cause autosomal recessive congenital ichthyosis in humans. PLoS Genet. 2013;9: e1003536. doi:10.1371/journal.pgen.1003536

21. Eckl K-M, Tidhar R, Thiele H, Oji V, Hausser I, Brodesser S, et al. Impaired epidermal ceramide synthesis causes autosomal recessive congenital ichthyosis and reveals the importance of ceramide acyl chain length. J Invest Dermatol. 2013;133: 2202–2211. doi:10.1038/jid.2013.153

22. Mizutani Y, Sun H, Ohno Y, Sassa T, Wakashima T, Obara M, et al. Cooperative Synthesis of Ultra Long-Chain Fatty Acid and Ceramide during Keratinocyte Differentiation. PLoS One. 2013;8: 2–9. doi:10.1371/journal.pone.0067317

23. Jennemann R, Rabionet M, Gorgas K, Epstein S, Dalpke A, Rothermel U, et al. Loss of ceramide synthase 3 causes lethal skin barrier disruption. Hum Mol Genet. 2012;21: 586–608. doi:10.1093/hmg/ddr494

24. Grond S, Eichmann TO, Dubrac S, Kolb D, Schmuth M, Fischer J, et al. PNPLA1 Deficiency in Mice and Humans Leads to a Defect in the Synthesis of Omega-O-Acylceramides. J Invest Dermatol. 2017;137: 394–402. doi:10.1016/j.jid.2016.08.036

25. Krieg P, Fürstenberger G. The role of lipoxygenases in epidermis. Biochim Biophys Acta - Mol Cell Biol Lipids. Elsevier B.V.; 2014;1841: 390–400. doi:10.1016/j.bbalip.2013.08.005

26. Behne M, Uchida Y, Seki T, de Montellano PO, Elias PM, Holleran WM. Omega-hydroxyceramides are required for corneocyte lipid envelope (CLE) formation and normal epidermal permeability barrier function. J Invest Dermatol. 2000;114: 185–92. doi:10.1046/j.1523-1747.2000.00846.x

27. Elias PM, Gruber R, Crumrine D, Menon G, Williams ML, Wakefield JS, et al. Formation and functions of the corneocyte lipid envelope (CLE). Biochim Biophys Acta - Mol Cell Biol Lipids. 2014;1841: 314–318. doi:10.1016/j.bbalip.2013.09.011

28. Grall A, Guaguère E, Planchais S, Grond S, Bourrat E, Hausser I, et al. PNPLA1 mutations cause autosomal recessive congenital ichthyosis in golden retriever dogs and humans. Nat Genet. Nature Publishing Group; 2012;44: 140–147. doi:10.1038/ng.1056

29. Oji V, Tadini G, Akiyama M, Blanchet Bardon C, Bodemer C, Bourrat E, et al. Revised nomenclature and classification of inherited ichthyoses: Results of the First Ichthyosis Consensus Conference in Sorze 2009. J Am Acad Dermatol. 2010;63: 607–641. doi:10.1016/j.jaad.2009.11.020

30. Akiyama M. The roles of ABCA12 in epidermal lipid barrier formation and keratinocyte differentiation. Biochimica et Biophysica Acta - Molecular and Cell Biology of Lipids. 2014. pp. 435–440. doi:10.1016/j.bbalip.2013.08.009

31. Firstskinfoundation.org. What is Ichthyosis? [Internet]. 2016. Available: http://www.firstskinfoundation.org/what-is-ichthyosis

32. Fachal L, Rodríguez-Pazos L, Ginarte M, Carracedo A, Toribio J, Vega A. Identification of a novel PNPLA1 mutation in a Spanish family with autosomal recessive congenital ichthyosis. Br J Dermatol. 2014;170: 980–2. doi:10.1111/bjd.12757

33. Ahmad F, Ansar M, Mehmood S, Izoduwa A, Lee K, Nasir A, et al. A novel missense variant in the PNPLA1 gene underlies congenital ichthyosis in three consanguineous families. J Eur Acad Dermatology Venereol. 2015; 1–4. doi:10.1111/jdv.13540

34. Lee E, Rahman OU, Khan MTM, Wadood A, Naeem M, Kang C, et al. Whole exome analysis reveals a novel missense PNPLA1 variant that causes autosomal recessive congenital ichthyosis in a Pakistani family. J Dermatol Sci. 2016;82: 46–48. doi:10.1016/j.jdermsci.2015.12.012

35. Vahidnezhad H, Youssefian L, Saeidian AH, Zeinali S, Mansouri P, Sotoudeh S, et al. Gene Targeted Next Generation Sequencing Identifies PNPLA1 Mutations in Patients with a Phenotypic Spectrum of Autosomal Recessive Congenital Ichthyosis: The Impact of Consanguinity. J Invest Dermatol. Elsevier Ltd; 2016;137: 678–685. doi:10.1016/j.jid.2016.11.012

36. Zimmer AD, Kim GJ, Hotz A, Bourrat E, Hausser I, Has C, et al. 16 novel mutations in PNPLA1 in patients with autosomal recessive congenital ichthyosis reveal the importance of an extended patatin domain in PNPLA1 that is essential for proper human skin barrier function. Br J Dermatol. 2017; doi:10.1111/bjd.15308

37. Kienesberger PC, Oberer M, Lass A, Zechner R. Mammalian patatin domain containing proteins: a family with diverse lipolytic activities involved in multiple biological functions. J Lipid Res. 2009;50 Suppl: S63–S68. doi:10.1194/jlr.R800082-JLR200

38. Rydel TJ, Williams JM, Krieger E, Moshiri F, Stallings WC, Brown SM, et al. The Crystal Structure, Mutagenesis, and Activity Studies Reveal that Patatin Is a Lipid Acyl Hydrolase with a Ser-Asp Catalytic Dyad ‡. Biochemistry. 2003;42: 6696–6708. doi:10.1021/bi027156r

39. Radner FPW, Fischer J. The important role of epidermal triacylglycerol metabolism for maintenance of the skin permeability barrier function. Biochimica et Biophysica Acta - Molecular and Cell Biology of Lipids. 2014. pp. 409–415. doi:10.1016/j.bbalip.2013.07.013

40. Zimmermann R, Lass A, Haemmerle G, Zechner R. Fate of fat: The role of adipose triglyceride lipase in lipolysis. Biochim Biophys Acta - Mol Cell Biol Lipids. Elsevier B.V.; 2009;1791: 494–500. doi:10.1016/j.bbalip.2008.10.005

41. Wilson P a, Gardner SD, Lambie NM, Commans S a, Crowther DJ. Characterization of the human patatin-like phospholipase family. J Lipid Res. 2006;47: 1940–1949. doi:10.1194/jlr.M600185-JLR200

42. Pelletier J, Sonenberg N. Internal initiation of translation of eukaryotic mRNA directed by a sequence derived from poliovirus RNA. Nature. 1988;334: 320–325. doi:10.1038/334320a0

43. Jang SK, Kräusslich HG, Nicklin MJ, Duke GM, Palmenberg AC, Wimmer E. A segment of the 5' nontranslated region of encephalomyocarditis virus RNA directs internal entry of ribosomes during in vitro translation. J Virol. 1988;62: 2636–43. Available: http://www.ncbi.nlm.nih.gov/pubmed/2839690

44. Baird SD, Turcotte M, Korneluk RG, Holcik M. Searching for IRES. RNA. 2006;12: 1755–1785. doi:10.1261/rna.157806

45. Wong E-T, Ngoi S-M, Lee C. Improved co-expression of multiple genes in vectors containing internal ribosome entry sites (IRESes) from human genes. Gene Ther. 2002;9: 337–344. doi:10.1038/sj/gt/3301667

46. de Felipe P. Skipping the co-expression problem: the new 2A "CHYSEL" technology. Genet Vaccines Ther. 2004;2: 13. doi:10.1186/1479-0556-2-13

47. Radcliffe PA, Mitrophanous KA. Multiple gene products from a single vector : " self-cleaving " 2A peptides. 2004; 1673–1674. doi:10.1038/sj.gt.3302361

48. Ibrahimi A, Velde G Vande, Reumers V, Toelen J, Thiry I, Vandeputte C, et al. Highly Efficient Multicistronic Lentiviral Vectors with Peptide 2A Sequences. Hum Gene Ther. 2009;20: 845–860. doi:10.1089/hum.2008.188

49. Verrier JD, Madorsky I, Coggin WE, Geesey M, Hochman M, Walling E, et al. Bicistronic lentiviruses containing a viral 2A cleavage sequence reliably co-express two proteins and restore vision to an animal model of LCA1. PLoS One. 2011;6: e20553. doi:10.1371/journal.pone.0020553

50. Szymczak AL, Workman CJ, Wang Y, Vignali KM, Dilioglou S, Vanin EF, et al. Correction of multi-gene deficiency in vivo using a single "self-cleaving" 2A peptide–based retroviral vector. Nat Biotechnol. 2004;22: 589–594. doi:10.1038/nbt957

51. Fan M. Plasmids 101: Multicistronic Vectors [Internet]. [cited 7 Nov 2016]. Available: http://blog.addgene.org/plasmids-101-multicistronic-vectors

52. Kim JH, Lee SR, Li LH, Park HJ, Park JH, Lee KY, et al. High cleavage efficiency of a 2A peptide derived from porcine teschovirus-1 in human cell lines, zebrafish and mice. PLoS One. 2011;6: 1–8. doi:10.1371/journal.pone.0018556

53. Wang Y, Wang F, Wang R, Zhao P, Xia Q. 2A self-cleaving peptide-based multi-gene expression system in the silkworm Bombyx mori. Sci Rep. Nature Publishing Group; 2015;5: 16273. doi:10.1038/srep16273

54. Boukamp P, Petrussevska RT, Breitkreutz D, Hornung J, Markham A, Fusenig NE. Normal keratinization in a spontaneously immortalized aneuploid human keratinocyte cell line. J Cell Biol. 1988;106: 761–71. doi:10.1083/jcb.106.3.761

55. Marinus MG, Morris NR. Isolation of deoxyribonucleic acid methylase mutants of Escherichia coli K-12. J Bacteriol. 1973;114: 1143–50. Available: http://www.pubmedcentral.nih.gov/articlerender.fcgi?artid=285375&tool=pmcentrez&rendertype=abstract

56. Geier GE, Modrich P. Recognition sequence of the dam methylase of Escherichia coli K12 and mode of cleavage of Dpn I endonuclease. J Biol Chem. 1979;254: 1408–13. Available: http://www.ncbi.nlm.nih.gov/pubmed/368070

57. May MS, Hattman S. Analysis of bacteriophage deoxyribonucleic acid sequences methylated by host- and R-factor-controlled enzymes. J Bacteriol. 1975;123: 768–70. Available: http://www.pubmedcentral.nih.gov/articlerender.fcgi?artid=235790&tool=pmcentrez&rendertype=abstract

58. Siegfried Z, Cedar H. DNA methylation: a molecular lock. Curr Biol. 1997;7: R305-7. Available: http://www.ncbi.nlm.nih.gov/pubmed/9115385

59. Grond S, Radner FPW, Eichmann TO, Kolb D, Grabner GF, Wolinski H, et al. Skin Barrier Development Depends on CGI-58 Protein Expression during Late-Stage Keratinocyte Differentiation. J Invest Dermatol. 2017;137: 403–413. doi:10.1016/j.jid.2016.09.025

60. Breiden B, Gallala H, Doering T, Sandhoff K. Optimization of submerged keratinocyte cultures for the synthesis of barrier ceramides. Eur J Cell Biol. 2007;86: 657–673. doi:10.1016/j.ejcb.2007.02.006

61. Logan S, Agbaga M-P, Chan MD, Brush RS, Anderson RE. Endoplasmic reticulum microenvironment and conserved histidines govern ELOVL4 fatty acid elongase activity. J Lipid Res. 2014;55: 698–708. doi:10.1194/jlr.M045443

62. Larsen MDB, Griesenbach U, Goussard S, Gruenert DC, Geddes DM, Scheule RK, et al. Bactofection of lung epithelial cells in vitro and in vivo using a genetically modified Escherichia coli. Gene Ther. Nature Publishing Group; 2008;15: 434–442. doi:10.1038/sj.gt.3303090

63. Fargo DC, Zhang M, Gillham NW, Boynton JE. Shine-Dalgarno-like sequences are not required for translation of chloroplast mRNAs in Chlamydomonas reinhardtii chloroplasts or in Escherichia coli. Mol Gen Genet. 1998;257: 271–82. Available: http://www.ncbi.nlm.nih.gov/pubmed/9520261

64. Skorski P, Leroy P, Fayet O, Dreyfus M, Hermann-Le Denmat S. The highly efficient translation initiation region from the Escherichia coli rpsA gene lacks a shine-dalgarno element. J Bacteriol. American Society for Microbiology; 2006;188: 6277–85. doi:10.1128/JB.00591-06

65. Rosano GL, Ceccarelli EA. Recombinant protein expression in Escherichia coli: advances and challenges. Front Microbiol. Frontiers Media SA; 2014;5: 172. doi:10.3389/fmicb.2014.00172

66. Gimeno RE. Fatty acid transport proteins. Curr Opin Lipidol. 2007;18: 271–276. doi:10.1097/MOL.0b013e3281338558

67. Klar J, Schweiger M, Zimmerman R, Zechner R, Li H, Törmä H, et al. Mutations in the Fatty Acid Transport Protein 4 Gene Cause the Ichthyosis Prematurity Syndrome. Am J Hum Genet. 2009;85: 248–253. doi:10.1016/j.ajhg.2009.06.021

68. Radner FPW, Streith IE, Schoiswohl G, Schweiger M, Kumari M, Eichmann TO, et al. Growth retardation, impaired triacylglycerol catabolism, hepatic steatosis, and lethal skin barrier defect in mice lacking comparative gene identification-58 (CGI-58). J Biol Chem. 2010;285: 7300–7311. doi:10.1074/jbc.M109.081877

69. Hirabayashi T, Anjo T, Kaneko A, Senoo Y, Shibata A, Takama H, et al. PNPLA1 has a crucial role in skin barrier function by directing acylceramide biosynthesis. Nat Commun. 2017;8: 14609. doi:10.1038/ncomms14609

70. Ohno Y, Kamiyama N, Nakamichi S, Kihara A. PNPLA1 is a transacylase essential for the generation of the skin barrier lipid ω-O-acylceramide. Nat Commun. 2017;8: 14610. doi:10.1038/ncomms14610